COMPUTATION OF DIFFUSION COEFFICIENTS AND PREDICTION OF CORROSION INITIATION IN CONCRETE STRUCTURES

by

Pratanu Ghosh

A dissertation submitted to the faculty of
The University of Utah
in partial fulfillment of the requirements for the degree of

Doctor of Philosophy

Department of Civil and Environmental Engineering

The University of Utah

May 2011

Copyright © Pratanu Ghosh 2011

All Rights Reserved

The University of Utah Graduate School

STATEMENT OF DISSERTATION APPROVAL

The dissertation of **Pratanu Ghosh**

has been approved by the following supervisory committee members:

Paul J. Tikalsky	, Chair	**1/19/2011** Date Approved
Chris Pantelides	, Member	**1/19/2011** Date Approved
Larry Reaveley	, Member	**1/19/2011** Date Approved
Terry A. Ring	, Member	**1/19/2011** Date Approved
Xuesong Zhou	, Member	**1/19/2011** Date Approved

and by **Paul J. Tikalsky** , Chair of the Department of **Civil and Environmental Engineering**

and by Charles A. Wight, Dean of The Graduate School.

ABSTRACT

Chloride induced reinforcement corrosion is one of the major problems in premature deterioration of several concrete structures such as bridge decks, concrete pavements and substructures in chloride laden environments. In this research, different ternary, binary and control cementitious concrete mixtures are studied for chloride induced corrosion initiation prediction of concrete structures. Diffusion coefficients are one of the primary variables that initiate chloride induced corrosion. The primary objective of the research is focused on investigation of chloride permeability of different cementitious materials and computation of reliable diffusion coefficients from the Chloride Ion Penetration Test (CIPT) and Wenner probe resistivity data using fundamentals of elctrochemistry. Several theoretical equations and methods are applied to compute improved diffusion coefficients of different ternary, binary based High Performance Cementitious (HPC) system. Correlation between the results of CIPT and the Wenner probe also measures their durability acceptance criterion for investigation of long term chlride penetration. This research also investigated electrical conductivity of different cementitius mixtures from the CIPT data and its effect on ternary cementitious systems. The other objective of this research is focused on the formulation of probabilistic corrosion initiation model with inclusion of apparent variation of previously computed HPC diffusion coefficients and the variation of surface chloride concentration with several corrosion resistant steel reinforcements. The distribution of the other governing parameters is generated from either detailed field survey or laboratory

experimental investigation. This study shows the variability and sensitivity of estimation of the time to onset of corrosion using the Monte Carlo technique and Simulation Based Reliability Approach (SBRA). Results from this probabilistic analysis estimate the corrosion free service life for the design of concrete structures in harsh chloride environments with respect to methods for diffusion coefficients computation.

TABLE OF CONTENTS

ACKNOWLEDGEMENTS

First and foremost, I wish to express my whole-hearted gratitude to Dr. Paul J Tikalsky for his help and invaluable guidance during the course of my doctorate research. I am grateful to Dr. Petr Konečný, who helped me last year to develop the probabilistc corrosion initiation model using SBRA approach. I would also like to thank all my committee members, Dr. Chris Pantelides, Dr. Larry Reaveley, Dr. Xuesong Zhou and Dr. Terry Ring, for their constructive suggestions.

I would like to thank all the past and present members of Dr.Tikalsky's research group especially Alex Hammond, Dave Thomas and Mike Virtis for their great help during my research.

I am grateful to my parents and wife Piyali for their complete support, patience, cooperation and giving me all the encouragement. I would also like to acknowledge my friends for their help.

Finally, I wish to express my gratitude and sincere appreciation to the Federal Highway Administration Pooled Fund Study TPF-5(117) for funding of this research work.

CHAPTER 1

INTRODUCTION

Concrete is the most versatile material in the world for construction of different structures such as bridges, highway pavements and marine facilities. It has been observed that the combination of concrete with reinforcing steel is a very good option from the point of view of long term performance in different distress mechanisms.

During winter, ice accumulates on the top surface of concrete slabs and bridge decks. For the purpose of removing the snow and ice, deicing agents, such as sodium chloride, magnesium chloride and calcium chloride are applied. These salts migrate down to the reinforcing steel through small pores in the concrete. Over time, the chlorides in these salts react with the reinforcing steel, breaking down the passivating layer and causing the steel to corrode. For low chloride concentrations the passivation layer is able to sustain itself and prevent active corrosion. However, when the concentration of the chlorides at the reinforcement reaches a critical level the passivation layer on the steel reinforcement surface will break down and active corrosion will initiate. Another source of chlorides is the seawater as many bridges are built in coastal areas and exposed to seawater. Chloride ion ingress is the primary catalyst of corrosion of reinforcing steel and premature deterioration of highway and marine structures.

The deterioration of concrete structures due to chloride induced corrosion is a major problem in the United States. The cost of repairing or replacing the structures has

become a major liability for highway agencies and DOTs. Approximately US$ 90 billion was required to repair or replace the 30% of the bridges in United States which are structurally deficient or functionally obsolete (1). Movement of chlorides through concrete can take place in several ways such as permeability, capillary movement in the pores (sorption) and diffusion (2). Diffusion is the dominating transport phenomenon for chloride ingress. Diffusion is the movement of chloride ions under a concentrated gradient. Since the interior of newly placed concrete contains very low levels of chloride ions, the difference in chloride concentration between the interior and the saturated exterior surface is enough to drive the diffusion process (3). Chloride ingress is governed by the micro-structural properties of concrete and chloride concentrations. The time required for the chlorides to reach the reinforcement in the bridge decks and other structures is determined by these factors as well as by the cover depth and presence of cracks. The corroding steel eventually delaminates the concrete, resulting in the need to replace bridge decks, substructures, and pavements. Once corrosion has been initiated, spalling and cracking of concrete in reinforced concrete bridge decks results.

Chloride induced corrosion is a complex electrochemical process. It requires flow of electric current and other chemical reactions. The three major components of corrosion cell are the cathode, anode and the electrolyte. The anode and the cathode can be present on the same reinforcing bar. The anode is present on the location of steel reinforcement. As this electrochemical process is a half cell reaction, cathodic and anodic reaction should occur simultaneously. Saturated concrete acts as an electrolyte and facilitates the flow of electrons from anode to cathode. The anode and the cathode can be located next to each other or separated. When they are present immediately next to each other, the

resulting corrosion is refereed as microcell and when they are separated, it is called macrocell. At the anode iron losses it's electrons to form Fe^{2+} (yellow) and this is an oxidation reaction. In the cathode, oxygen dissolves to form hydroxyl ions (OH^-) and this is a reduction reaction. The anodic product Fe^{2+} reacts with the cathodic product OH^- to produce ferrous oxide ($Fe(OH)_2$). This hydrated ferrous oxide can be further converted to red brown rust and black magnetite to form a stable passive layer around the steel reinforcement. Now, chloride diffuses through the depth of the reinforcing steel and starts to attack this passive film. When the concentration of chlorides reaches a critical level that is generally referred as critical chloride threshold, passive layer breaks down and the corrosion initiation starts.

While the ingress of chlorides is typically modeled as strictly a diffusion process it is a much more complex process. The initial movement of chlorides at the surface of the concrete can be affected by capillary suction, sorption, depending upon the percent saturation of the concrete. The chlorides within the concrete can also be affected by the fluxes of other ionic species. Due to the complexity of these processes and their strong dependence upon the chemical composition of the concrete paste made for concrete structures can be enhanced by reducing the chloride penetration or by providing protection to the reinforcement bars against corrosion. Improvement of material properties of concrete and use of more corrosion resistant reinforcements slow the chloride ingress process.

In order to provide useful remedies to enhance the service life of concrete structures in chloride induced corrosion, the following goals need to be achieved to address the problems:

1) Computation of reliable improved high performance concrete (HPC) diffusion coefficients from different testing procedures to include in the corrosion initiation model
2) Determination of reliable correlation between the data sets of different testing procedure to investigate chloride ingress as part of the durability acceptance criterion
3) Investigation of influence of diffusion coefficients, electrical resistivity and conductivity on different HPC systems
4) Development of probabilistic corrosion initiation model with inclusion of several corrosion resistant reinforcements and variation of HPC diffusion coefficients, surface chloride concentrations, holidays and cracks.

For this reason, this dissertation has achieved previously mentioned goals through Chapter 3-7. Chapter 2 describes all the previous studies for determination of diffusion coefficients, resistivity measurements of different high performance concrete and how it affects the corrosion initiation of different concrete structures. Previous research related to probabilistic corrosion initiation model is also described in this chapter. Chapter 3 demonstrates prediction of equivalent steady state diffusion coefficients from chloride ion penetration test (CIPT) data. Chapter 4 describes the computation of diffusion coefficients from both the CIPT and experimental resistivity data. Chapter 5 discusses correlation of the CIPT and resistivity data in different curing conditions. Chapter 6 describes the effect of ternary cementitious system on conductivity and diffusion coefficients. Additionally, corrosion initiation time for different ternary based cementitious mixtures are calculated and compared with each other. Chapter 7 discusses

the Simulation Based Reliability Assessment model for concrete structures made with different cementitious mixtures and with different corrosion resistant steel reinforcements. Chapter 8 explains the discussion and conclusion of the results obtained from the whole research study. Chapter 9 proposes future research study.

To summarize, one of the goals of this research is to establish high performance cementitious mixtures with reduction of diffusion coefficients and increase of resistivity. The other goal of this research is focused on the formulation of probabilistic corrosion initiation model with inclusion of apparent variation of diffusion coefficients of HPC systems based on performance based specification and with several corrosion resistant steel reinforcement. The significance of the model is based on the prediction of corrosion initiation of the concrete bridge decks within the intended service life. These inclusions would be the additional important data component in the proposed model in comparison with previous existing model. This probabilistic corrosion initiation model would also serve the durability assessment of concrete bridge decks, pavements and other concrete structures.

1.1 References

1. Kirkpatrick, T.J., "Impact of Specification Changes on Chloride Induced Corrosion Service Life of Virginia Bridge Decks" Master's thesis at Virginia Polytechnic Institute and State University, Virginia USA, 2002.

2. Ahmad, S., Al-Kutti, W.A, Al-Amoudi, B.S.O., and Maslehuddin, M., "Correlations Between Depth of Water Penetration, Chloride Permeability, and Coefficient of Chloride Diffusion in Plain, Silica Fume, and Fly Ash Cement Concretes", *Journal of Testing and Evaluation*, V.36, 2009, pp.1-4.

3. Tikalsky, P.J., "Statistical Variations in Chloride Diffusion in Concrete Bridges", *ACI Structural Journal*, V.102, No.3, 2005, pp.481-486.

CHAPTER 2

LITERATURE REVIEW

Several research studies have been reported for prevention of corrosion initiation of concrete structures such as reliable diffusion coefficient determination, use of corrosion resistant steel reinforcements, and several Finite Elements (FE) based numerical models to predict the corrosion initiation. Chloride diffusion coefficient is useful in predicting the time of initiation and rate of propagation of corrosion (1). However, determination of chloride diffusion coefficient is not an easy process and it is time consuming. It is widely believed that Fick's law of diffusion can describe the rate of penetration of chloride to the depth of steel reinforcement to initiate corrosion in bridge decks (2), since the effect of hydraulic pressure and absorption are negligible in comparison for bridge decks and nonsaturated structures.

There are two general processes to determine diffusion coefficient, one under nonsteady state condition and the other under steady state condition. Under nonsteady condition apparent diffusion coefficients for various concretes are often determined by fitting profiles of acid soluble chloride concentration versus depth with Crank's solution (Equation (2.1)) to Fick's Second Law of diffusion (Equation (2.2)) (3),

$$C(x,t) = C_0(1 - erf(\frac{x}{2\sqrt{Dt}})) \tag{2.1}$$

$$\frac{\partial c}{\partial t} = D_a \frac{\partial^2 c}{\partial x^2} \tag{2.2}$$

where C_0-surface chloride concentration, D_a- apparent diffusion coefficient $C_{(x,t)}$- the chloride concentration at depth x, and time t, and erf()- standard error function.

The main weakness of the Equation 2.1 is the assumption of constant diffusion coefficient and surface concentration over time. It also does not take into account the influence of water transport on the transport of chemical compounds. As a consequence a single value of the diffusion coefficient can never be obtained from the measured concentration profiles, particularly if the measurements are performed over longer time periods (4). Some researchers consider surface diffusion coefficient and chloride concentration to be time dependent. Costa et al. considers time for chloride concentration build up from zero to C_0 by linear function (5). Bentz and Thomas, consider the chloride diffusion coefficient D_a, a function of both time and temperature (6). However, the use of Fick's second law for determination of diffusion coefficient proved to be useful in practical applications because it can be compared in different types of concrete and different environments. It is also promising with probability based approaches (4).

Under steady state condition, the rate of diffusion is expressed by Fick's first law as follows:

$$Q = -D \frac{\partial c}{\partial x} \tag{2.3}$$

where, Q- mass transport rate, D- diffusion coefficient, $\frac{\partial c}{\partial x}$- Concentration gradient of the chloride ions. Some researchers have performed chloride migration tests to determine

diffusion coefficient for nonsteady and steady state condition (7). They obtained relationship between the pore structure and chloride diffusivity in cement based materials, obtained a linear relationship between the steady state migration coefficient and nonsteady state migration coefficient based on the experimental setup and specimens. These migration tests are time consuming and are not easy to perform and also require continuous measurement of concentration of chloride ions in cathodic and anodic regions to investigate the steady state condition. Yang et al. have found a linear correlation between the chloride diffusion coefficient and charge passed (8). The existing method for determination of chloride ingress and computation of diffusion coefficient is the chloride ion penetration test (CIPT) according to ASTM C1202-05. In this testing procedure transport of ions is accelerated by applying external electrical field. In CIPT, the current passed through each of the mixture is measured at each 5- minute interval for a 6- hour time period and the resistance to chloride ion penetration is assessed by the total charge passed (9). The one major limitation of CIPT is that it accounts the current flow due to chloride ions only but not for other ions such as Na^+, K^+, OH^- which are also present in the migration process (10). The other limitation with the CIPT test is the high current flow due to application of 60V DC resulting joule effect. The increase in temperature will encourage the current to flow rapidly and produce considerable heat in a 6- hour time period especially through some of the permeable concrete mixtures (11). However, this is one of the most popular and simplest, quickest migration test methods accepted in the world and it is repetitive.

Several studies have been documented on ternary based cementitious mixtures and other supplementary cementitious mixtures for their effect on reduction of diffusion

coefficients and increase of resistivity as these two parameters are important in durability modeling of concrete structures. The electrical resistivity is the property of the material that reflects the ability to transport electrical charge, which accounts for the key parameter related to reinforcement corrosion problems (12). Ganesan et al. have shown that 20% reduction of portland cement with well burnt bagasse ash can make the concrete highly resistant to chloride ion penetration and diffusion (13). Smith et al. have shown the significant advantage of using supplementary cementitious materials (SCM) in development of high performance concrete. Their study revealed that use of SCM results in high values of concrete resistivity, thus causing a smaller likelihood of corrosion initiation (14). Ahmed et al. indicated that their results emphasized ternary blends of 25% fly ash and 10% silica fume exhibited significant decrease in charge passed in CIPT. Similarly, the charge passed in the ternary blends of 25% Blast Furnace Slag (BFS) and 50% BFS with addition of 10% silica fume showed lower charge compared to their respective binary blends (15). Ahmadi et al. showed that zeolite, a natural pozzolan improved the pore structure of the concrete significantly in mitigation of corrosion and comparable to or better than the concrete prepared with silica fume replacement in some cases (16). Kurgan et al. investigated the concrete with chloride ion penetrability and resistivity proportioned with different binary and ternary cement blends of Class F fly ash, blast furnace slag and silica fume. Their study proved that supplementary cementitious materials significantly reduced chloride ion ingress and increase resistivity (17). Thomas et al. showed that concrete produced with ternary cementitious blends has a

very high resistance to the penetration of chloride ions. Their results also emphasized that the diffusivity of the concrete that contains ternary blends continues to decrease with age. The reductions are very significant and have a considerable effect on service life modeling of concrete structures exposed chloride laden environments (18). Sun et al. investigated the chloride induced corrosion mitigation strategy with two or three different types of mineral admixtures added at the same time. Their results showed that mineral admixtures greatly increased the electrical resistance of concrete, which led to a delay in the initial time of corrosion and a decrease in the corrosion rate of steel bars. Additionally, double- and triple-adding mineral admixtures, instead of single adding, fly ash can reduce the corrosion of steel bars when a large amount of fly-ash replacement was used (19). Stundebeck showed that binary and ternary mixtures containing 25% fly ash provides chloride permeability resistance at 56 days similar to control mixtures without fly ash. The 50% fly ash replacement also produces high resistance to chloride penetration that is superior to the control mixture and the 25% fly ash binary mixture. The high volume (50%) fly ash mixture provides chloride permeability that is approximately half of that of the control mixture (20).

Several studies have reported for the application of different types of corrosion resistant steel reinforcement for prevention of corrosion initiation of concrete structures. One of the major types is epoxy coated rebar which is designed to seal the surface of the bar from any moisture, oxygen or any corrosive elements. Epoxy-coated bar is simply normal “black bar” from mild steel, cleaned and painted with an epoxy coating *(4)*. The protective effect of epoxy-coating may be damaged by a mashed area, bare area, or

holiday (pinhole), and is widely discussed (21-25). However, cracking and spalling of bridge substructure concrete components from corrosion of epoxy coated reinforcement occurred for splash and near splash zone locations of the overseas highway to Key West, FL, only 7 years after construction (26). Stainless steel or stainless steel cladding has been considered for reinforcing concrete undergoing severe exposure. Of the options that have been studied, epoxy coated reinforcing steel is the most prominent and galvanized rebar been applied in concrete with limited exposures. Nagi et al. showed application of galvanized rebar to prevent chloride induced corrosion and increase the service life of bridge decks. Evaluation testing results of two bridges in Michigan and Wyoming revealed that the galvanized reinforcing steel exhibited little evidence of corrosion in these two concrete decks. Field investigation also showed no evidence of concrete deterioration related to corrosion of embedded steel reinforcement even after 30 years of service (27). Yeomans studied the application of galvanized rebar in reinforced concrete structures. The experimental results showed that galvanized rebar has substantially higher chloride threshold than conventional black bar and it is effective in delaying the corrosion initiation and extends the life of the structures. However, the extent of this life extension depends to a large extent on the quality of the concrete used and the severity of the environment to which it is exposed (28).

It seems that research on the use of different high performance steel reinforcement is inconclusive and it needs more research for justification of their implementation.

Another method of corrosion prevention is the prediction of corrosion initiation through finite element (FE) based numerical models. Tikalsky et al. applied simulation based reliability assessment (SBRA) in the area of performance design and the durability

assessment of concrete structures (29). SBRA method developed in the late 80s by Pavel Marek and Milan Gusťar (30) is a modern simulation tool that can be used to predict the behavior of a structural element in a deleterious environment, as documented in (31-32) and thus evaluates performance-based criteria. The research provides the very first application of SBRA to combine in-place statistical data from concrete structures to assess the chloride penetration of concrete bridge decks. This paper illustrates the effect of variation in diffusion coefficients and cover depths using histograms by the application of Monte Carlo simulation. The results showed that the initiation of corrosion from the diffusion of chlorides can be delayed for decades by using high performance concrete with lower diffusion coefficients. A future area of this research would be development of a more comprehensive corrosion model based on reliability rather than deterministic equations. Konečný et al. developed comprehensive corrosion model and evaluated the performance of concrete bridge decks based on the probability of corrosion initiation on the bridge decks with crack and epoxy-coating protection of the reinforcement (33). Their model helps to compare the performance of epoxy-coating with the behavior of the black bar. The main objective of the research was to put on the stochastic evaluation of the epoxy-coated reinforcement of the bridge decks with respect to chloride induced corrosion. This research presents the interconnection of simulation based reliability assessment with Monte Carlo simulation and with respect to histogram-based random variables. Shim used this Monte Carlo technique in a corrosion model to show the variability on estimation of the time to onset of corrosion and the required depth of

concrete cover to extend the service life up to 100 years. His work demonstrated that the resulting probability distribution is most sensitive to the chloride diffusion coefficient (34). Lounis et al. presented a research approach for the probabilistic modeling of the chloride induced corrosion of carbon steel reinforcement in concrete structures. They also considered the uncertainties of the governing parameters such as concrete diffusivity, surface chloride concentration, concrete cover depth, and threshold chloride level. The parameters were modeled as random variables and the distribution of the corrosion time and probability of corrosion rate are determined by using Monte Carlo simulation (35). This method was incorporated to predict the level of corrosion in the top layer of reinforcing carbon steel of a highway bridge deck that was exposed to chlorides from deicing salts for 40 years. The prediction of the proposed model correlated very well with the field data which clarifies the usefulness of the probabilistic models to characterize the corrosion response and the actual condition of reinforced concrete structures. Kirkpatrick developed a model which determined the time to first repair and subsequent rehabilitation of concrete bridge decks exposed to deicing salts. The model works on the basis of existing deterministic model using Monte Carlo simulation (MCS) technique. The objective of the research was focused on the diffusion coefficient of the diffusion cracking model. Data for the surface chloride concentration, concrete cover depth, and apparent diffusion coefficient were collected from 10 Virginia bridge decks. Two types of resampling technique within MCS such as parametric bootstrap and simple bootstrap

were used to predict the first repair and rehabilitation based on the field data. This method substantially agreed for all bridge decks investigated (36).

Most of the previously mentioned probabilistic corrosion initiation models lack the distribution of reliable diffusion coefficients data of various high performance cementitious materials or performance of several corrosion resistant steel reinforcements. Some research needs to be performed to incorporate the reliable diffusion coefficients of HPC materials to investigate the performance of several steel reinforcements in order to extend chloride induced corrosion initiation in concrete structures exposed to chloride laden environments.

2.1 References

1. Azad, A.K., Sharif, A.M., Navaz, M., and Loughlin, K.F., "Chloride Diffusion Coefficient of Concrete in the Arabian Gulf Environment", *Arabian Journal of Science and Engineering*, V.22, No. 2B, 1997, pp.169-182.

2. Hooton, R.D., Thomas, M.D.A., and Standish, K., "Prediction of Chloride Penetration in Concrete, Federal Highway Administration, Washington, D.C., No.FHWA-RD-00-142, 2001, pp.405.

3. Nokken, M.R., Boddy, A., Hooton, R.D., and Thomas, M.D.A., "Time Dependent Diffusion in Concrete", *Cement and Concrete Research*, V.36, No.1, 2006, pp. 200-207.

4. Konečný, P., "Reliability of Reinforced Concrete Bridge Decks with Respect to Ingress of Chlorides", Doctoral Dissertation, Faculty of Civil Engineering, Ostrava, CZ, 2007.

5. Costa, A., and Appleton, J., "Chloride Penetration into Concrete in Marine Environment-Part II: Prediction of Long Term Chloride Penetration", *Materials and Structures*, V.32, 1999, pp.354-359.

6. Bentz, E., Thomas, M.D.A., and Rogers, C.A., "Durability of Ternary Blend Concrete with Silica Fume and Blast-Furnace Slag: Laboratory and Outdoor Exposure Site Studies", *ACI Materials Journal*, V.99, No.5, 2002, pp.499-508.

7. Sugiyama, T., Tsuji, Y., and Bremner, T.W., "Relationship between Coulomb and Migration Coefficient of Chloride Ions for Concrete in a Steady State Chloride Migration Test", *Magazine of Concrete Research*, 2001, V.53, No.1, pp. 13-24.

8. Yang, C.C., and Cho., S.W., "The Relationship between Chloride Migration Rate for Concrete and Electrical Current in Steady State using Accelerated Chloride Migration Test", *Materials and Structures*, V.37, 2004, pp.456-463.

9. Whiting, D., "Rapid Measurements of Chloride Permeability of Concrete", *Public Roads*, 1981, V.45, pp.101-112.

10. Suryavanshi, A.K., Swami, R.N., and Cardew, G.E., "Estimation of Diffusion Coefficients for Chloride Ion Penetration into Structural Concrete", *ACI Materials Journal*, 2002, V.99, pp.441-449.

11. Betancourt, J.G.A., and Hooton, R.D., "Study of the Joule Effect on Rapid Chloride Permeability Values and Evaluation of Related Electrical Properties of Concrete", *Cement and Concrete Research*, 2004, V.34, pp. 1007-1015.

12. Andrade, C., Rio, O., Castellote M., and Andrea, R.D., "A NDT Performance Method Based on Electrical Resistivity for the Specification of Concrete Durability", ECOOMAS Thematic Conference on Computational Methods in Tunneling, Vienna, Austria, August 27-29, 2007, pp.1-9.

13. Ganesan, K., Rajagopal, K., and Thangavel, K., "Evaluation of Bagasse Ash as Supplementary Cementitious Material", *Cement & Concrete Composites*, V.29, 2007, pp.515-524.

14. Smith, M.K., Andrea, J.S., and Tikalsky, P.J., "Performance of Supplementary Cementitious Materials in Concrete Resistivity and Corrosion Monitoring Evaluation", *ACI Materials Journal*, V.101, No.5, 2004, pp.385-390.

15. Ahmed, S.M., Kayali, O., and Anderson, W., "Chloride Penetration in Binary and Ternary Blended Cement Concretes as Measured by Two Different Rapid Methods", *Cement & Concrete Composites*, V.30, 2008, pp.576-582.

16. Ahmadi, B., and Shekarchi, M., "Use of Natural Zeolite as a Supplementary Cementitious Material", *Cement & Concrete Composites*, V.32, 2010, pp.134-141.

17. Kurgan, G.J., Tepke, D.G., Schokker, A.J., Tikalsky P.J., and Scheetz B.E., "The Effects of Blended Cements on Concrete Porosity, Chloride Permeability and Resistivity", SP-221(6).

18. Thomas, M.D.A., Shehata, M.H., Shashiprakash, S.G., Hopkins, D.S., and Cali, K., "Use of Ternary Cementitious Systems Containing Silica Fume and Fly Ash in Concrete", *Cement and Concrete Research*, V.29, 1999, pp.1207-1214.

19. Sun, W., Zhang, Y., Liu, S., and Zhang, Y., "The Influence of Mineral Admixtures on Resistance to Corrosion of Steel Bars in Green High-Performance Concrete", *Cement and Concrete Research*, V.34, 2004, pp.1781-1785.

20. Stundebeck, J.C., "Durability of Ternary Blended Cements in Bridge Applications" Master's thesis, May 2007, Missouri-Columbia, pp.1-102.

21. Benjamin, S.E., and Sykes, J.M., "Chloride Induced Pitting Corrosion of Swedish Iron in Ordinary Portland Cement Mortars and Alkaline Solutions: The Effect of Temperature", *Corrosion of Reinforcement in Concrete*, SCI, Elsvier, London, 1990, pp.59-64.

22. Sagues, A., Powers, R., and Zayed, A., "Marine Environment Corrosion of Epoxy-Coated Reinforcing Steel", *Corrosion of Reinforcement in Concrete*, SCI, Elsevier, London, 1990, pp.539-549.

23. Aarstein, F., Rindaroy, O. E., Liodden, O., and Jenssen, B.W., "Effect of Coatings on Chloride Ion Penetration into Offshore Concrete Structures", Concrete under severe conditions 2: Environment and loading, V.2, E&FN, London, 1998, pp.921-929.

24. Bentz, E., and Thomas, M.D.A., and Rogers, C.A., "Durability of Ternary Blend Concrete with Silica Fume and Blast-Furnace Slag: Laboratory and Outdoor Exposure Site Studies" *ACI Materials Journal*, V.99, No.5, 2002, pp.499-508.

25. Weyers, Brown, Kirkpatrick, Mokarem and Sprinkel, "Field Assessment of The Linear Cracking of Concrete Bridge Decks and Chloride Penetration" A paper submitted for presentation at TRB annual meeting, 2002, pp.1-18.

26. Houston, J.T., Atimay, E., and Ferguson, P.M., "Corrosion of Reinforcing Steel Embedded in Structural Concrete", Report No. CFHR-3-5-68-112-1F, Center for Highway Research, University of Texas, Austin, TX, 1972.

27. Nagi, M., and Alhasan, S., "Long Term Performance of Galvanized Reinforcing Steel in Concrete Bridges - Case Studies" Corrosion 2005, April 3-7, 2005, Houston, TX.

28. Yeomans, S.R., "Applications of Galvanized Rebar in Reinforced Concrete Structures", Corrosion 2001, March 11-16, 2001, Houston, TX.

29. Tikalsky, P.J., "Chapter 20- Durability and Performance Design Using SBRA" In (Marek et al., 2003).

30. Marek, P., and Gusťar, M. (1988). "Probabilistic Analysis of the Simultaneous Load Effects - Source of Steel Savings)", Proceedings: Conference "Ocelové konstrukce pro skladové hospodárství", ZP SVTS OK Mostárna Hustopece, December.1988. (in Czech).

31. Bradac, J., and Marek, P., "Application of Simulation-based Reliability Assessment, SBRA, for Lifetime Prediction of Concrete Structures". In proceedings: 8th International Conference on Life Prediction and Aging Management of Concrete Structures, RILEM, Bratislava, July 1999.

32. Korous, J.A., and Marek, P., "Durability and Plan of Inspections of Steel Component Exposed to Corrosion", *Journal: Stavebni obzor 2002/6*, CVUT Praha, Czech.

33. Konečný, P., Tikalsky, P.J., and Tepke, D.G., "Performance Assessment of a Concrete Bridge Decks Affected by Chloride Ingress by using Simulation Based Reliability Assessment and Finite Element Modeling", *Journal of Transportation Research Board*, Washington, DC, USA, 2007.

34. Shim, H., "Design and Analysis of Corrosion Free Service Life of Concrete Structures using Monte Carlo Method", *KSCE Journal of Civil Engineering*, V.9, No.5, 2005, pp.377-384.

35. Lounis, Z., Zhang, J., and Daigle, L., "Probabilistic Study of Chloride Induced Corrosion of Carbon Steel in Concrete Structures", 9th ASCE Joint specialty conference on Probabilistic Mechanics and Structural Reliability, Albuquerque, New Mexico, July 26-28, 2004, pp.1-6.

36. Kirkpatrick, T.J., "Impact of Specification Changes on Chloride Induced Corrosion Service Life of Virginia Bridge Decks", Master's thesis, Virginia Polytechnic Institute and State University, Virginia USA, 2002.

CHAPTER 3

PREDICTION OF EQUIVALENT STEADY STATE CHLORIDE DIFFUSION COEFFICIENTS

Pratanu Ghosh, Alex Hammond and Paul J. Tikalsky

Biography: ACI student member **Pratanu Ghosh** is a Research Assistant at the Materials and Structures Research Laboratory at the University of Utah. He received his B.S. from Bengal Engineering College (D.U), India and MASc. from the University of Windsor, Canada.

ACI student member **Alex Hammond** is a Research Assistant at the Materials and Structures Research Laboratory at the University of Utah. He received his B.S. from Boise State University and his M.S. from the University of Utah.

ACI Fellow **Paul Tikalsky** is the Chair of the Department of Civil and Environmental Engineering at the University of Utah. He is a member and former Chair of ACI Committee 232 (Fly Ash and Natural Pozzolans), member of ACI Committee 201 (Durability), and Chair of TRB Committee AFN10 (Basic Research and Emerging Concrete Technologies).

(Accepted for publication in ACI Materials Journal)

3.1 Abstract

This paper presents an approach for determining the chloride migration rate of hardened concrete by applying fundamental electrochemistry for different cementitious mixtures using the measurements from chloride ion penetration test (CIPT) data following ASTM C1202 specifications. The steady state condition is verified by comparing the numerical values of chloride migration rates during 5 minutes, 30 minutes and 360 minutes of testing. Three different theoretical approaches, Nernst-Plank, Nernst-Einstein and the Zhang-Gjorv method, are applied to obtain the equivalent steady state diffusion coefficients for different cementitious materials. These results are compared with the diffusion coefficients obtained from Berke's empirical equation using CIPT data. These methods for computation of diffusion coefficients include both the joule effect and temperature dependency and eliminate the need for other extended migration tests to obtain the steady state conditions. Overall, this research presents a reliable method of determining the chloride migration rate for diffusion coefficient prediction.

Keywords: Chloride diffusion, migration rate, corrosion, joule effect, steady-state

3.2 Introduction

Chloride ion ingress is one of the major problems that affect the durability of concrete structures such as bridge decks, concrete pavements and other structures exposed to harsh saline environments. It is one of the prime catalysts for corrosion of reinforcing steel and premature deterioration of highway, industrial and marine structures. Diffusion is one of the primary properties that control the rate of chlorides and ions entering into concrete structures. The chloride salt ingression into concrete can take place in several ways, such as flow under a pressure differential, termed as

"permeability" capillary movement in the pores termed as "adsorption" and due to the difference in concentration, termed as "diffusion" phenomena (1). Among these transport phenomena, diffusion is the most detrimental process related to the initiation of corrosion in steel reinforcement. Since the interior of newly placed structural concrete contains very low levels of chloride ions, the difference in chloride concentration between the interior and the saturated exterior surface are enough to drive the diffusion process (2). These salts migrate down to the reinforcing steel through small pores in the concrete, driven by the diffusion process. Over time, the chlorides in these salts react with the reinforcing steel, breaking down the passivating layer on the steel and causing the steel reinforcement to oxidize and subsequently corrode. As a consequence, the chloride diffusion coefficient is a necessary component in predicting the time of corrosion initiation and the rate of reinforcement corrosion (3). However, the determination of the chloride diffusion coefficient has not been easily obtained for production concrete. Several chloride diffusion testing procedures have been used to investigate the diffusivity of cement based materials. Typically the diffusion coefficients are determined by sampling concrete at different depths and fitting the profiles of water soluble chloride concentrations versus sample depths using Crank's solution following Fick's second law (4). This was the only method a decade ago despite being highly variable. The problem of such a method is that a powdered concrete sample at any depth sample may represent a mortar or an aggregate material at a particular location, not the composite behavior of concrete material. Long term chloride migration tests have been performed to determine migration coefficient under steady state conditions (5). These tests are time consuming and are not easy to perform for production mixture designs and they also require

continuous measurement of the concentration of chloride ions in the cathode and anode of the test to determine if steady state has been reached. The existing method is the chloride ion penetration test (CIPT) following ASTM C1202 specification (6). In this testing procedure, the transport of chloride ions is accelerated by applying an external electrical field. The current passed through an electrical cell containing the concrete specimen is measured at 5 minute intervals for a 6- hour time period. The resistance to chloride ion penetration is assessed by the total charge passed during the 6 hours (7). One major limitation of the CIPT results is that they do not account for the current exclusively carried by chloride ions as distinguished from the total ions in the migration process (8). Another limitation of the CIPT is that the high current flow in permeable concrete mixtures results in a "joule effect." The increase in temperature effectively decreases the electrical resistance and encourages the current to flow more rapidly and produce more heat which further accelerates the current flow (9). Berke et al. (10) developed empirical equations for the computation of diffusion coefficients using CIPT test data and experimental resistivity data. A strong influence of temperature on the diffusion coefficients was investigated by Berke and Hicks (11). This research involved conversion of the diffusion coefficients determined at lab temperatures to the average in service temperature by using an Arrhenius type equation. In spite of the repeatability of CIPT data, the test remains a comparative measure not a fundamental physical property. The computation of diffusion coefficients needs a stronger theoretical basis and considerations for the joule effect and the temperature normalization. The emphasis of this paper is on a reliable estimation of the diffusion coefficients directly from CIPT data and for the qualitative comparison of different approaches.

3.3 Research Significance

It is necessary to understand the variations of the diffusion coefficient of concrete with different cementitious materials to enhance the service life prediction of concrete structures, and establish some concrete mixtures with diffusion coefficients that minimize the ingress of chlorides. This research presented herein addresses the computation of diffusion coefficients from different theoretical and empirical approaches with the incorporation of essential adjustments for the joule effect and temperature dependency. These adjustments of data provide an improved prediction of chloride diffusion coefficients in concrete structures.

3.4 Experimental Investigation

Different types of binary and ternary cementitious mixtures with a water/cementitious materials ratio of 0.44, typical of exposed bridge deck concrete, were designed to give a wide range of values for this experimental program. All mixtures contained 564 lbs (256 kg) of the cementitious material with a CAF of 0.67. Limestone coarse aggregate meeting ASTM C33 No.67 gradation and ASTM C33 silica sand was used. Tests performed on mixtures using:

- ASTM Type I cement (TI)
- Limestone blended cement (E)
- Portland-pozzolan cement(TIP (20))
- Slag modified portland cement (TISM[TIS (25)])

Mineral additives used:

- Ground granulated blast furnace slag (G120S)
- Fly ash (Types C, F and F2)

- Silica fume(SF)
- Metakaolin(M)
- Volcanic tuft (S)

Medium range water reducing admixture and an air entraining agent were also used to meet required slump flow and other durability performance specifications. For each mixture, two 100 mm x 200 mm (4 inches x 8 inches) cylinders were cast and wet cured for 14 days and then they were air cured in lab conditions until the 98th day for testing. 98 days is 14 weeks, a sufficient time for pozzolanic reaction to develop. The concrete cylinders were cut to 50 mm (2 inches) slices and vacuum saturated with de-aerated water. In the testing process, each cell was filled with 3% NaCl solution on one side (cathode) and 0.3N NaOH solution on the other side (anode). A potential difference of 60Vdc was applied across each cell during which the current and temperature were recorded every 5 minutes for 6 hours. A minimum of two specimens were tested for each of the concrete mixtures. The average value of the specimen readings was reported to minimize the variation.

3.5 Chloride Migration Rate and Joule Effect

The electrical current is correlated to the flux of ions by a fundamental electrochemical equation. An electrical current is defined as the amount of electricity passing through a cross-sectional area, S, in a unit time (12) as expressed in Equation 3.1,

$$I = z \times F \times J \times S \tag{3.1}$$

where z is the valency of the chloride ion, J is the flux of the chloride ion species, S is the cross sectional area and F is the Faraday constant. The ionic flux, J, can be related to chloride migration rate (k), as shown in Equation 3.2,

$$J = k \times V/A \tag{3.2}$$

where V is the volume of the solution used in CIPT and A is the cross sectional area exposed to the chloride ions. In the CIPT, the volume of the solution is maintained at 250 ml (8.45 oz) in each electrode. The cathode is filled with 3% sodium chloride solution and the anode is filled with 0.3M sodium hydroxide solution. This 3% sodium chloride solution is equivalent to 2.05 mole/l (58.06 mole/ft^3) chloride ion concentration in the cathode cell. The negative ion (Cl^-) migrates towards the anode due to the application of the external applied potential of 60 Vdc. The data logger records the current at each 5-minute interval for a 6- hour duration of the test. The total charge passed through each of the mixtures is computed in coulombs (amp-sec). The charge passed, Q, is determined by integrating the current-time relationship as shown in Equation 3.3,

$$Q = \int_0^t I dt \tag{3.3}$$

where I is the current and t is the total elapsed testing time. The application of the high magnitude 60 Vdc induces an increase in temperature of the electrode solution throughout the 6- hour test period. This accelerates the current flow through permeable concrete mixtures during the test period resulting in a high value of charge passed. Betancourt et al. *(9)* applied a temperature adjustment to reduce or eliminate this “joule

effect" and improve the prediction of charge passed during 6- hour time period. The adjusted charge during the 6- hour test can be expressed in Equation 3.4.

$$Q_0 = e^{[\ln(Q_{c\,6hr})+\beta(1/\delta T - 1/273)]} \tag{3.4}$$

In Equation 3.4, Q_0 is the joule effect adjusted charge passed through 6 hour CIPT and β is an experimental constant equal to 1245, Q_{c6hr} is the original charge passed through 6- hour CIPT test, and δT is the difference in temperature increment in Kelvin during the 6- hour test (9). The adjusted average current is obtained by dividing the joule effect adjusted charge passed (Q_0) by time in seconds. The adjusted average electrical current during 360 minutes can be substituted into Equation 3.1 to obtain flux and then Equation 3.2 to obtain the adjusted chloride migration rate during 360 minutes. Table 3.1 shows the chloride migration rate during 5- minute, 30- minute and 360- minute intervals. It also depicts adjusted average charge passed using Equation 3.4 and adjusted chloride migration rate using Equation 3.2 during the 6- hour test for all of the concrete mixtures.

The "joule effect" further was examined by performing extended migration test (36 hours with 10 Vdc) along with CIPT procedure for 6- hour test for four different mixtures. Fig. 3.1 and 3.2 show the joule effect on two concrete mixtures for the CIPT as well as long term migration test in terms of excessive current passed and temperature rise. Fig. 3.3 shows the need for the incorporation of the joule effect adjustments.

3.6 Diffusion Coefficients from Three Theoretical Equations

In steady state conditions, the total chloride ion flux consists of three components, namely diffusion, migration and convection as shown in Equation 3.5 (13),

$$J = -D_i \frac{\partial C_i}{\partial x} - \frac{zF}{RT} D_i C_i \frac{\partial E}{\partial x} + C_i u \tag{3.5}$$

where D_i is the diffusion coefficient of chloride ion i in m^2 /sec (ft^2/sec); C_i is the chloride ion concentration in mole/m^3 (mole/ft^3); E is the applied electric potential and u is the velocity of the solute in m/sec (ft/sec). The first and third term in the Equation 3.5 describes the pure diffusion and convection processes. Since the specimen is saturated for the CIPT, the velocity of the solute can be neglected. As the electrical field is applied across the concrete specimen, the effect of pure diffusion in concrete is small since there is no concentration gradient at x=0 and diffusion can be neglected (13). As a result, the dominant term subjected to investigation is the second term, i.e., migration of chloride ions through diffusion and Equation 5 can be reduced to Equation 3.6.

$$J = -\frac{zF}{RT} D_i C_i \frac{\partial E}{\partial x} \tag{3.6}$$

The equivalent steady state chloride diffusion coefficient can be calculated by the Nernst-Plank equation as follows:

$$D = \frac{RTKV}{zC_o F(E/L)A} \tag{3.7}$$

In the Equation 3.7, R is the universal gas constant [8.314 Joule/mole/K] (1.98 Calorie/K/mole); T is the absolute temperature in Kelvin; z is the valency of chloride ions; C_o is the chloride ion concentration [2.05 mole/l] (58.06 mole/ft^3); E is the applied

electrical potential (60 Vdc); F is the Faraday constant; and L is the thickness of the concrete specimen [50 mm] (2 inches).

The diffusion coefficient in steady state can be calculated by another theoretical equation, based on the Nernst-Einstein Equation and is expressed by Equation 3.8 (14),

$$D = \frac{it_i RTL}{ZF^2 \Psi C_o} \tag{3.8}$$

where t_i is the transport number or transference number of chloride ions, and ψ is the applied electrical potential. The application of the Nernst-Einstein equation corresponds to the determination of diffusivities of aggressive ions in concrete, establishment of rapid tests for the permeability of concrete, monitoring the reinforcement of corrosion and predicting the service life of concrete structures (15).

The transference number of an ion in an electrolyte solution is the ratio of current carried by that particular ion to the total current carried in the solution (13). It can be expressed by Equation 3.9,

$$t_{cl} = \frac{I_{cl}}{I} = \frac{Q_{cl}}{Q} \tag{3.9}$$

where I_{cl} and Q_{cl} are the current and the charge passed due to chloride ions only. According to Equation 9, the transference number will be different for different mixtures. However, it has been shown that the diffusivity of chloride ions in concrete can be determined by the Nernst-Einstein equation only if the transference number is equal to one (15). This is the simplified approach, though it is not always correct. If the diffusivity of chlorides is to be determined, the concrete can be filled with a concentrated salt

solution. In this condition, the transference number of chloride ion can be assumed to be 1.0 (15).

Another simple approach of determining the diffusion coefficients of chloride ions would be application of the method developed by Zhang and Gjorv (16), and is expressed by Equation 10,

$$D = \beta \frac{T}{\Psi} \frac{LV}{C_o A} \frac{dc}{dt} \tag{3.10}$$

where dc/dt is the concentration gradient or chloride migration rate (k), and β is the empirical correction factor introduced by Zhang and Gjorv (16). This factor β was developed to explain the interactions between the ionic drift and it can be defined as the ratio of ideal to the actual drift velocity of ions. The value of β has been calculated for some NaCl solutions with chloride ion concentrations up to 0.5 M and a value of 1.48 x 10^{-4} $JK^{-1}C^{-1}$($0.43CalorieK^{-1}C^{-1}$) can be used for this purpose. The factor β allows for the determination of the chloride diffusion coefficient during testing by introducing concentration related retardation in the ionic migration velocity up to 41% for a 0.5 M NaCl solution (16). The only unknown parameter in Equation 3.10 is the concentration gradient which can be calculated by Equation 3.2. Table 3.2 shows the numerical values of diffusion coefficients for 24 mixture designs using the three previously mentioned theoretical approaches and they are discussed in the results section.

3.7 Empirical Method for Calculation of Diffusion Coefficients

The determination of diffusion coefficients by measurement of concentration profiles is a time consuming process. Therefore, it is beneficial to estimate the diffusion

coefficients directly from CIPT data. Berke et al. (10) developed an empirical equation to obtain diffusion coefficients from CIPT data as this test is frequently used in quality control and concrete specifications for construction projects. Data for permeability values above 2000 coulomb were not included in the correlation due to the high currents producing significant heating of the concrete, in which case the specimen can no longer be assumed to be at ambient temperature. Equation 3.11 was used to derive correlations between the effective diffusion coefficients and the CIPT Coulomb data. In the study presented herein, the joule effect is included in the computation of the adjusted CIPT data. Equation 3.11 is the prediction of the effective diffusion coefficients.

$$D_{eff} = 0.0103 \times 10^{-8} \times (Q_0)^{0.84} \tag{3.11}$$

Table 3.3 shows the numerical values of diffusion coefficients of the 24 mixture designs from Berke's empirical method. Diffusion coefficients from theoretical approaches are compared with Berke's empirical equation for the 24 mixture designs in Fig. 3.4 and the details are discussed in the results section.

Diffusion coefficients assist in the understanding of the rate of migration of chloride and other ions in concrete. The CIPT used throughout the industry to indicate the potential rate of chloride ingress. The chloride migration rate of the mixtures in this study versus computed steady state diffusion coefficients using the Nernst-Plank equation are plotted in Fig. 3.5. The substantial scatter in the data is generated by the heating of the CIPT system during testing.

3.8 Arrhenius Correction Factor

The diffusion coefficients obtained from the theoretical and empirical approaches presented in the previous sections are based on the temperature of the solution for the 6 hour CIPT experiment for each particular mixture. It has been observed that even a 10°C (18°F) increase of solution temperature results in approximately doubling the value of diffusion coefficients (11). Thus, diffusion coefficients determined on different temperature ranges must be converted to room temperature (21°C) (70°F) to get a uniform distribution of diffusion coefficients for all the cementitious mixtures. An Arrhenius type factor can be implemented to obtain diffusion coefficients at room temperature for all the mixtures designs as expressed in Equation 3.12.

$$D_2 = D_1(\frac{294}{T})e[\frac{U}{R}(\frac{1}{273+T} - \frac{1}{294}) \quad (3.12)$$

In Equation 3.12, T is temperature of the solution after 6- hour CIPT in Kelvin (Fahrenheit), U/R is the activation energy divided by the universal gas constant and it has been estimated to vary between 3850°K (6470°F) and 6000°K (10340 °F) for concrete with water to cementitious materials ratio of 0.6 to 0.4, respectively. Fig. 3.6 shows the effect of the Arrhenius correction factor on diffusion coefficients predicted from the Nernst-Plank equation.

3.9 Results

The values of chloride migration rate (k) are in a similar range where computed with data from 5 minutes and 30 minutes. However, high values are obtained where 360 minutes data is used. Insitu concrete does not attain such highly elevated temperatures.

This phenomenon is evidenced by Fig. 3.1 and 3.2 for two different mixtures one with 60Vdc for 6 hours and the other with 10Vdc for 36 hours of time. Fig. 3.1 and 3.2 show that temperature and current become nearly constant with the application of 10V dc over a 36- hour time period in comparison with high temperature and current passed due to application 60V dc over a 6- hour time period. Considerations for the joule effect are necessary to adjust the current and therefore chloride migration rate. Fig. 3.3 depicts this adjustment of chloride migration rate and shows that the chloride migration is comparable as compared to the 5- minute chloride migration rate. This small difference in values of chloride migration rate (k) implies steady state condition has nearly been reached within the 6- hour CIPT test where adjustments for the joule effect are incorporated.

It has been observed from Table 3.2 that the Nernst-Plank and the Nernst Einstein equations compute diffusion coefficients within similar ranges. The Zhang-Gjorv method computes high values of diffusion coefficients compared to Nernst-Plank and Nernst-Einstein method due to the introduction of empirical correction factor β to explain the ionic interactions between the ionic drift. Diffusion coefficients obtained from the empirical method (Berke's equation) also provide diffusion coefficients using CIPT data. The Empirical method of computation of diffusion coefficients is completely based on an equation developed by Berke on the basis of his experimental results curve fit rather than physics based model. While these methods are proportional with the Nernst-Plank method in Fig. 3.4**,** they do not provide the same values. These theoretical and empirical methods are useful to predict reliable equivalent steady state diffusion coefficients for different cementitious mixtures directly from 6- hour CIPT data.

Chloride migration rate is an important component in the computation of diffusion coefficients. For some permeable mixtures namely 100 TI, 75TISM/25C the adjusted chloride migration rate reduces the diffusion coefficients by a large extent (25 to 30%). It has been observed from Fig. 3.5 that the adjusted chloride migration rate correlated well with the diffusion coefficients predicted by the Nernst-Plank equation. It can be concluded from Fig. 3.5 that the joule effect is the prominent factor in computing diffusion constants for permeable concrete mixtures and the joule effect does not have a predominant effect on impermeable concrete mixtures.

The Arrhenius correction factor shows the temperature effect on the diffusion coefficients of cementitious mixtures, as shown in Fig. 3.6. Permeable cementitious mixtures have the greatest reduction in diffusion coefficients due to conversion of temperature from 6 hour CIPT test to 21°C (70°F).

3.10 Summary and Conclusion

The work presented in this paper demonstrates the necessity of the temperature adjustment due to the joule effect in understanding the steady state condition of the diffusion process. As a result, this adjustment achieved a more accurate and reliable prediction of the chloride migration rate in hardened concrete within 6 hours of the CIPT. Thus, the Nernst-Plank and the Nernst-Einstein equations are most applicable to compute equivalent steady state diffusion coefficients from the CIPT data. This adjustment due to joule effect has a predominant effect on permeable concrete mixtures by reducing their apparent chloride migration rate within the 6 hour CIPT. This adjustment eliminates the need for extended migration tests and other bulk diffusion tests to obtain the steady state conditions. The Arrhenius correction factor is also necessary to obtain the diffusion

coefficients from different temperature ranges to a standardize test temperature of 21°C (70°F).

3.11 Acknowledgements

The authors wish to express their gratitude and sincere appreciation to the Federal Highway Administration Pooled Fund Study TPF-5(117) for support of this research work.

3.12 Notation

C_0 = Chloride ion concentration

I = Electrical current

Z =Valency of chloride ion

J = Flux of chloride ion species

F = Faraday constant

S = Cross-sectional area

A = Cross-sectional area

K = Chloride migration rate

D = Diffusion coefficient

u = Velocity of solute

R = Universal gas constant

T = Absolute temperature in Kelvin

V = Volume of the solution used in CIPT

E = Applied electrical field

L = Thickness of the concrete specimen

I = Current density

t_i = Transport or Transference number of chloride ion

ψ = Applied electrical field

Q_{cl} = Charge carried by only chloride ions

I_{cl} = Current carried by chloride ions

β = Empirical correction factor introduced by Zhang and Gjorv in their equation

β = Experimental constant developed by Betancourt et al. due to the joule effect

dc/dt = Concentration gradient

Q_{c6hr} = Charge passed during 6 th hour

Q_0 = Corrected charge passed through 6 hr CIPT

U = Activation energy

x = Depth

δt = Difference in temperature increment during 6 hr test

3.13 References

1. Ahmad, S., Al-Kutti, W.A., Al-Amoudi, B.S.O., and Maslehuddin, M.," Correlations Between Depth of Water Penetration, Chloride Permeability, and Coefficient of Chloride Diffusion in Plain, silica fume, and fly ash Cement Concretes", *Journal of Testing and Evaluation,* V.36, No.2, 2009, pp.1-4.

2. Tikalsky, P.J., Pustka, D., and Marek, P., "Statistical Variations in Chloride Diffusion in Concrete Bridges", *ACI Structural Journal,* V.102, No.3, May 2005, pp.481-486.

3. Azad, A.K., Sharif, A.M., Navaz, M., and Loughlin, K.F., "Chloride Diffusion Coefficient of Concrete in the Arabian Gulf Environment", *Arabian Journal of Science and Engineering,* Dhahran, Saudi Arabia, V.22, No.2B, 1997, pp.169-182.

4. Nokken, M., Boddy, A., Hooton, R.D., and Thomas, M.D.A, "Time Dependent Diffusion in Concrete-Three Laboratory Studies", *Cement and Concrete Research*, V.36, No.1, January 2006, pp.200-207.

5. Sugiyama, T., Tsuji, Y., and Bremner, T.W., "Relationship between Coulomb and Migration Coefficient of Chloride Ions for Concrete in a Steady State Chloride Migration Test", *Magazine of Concrete Research,* V.53, No.1, 2001, pp. 13-24.

6. ASTM C1202-05, "Electrical Indication of Concrete's Ability to Resist Chloride Ion Penetration", *ASTM V04.02,* ASTM*,* Philadelphia, PA, 2005.

7. Whiting, D., "Rapid Measurements of Chloride Permeability of Concrete", *Public Roads,* V.45, No. 3, 1981, pp.101-112.

8. Suryavanshi, A.K., Swami, R.N., and Cardew, G.E., "Estimation of Diffusion Coefficients for Chloride Ion Penetration into Structural Concrete", *ACI Materials Journal,* V.99, No.5, September 2002, pp.441-449.
9. Betancourt, J.G.A., and Hooton, R.D., "Study of the Joule Effect on Rapid Chloride Permeability Values and Evaluation of Related Electrical Properties of Concrete", *Cement and Concrete Research,* V.34, No.6, June 2004, pp. 1007-1015.

10. Berke, N.S., and Hicks, M.C., "The Life Cycle of Reinforced Concrete Decks and Marine Piles Using Laboratory Diffusion and Corrosion Data", *In corrosion forms and control of infrastructure*, V.Chaker, ASTM STP 1137, *American Society for Testing and Materials,* Philadelphia, 1992, pp.207-31.

11. Berke, N., and Hicks, M., "Predicting Chloride Profiles in Concrete, Proceedings, Corrosion 93, *National Association of Corrosion Engineers Annual Conference,* Houston, 1993, pp.341/1-341/15.

12. Bockris, J.O'M., and Reddy, A.K.N., "Modern Electrochemistry", *Plenum press,* V.1, 1998.

13. Andrade, C., "Calculation of Chloride Diffusion Coefficients in Concrete from Ionic Migration Experiments", *Cement and Concrete Research,* V.23, No.3, 1993, pp.724-742.

14. Delagrave, A., Marchand, J., and Samson, E., "Prediction of Cement Based Materials on the basis of Migration Experiments", *Cement and Concrete Research,* V.26, No.12, 1996, pp.1831-1842.

15. Lu, X., "Application of the Nernst-Einstein Equation to Concrete", *Cement and Concrete Research,* V.27, No.2, February1997, pp.293-302.

16. Zhang, T., and Gjorv, O.E., "Effect of Ionic Interaction in Migration Testing of Chloride Diffusivity in Concrete", *Cement and Concrete Research,* V.25, No.7, October 1995, pp.1535-1542.

Table 3.1- Chloride migration rate and charged passed for different mixtures

Mix ID	Charge passed 6 hr (Coulomb)		Chloride migration rate (mol/l/sec) (mole/ft^3/sec) X 10^{-6}			
	Raw	Adjusted	5 min	30 min	Raw 360 min	Adjusted 360 min
100 TI	4562	3068	7.5(212.4)	7.8(220.9)	11.0 (311.6)	4.3 (121.8)
80TI/20F	6059	3729	9.1 (257.7)	9.9 (280.4)	14.0 (396.6)	5.3 (150.1)
80TI/20F2	2200	1761	3.8 (107.6)	3.7 (104.8)	5.4 (152.9)	3.0 (84.9)
65 TI/35G120S	1348	1165	2.7 (76.4)	2.5 (70.8)	3.1 (87.8)	1.8 (50.9)
60 TI/20C/20F2	4549	2709	9.4 (266.2)	10.0 (283.2)	14.0 (396.6)	9.9 (280.4)
60TI/30F2/10C	6137	3560	8.4 (237.9)	9.6 (271.9)	15.0 (424.9)	5.2 (147.3)
60TI/20F/20F2	4963	3247	7.3 (206.7)	8.1(229.4)	11.0 (311.6)	5.1 (144.4)
75TI/20F/5SF	1163	1032	2.3 (65.1)	2.1 (59.4)	2.8 (79.3)	1.6 (45.3)
60TI/20F/20G120S	1281	1143	3.0 (84.9)	3.0 (84.9)	2.4 (67.9)	1.4 (39.6)
75TI/20F/5M	1621	1372	2.9 (82.1)	2.9 (82.1)	3.9 (110.4)	2.4 (67.9)
65TI/30F/5SF	740	670	1.4 (39.6)	1.4 (39.6)	1.7 (48.1)	1.2 (33.9)
67TI/30F/3SF	1176	1033	2.2 (62.3)	2.1 (59.4)	2.8 (79.3)	1.8 (50.9)
50TI/30F/20G120S	1044	927	2.0 (56.65)	1.9 (53.8)	2.5 (70.8)	1.6 (45.3)
65TI/30F/5M	1159	1012	2.2 (62.3)	2.1 (59.4)	2.9 (82.1)	1.7 (48.1)
50TI/35G120S/15F	1124	979	2.3 (65.1)	2.1 (59.4)	2.6 (73.6)	1.5 (42.4)
75TI/20F2/5SF	1720	1408	3.0 (84.9)	3.1(87.8)	4.1(116.1)	2.5(70.8)
77TI/20F2/3SF	2137	1710	4.0 (113.3)	4.0 (113.3)	4.8 (135.9)	2.6 (73.6)
60TI/20F2/20G120S	2316	1808	4.0 (113.3)	4.0 (113.3)	5.6 (158.6)	2.9 (82.1)
75TI/20F2/5M	2363	1743	4.3 (121.8)	4.2 (118.9)	5.6 (158.6)	2.4 (67.9)
65TI/30F2/5SF	1168	1067	2.4 (67.9)	1.1 (31.1)	1.3 (36.8)	1.7 (48.1)
67TI/30F2/3SF	1987	1615	3.6 (101.9)	3.5 (99.1)	4.7 (133.1)	2.6 (73.6)
65TI/30F2/5M	3127	2299	5.1 (144.4)	5.1 (144.4)	7.6 (215.2)	3.8 (107.6)
50TI/35G120S/15F2	1264	1093	2.5 (70.8)	2.4 (67.9)	2.9 (82.1)	1.7 (48.1)
62TI/35G120S/3SF	1024	888	2.1 (59.4)	2.0 (56.65)	2.3 (65.1)	1.3 (36.8)
60TI/35G120S/5M	927	814	1.8 (50.9)	1.8 (50.9)	2.1(59.4)	1.3 (36.8)
100TIP	3583	2432	5.3 (150.1)	5.5 (155.8)	9.1 (257.7)	4.0 (113.3)
85TIP/15C	4913	3099	8.1 (229.4)	8.7 (246.4)	12.0 (339.9)	3.8 (107.6)
85TIP/15F	3877	2663	6.1 (172.8)	6.3 (178.4)	9.2 (260.6)	4.1 (116.1)
85TIP/15F2	1890	1505	3.4 (96.3)	3.2 (90.6)	4.9 (138.8)	2.4 (67.9)
65TIP/35G120S	1845	1546	2.8 (79.3)	2.7 (76.4)	3.7 (104.8)	3.1 (87.8)
97TIP/3SF	977	876	1.9 (53.8)	1.9 (53.8)	2.3 (65.1)	1.5 (42.4)
95TIP/5M	755	684	1.5 (42.4)	1.5 (42.4)	1.8 (50.9)	1.2 (33.9)
75TIP/25C	7515	4341	9.4 (266.2)	11.0 (311.6)	16.0 (453.2)	7.3 (206.7)
75TIP/25F	4535	3079	7.0 (198.3)	7.6 (215.2)	11.0 (311.6)	4.8 (135.9)
75TIP/25F2	5847	3497	8.3 (235.1)	9.2 (260.6)	13.0 (368.2)	5.1 (144.4)
50TIP/50G120S	955	873	1.9 (53.8)	1.8 (50.9)	2.2 (62.3)	1.5 (42.4)
100 TISM	4013	2687	5.6 (158.6)	6.5 (184.1)	10.0 (283.2)	4.7 (133.1)
75TISM/25C	4023	2725	6.0 (169.9)	6.5 (184.1)	9.6 (271.9)	4.5 (127.4)
75TISM/25F2	3032	2173	4.8 (135.9)	4.9 (138.8)	7.7 (218.1)	3.5 (99.1)
65TISM/35G120S	2735	2048	4.8 (135.9)	4.7 (133.1)	6.4 (181.3)	3.1 (87.8)
97TISM/3SF	935	847	1.8 (50.9)	1.7 (48.1)	2.3 (65.1)	1.5 (42.4)
100E	4774	3081	7.4 (209.6)	7.7 (218.1)	12.0 (339.9)	4.5 (127.4)
80E/20S	4560	2983	6.5 (184.1)	6.6 (186.9)	11.0 (311.6)	5.0 (141.6)
80E/20F	3878	2682	6.2 (175.6)	6.1 (172.8)	9.9 (280.4)	4.1 (116.1)
80E/20F2	4169	2884	6.4 (181.3)	7.1 (201.1)	10.0 (283.2)	4.6 (130.3)
80E/20G120S	2692	2040	4.8 (135.9)	4.6 (130.3)	6.8 (192.6)	3.0 (84.9)
80E/20C	3380	2440	5.5 (155.8)	5.6 (158.6)	8.3 (235.1)	3.9 (110.4)
95E/5SF	779	695	1.4 (39.6)	1.4 (39.6)	1.9 (53.8)	1.3 (36.8)
95E/5M	1350	1140	2.4 (67.9)	2.4 (67.9)	3.3 (93.4)	2.0 (56.6)

(Legend used to describe percentage of cementitious materials in mix proportions)

Table 3.2- Diffusion coefficients from theoretical approaches

Mix ID	Diffusion coefficients (m^2/sec) (ft^2/sec)x10^{-12}		
	Nernst-Plank	Nernst-Einstein	Zhang-Gjorv
100 TI	2.4 (25.7)	2.7(29.4)	4.7 (50.4)
100 TIP	1.9 (20.0)	2.1 (22.9)	3.7 (39.4)
60TI/20C/20F2	2.8 (30.4)	3.2 (34.8)	5.5 (58.6)
60TI/20F/20F2	2.5 (27.1)	2.9 (31.0)	4.9 (53.2)
75TI/20F/5SF	0.7 (8.1)	0.9 (9.3)	1.5 (15.9)
75TI/20F/5M	1.0 (10.9)	1.1 (12.5)	2.0 (21.4)
60TI/20F2/20G120S	1.4 (14.6)	1.5 (16.7)	2.7 (28.7)
75TI/20F2/5M	1.3 (14.1)	1.5 (16.1)	2.6 (27.7)
65TI/30F2/5SF	0.7 (7.9)	0.8 (9.1)	1.5 (15.7)
67TI/30F2/3SF	1.2 (13.0)	1.4 (14.8)	2.4 (25.6)
65TIP/35G120S	1.1 (12.2)	1.3 (13.9)	2.2 (23.9)
75TISM/25C	2.1 (22.5)	2.4 (25.7)	4.1 (44.1)
75TISM/25F2	1.6 (17.8)	1.9 (20.2)	3.2 (34.8)
97TISM/3SF	0.6 (6.7)	0.7 (7.5)	1.2 (13.0)
60TI/30F/10F2	2.5 (26.8)	2.8 (30.5)	4.9 (52.5)
77TI/20F/3SF	1.5 (16.5)	1.7 (18.7)	3.0 (32.3)
60TI/30C/10F2	2.7 (28.6)	3.0 (32.7)	5.2 (56.3)
60TI/30C/10F	2.9 (31.7)	3.4 (36.3)	5.8 (62.2)
80TI/20C	2.6 (28.7)	3.0 (32.7)	5.2 (56.3)
62 TI/35G120S/3SF	0.6 (6.9)	0.7 (7.9)	1.3 (13.6)
60TI/35G120S/5M	0.6 (6.3)	0.7 (7.3)	1.2 (12.5)
50TI/35G120S/15F	0.7 (7.6)	0.8 (8.7)	1.4 (15.1)
85TIP/15F	2.1 (22.1)	2.3 (25.2)	4.0 (43.1)
65TISM/35G120S	1.5 (16.6)	1.8 (18.9)	3.0 (32.5)

Table 3.3- Diffusion coefficients from empirical method

Mix ID	Diffusion coefficients m^2/sec (ft^2/sec) x10^{-12}
100 TI	8.7 (93.6)
100 TIP	7.2 (77.5)
60 TI/20C/20F2	7.9 (85.0)
60TI/20F/20F2	9.2 (99.0)
75TI/20F/5SF	3.5 (37.6)
75TI/20F/5M	4.5 (48.4)
60TI/20F2/20G120S	5.6 (60.2)
75TI/20F2/5M	5.4 (58.1)
65TI/30F2/5SF	3.4 (36.6)
67TI/30F2/3SF	5.1 (54.8)
65TIP/35G120S	4.9 (52.7)
75TISM/25C	7.9 (85.0)
75TISM/25F2	6.5 (69.9)
97TISM/3SF	3.0 (32.2)
60TI/30F/10F2	9.0 (96.8)
77TI/20F/3SF	6.1 (65.6)
60TI/30C/10F2	9.4 (101.1)
60TI/30C/10F	10 (107.6)
80TI/20C	9.5 (102.2)
62TI/35G120S/3SF	3.1 (33.3)
60TI/35G120S/5M	2.9 (31.2)
50TI/35G120S/15F	3.4 (36.5)
85TIP/15F	7.8 (83.9)
65TISM/35G120S	6.2 (66.7)

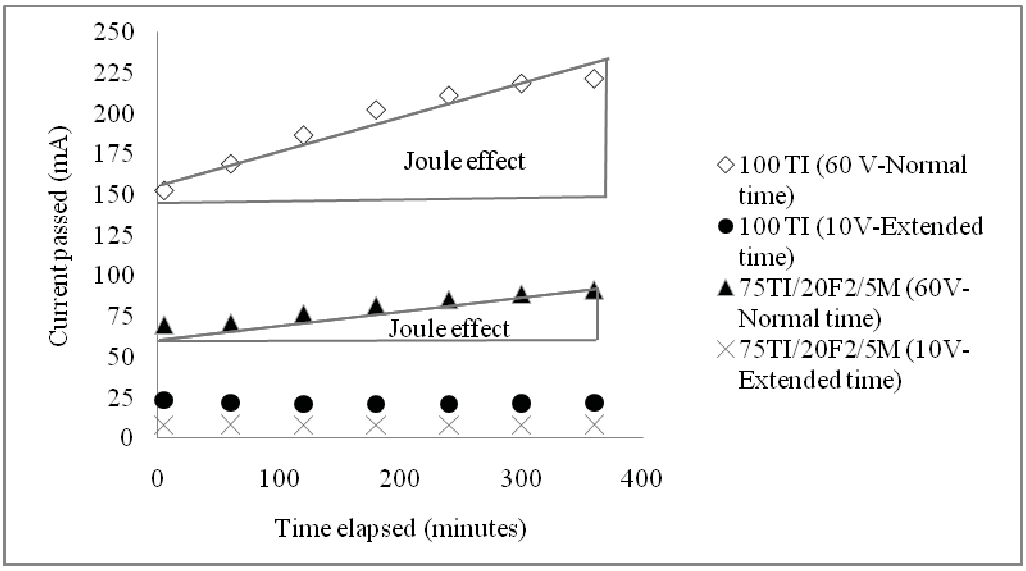

Fig. 3.1- Joule effect on two concrete mixtures in terms of current passed

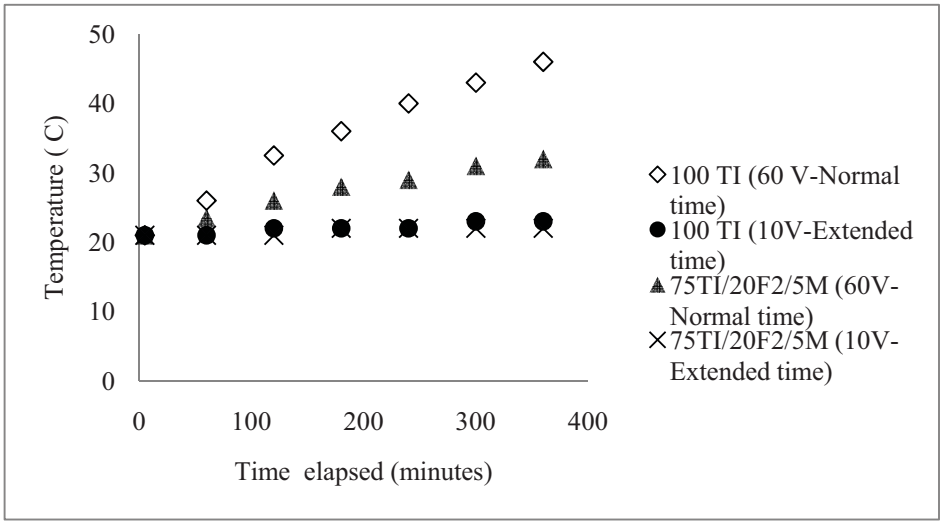

Fig. 3.2- Joule effect on two concrete mixtures in terms of temperature rise (1°F = °C x 1.8+32)

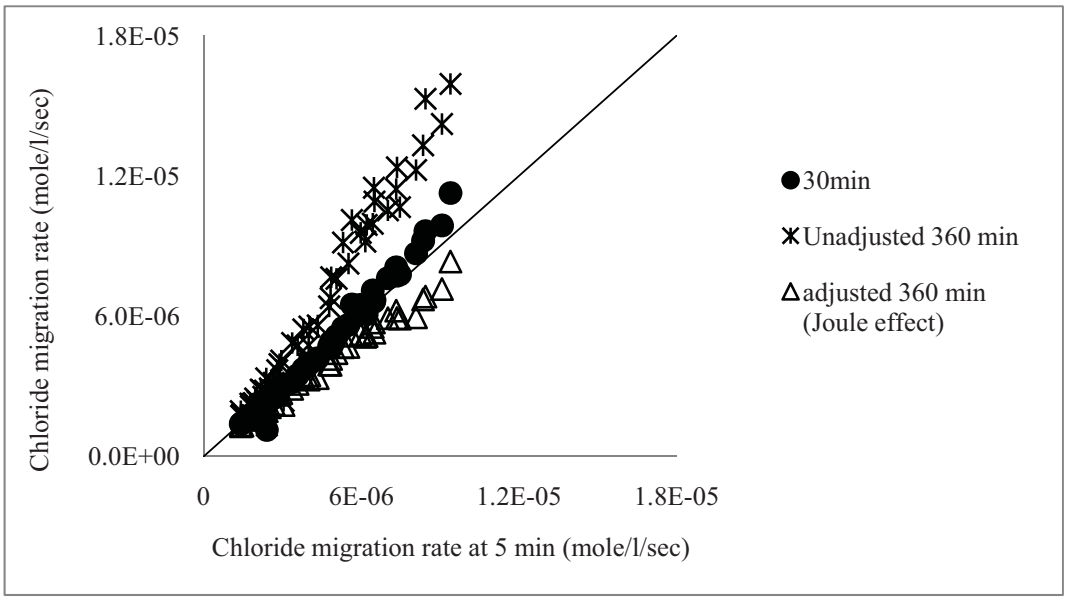

Fig. 3.3- Comparison of chloride migration rate from 5 minutes to 360 minutes

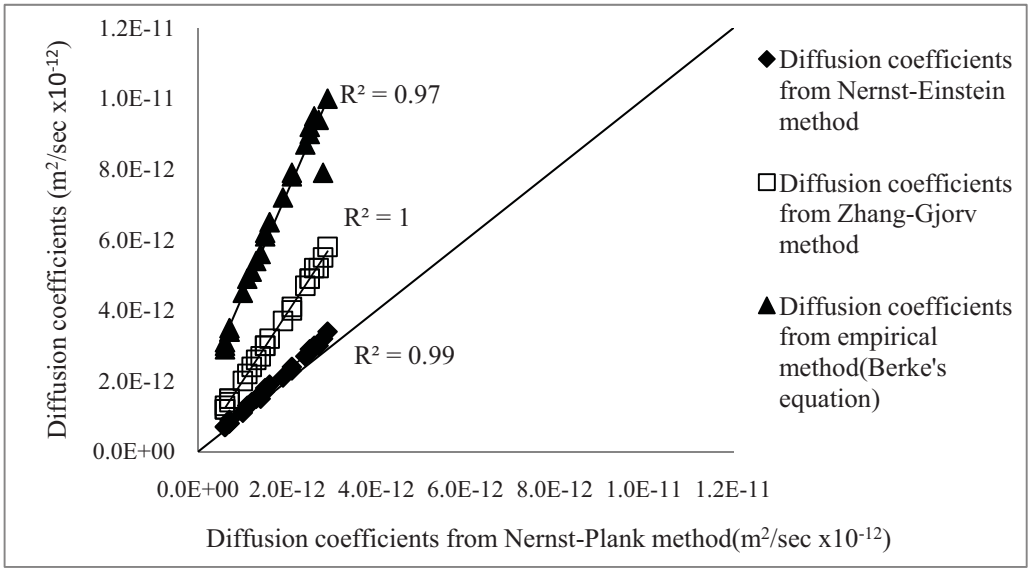

Fig. 3.4- Comparison of diffusion coefficients from CIPT data (1 m^2= 10.76 ft^2)

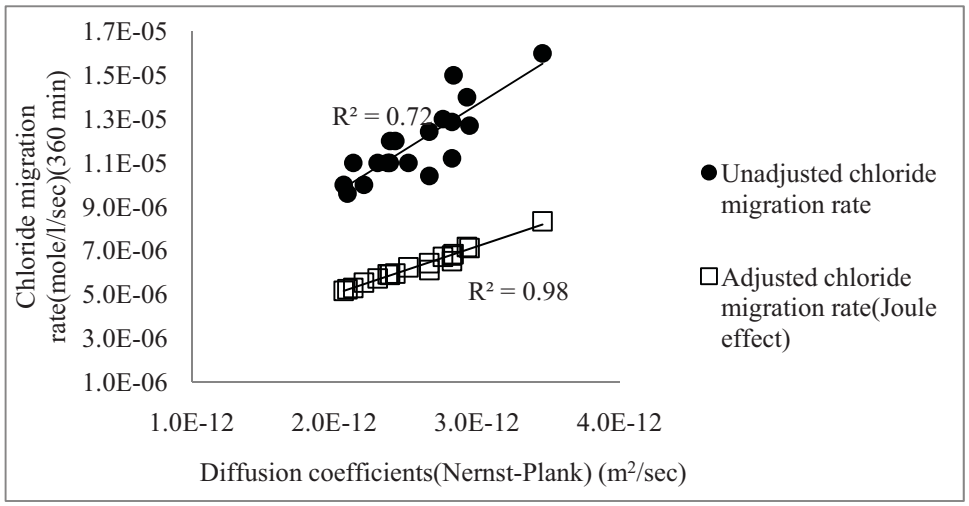

Fig. 3.5- Chloride migration rate vs. diffusion coefficients (1 m^2= 10.76 ft^2) (1 l= 0.0353 ft^3)

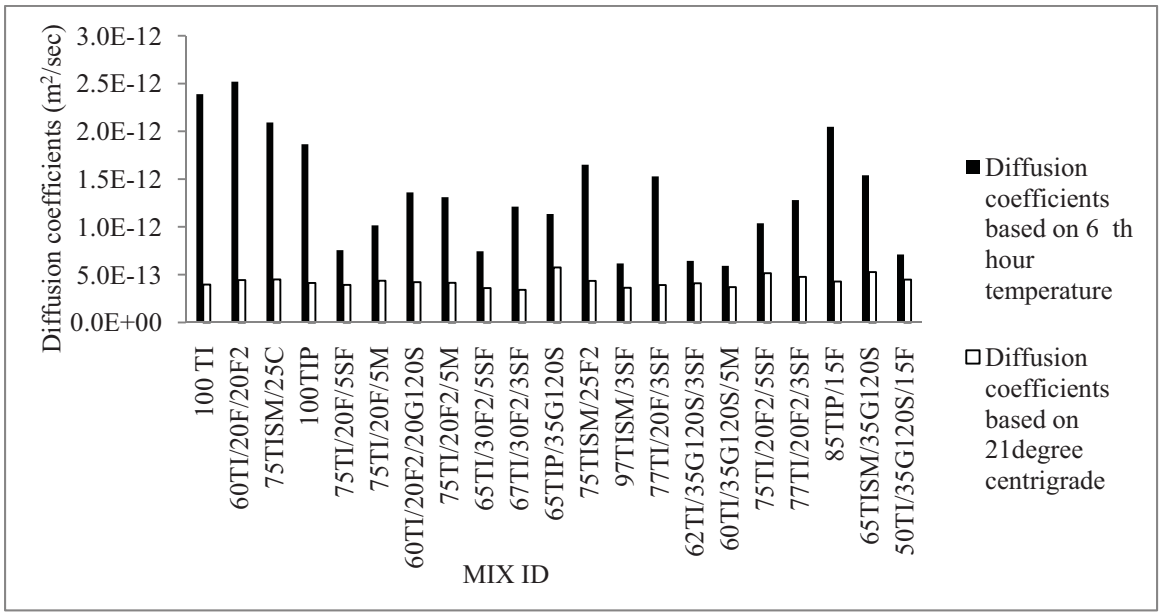

Fig. 3.6- Effect of Arrhenius correction factor on diffusion coefficients (Nernst-Plank) (1 m^2= 10.76 ft^2)

CHAPTER 4

DIFFUSION COEFFICIENTS FROM EXPERIMENTAL RESISTIVITY AND CIPT DATA

Pratanu Ghosh and Paul J. Tikalsky

Biography: ACI student member **Pratanu Ghosh** is a Research Assistant at the Materials and Structures Research Laboratory at the University of Utah. He received his B.S from Bengal Engineering College (D.U), India and MASc from University of Windsor, Canada.

ACI Fellow **Paul Tikalsky** is the Chair of the Department of Civil and Environmental Engineering at the University of Utah. He is a Fellow of the Engineering Academy of the Czech Republic. He is a member and former Chair of ACI Committee 232 (Fly Ash and Natural Pozzolans), member of ACI Committee 201 (Durability), and Chair of TRB Committee AFN10 (Basic Research and Emerging Concrete Technologies).

(To be submitted in ACI Materials Journal)

4.1 Abstract

Prediction of diffusion coefficients has been the subject of increasing research interest for last few years related to reinforcement corrosion problem. In this research, several approaches have been incorporated to compute the diffusion coefficients based on the experimental resistivity data along with the CIPT data for different cementitious

mixtures. Several theoretical approaches namely the Nernst-Einstein equation, one of the Nernst-Einstein laws is used to obtain the diffusion coefficients. Diffusion coefficients for chloride ions only excluding the effect of other ions in the migration process are also determined by the application of plug flow model. All of these theoretical methods are based on fundamentals of electrochemistry and incorporation of essential adjustments due to the joule effect and geometric shape difference. These theoretical approaches are compared with Berke's empirical method for determination of the diffusion coefficients from experimental resistivity data. Overall, this research presents a reliable method of prediction of the diffusion coefficients in corrosion initiation model in concrete structures.

Keywords: Chloride diffusion, resistivity, corrosion, Morris adjustment factor.

4.2 Introduction

There is an increasing demand to compute diffusion coefficients for durability protection of concrete structures. It is one of the prime reasons for corrosion of reinforcing steel and premature deterioration of highway and marine structures. Diffusion is one of the primary properties that control the rate of chlorides and ions entering into concrete structures. The chloride salt ingression into concrete can take place in several ways, such as flow under a pressure differential, termed as "permeability," capillary movement in the pores termed as "adsorption" and due to the difference in concentration, termed as "diffusion" phenomena (1). Among these transport phenomena, diffusion is the most detrimental process related to the initiation of corrosion in steel reinforcement. Since the interior of newly placed structural concrete contains very low levels of chloride ions, the difference in chloride concentration between the interior and the saturated

exterior surface are enough to drive the diffusion process (2). As a consequence, chloride diffusion coefficient is useful component in predicting the time of initiation and rate of reinforcement corrosion (3). The control of the chloride diffusivity is based on different short term and long term migration testing. However, these tests are both extensive and sometimes requires at least 2 to 3 days of testing compared to inexpensive non-destructive electrical resistivity testing (4). One major limitation of the migration test is that it does not account for the current exclusively carried by chloride ions as distinguished from the total ions in the migration process (5). Another limitation of short term migration testing, namely the Chloride Ion Penetration Test (CIPT), is the high current flow in permeable concrete mixtures results in a "joule effect." The increase in temperature effectively decreases the electrical resistance and encourages the current to flow more rapidly and produce more heat which further accelerates the current flow (6).

Concrete resistivity is another important parameter in durability modeling of concrete structures. The electrical resistivity is the property of the material that reflects the ability to transport electrical charge and provides indications on the concrete resistance to penetration of liquid or gas substances which accounts for the key parameter related to reinforcement corrosion problem (7). Corrosion current density decreases as the electrical resistivity increases, which subsequently reduces corrosion rate. As a result, electrical resistivity plays an important role in active corrosion propagation of the reinforcements. There is always research interest to obtain reliable diffusion coefficients from experimental resistivity data to include in corrosion initiation model. Riding et al. developed a simplified method which is similar to CIPT procedure except the specimen and gasket size to determine concrete resistivity as an index of concrete permeability. To

eliminate the gradual temperature rise problem only one current reading was taken (after 5 minutes) that could be applied to measure the concrete resistivity. An empirical correlation between the new method and the standard CIPT method established the validity and promise of the new simplified method. It also eliminates the difficulties associated with chloride ion penetration test such as cutting samples, desiccation, sample heating etc. and it is significantly faster and easier to perform (8). Berke et al. (9) developed empirical equations for computation of the diffusion coefficients using experimental resistivity data as these tests are frequently used in quality control and concrete specifications for construction projects. A strong dependence of temperature on the diffusion coefficients was also investigated by Berke and Hicks (10). This study involved the conversion of the diffusion coefficients determined at lab temperature to the average in service temperature by using an Arrhenius type equation.

It seems that the computation of diffusion coefficients needs a stronger theoretical basis and considerations for the joule effect, geometric shape factor and the temperature normalization. The emphasis of this paper is on a reliable estimation of the diffusion coefficients using electrical resistivity data along with the CIPT data from different theoretical and empirical approaches and for the qualitative comparison of different approaches.

4.3 Research Significance

Concrete structures exposed to chloride laden environments require computation of diffusion coefficients for alternative protection strategy. Earlier limited efforts were attempted to compute the diffusion coefficients from both experimental resistivity and the

CIPT data. This research addresses in depth computation of the diffusion coefficients using concrete resistivity along with the CIPT data from different theoretical and

empirical methods with incorporation of essential adjustments due to the joule effect, geometric shape difference and temperature dependency. Each of these theoretical methods in computation of the diffusion coefficients is based on fundamentals of electrochemistry and provides a reliable prediction of the chloride diffusion coefficients in concrete structures with less effort and expense.

4.4 Experimental Investigation

Different types of ternary cementitious mixtures along with control mixtures with a water/cementitious materials ratio of 0.44, typical of exposed bridge deck concrete, were designed to give a wide range of values for this experimental program. All mixtures contained 256 kg (564 lb) of the cementitious material with a Coarse Aggregate Factor (CAF) of 0.67. Limestone coarse aggregate of size 19 mm (3/4 inch) meeting ASTM C33 No.67 gradation and ASTM C33 silica sand was used. Tests performed on mixtures using:

- ASTM Type I cement (TI)
- Portland-pozzolan blended cement(TIP (20))
- Slag blended portland cement (TISM[TIS (25)])

Mineral additives used:

- Ground granulated blast furnace slag (G120S)
- Fly ash (Types C, F and F2)
- Silica fume(SF)
- Metakaolin(M)

Table 4.1 shows the concrete mixture compositions. Medium range water reducing admixture and air entraining agent were also used to meet required slump flow and other durability performance specifications. Chloride ion penetration test (CIPT) was performed with different ternary cementitious mixtures including the control mixtures to use its data for computation of equivalent steady state diffusion coefficients. For each mixture, two 100 mm x 200 mm cylinders were cast and wet cured for 14 days and then they were air cured in lab conditions until the 98^{th} day for testing. Ninety eight days (i.e 14 weeks) was selected as sufficient time for pozzolanic reaction to develop. Experimentation with a Wenner Probe device was conducted for 21 concrete mixtures to determine concrete cylinder resistivity on 98 days and these data were utilized to determine diffusion coefficients for chloride ions only using plug flow model. Concrete cylinders of 100 mm x 200 mm (4 inch x 8 inch) were cast and placed in a wet curing room in accordance with ASTM C192. They were wet cured for 98 days for electrical resistivity measurements to comply with Saturated Surface Dry (SSD) condition. A minimum of two specimens were tested for each of the concrete mixtures for CIPT and electrical resistivity data measurement. The average value of the specimen readings was reported to minimize the variation.

4.5 Plug Flow Model

Generally, CIPT and other extended migration tests include the influence of several ions such as Na^+, K^+, OH^- along with the effect of Cl^- ions. Therefore, it may be difficult to distinguish the effect of other ions in the computation of diffusion coefficients. The approach presented here involves the determination of diffusion

coefficients for chloride ions only using the rough order magnitude of velocity of chloride front from the CIPT and experimental resistivity data.

4.5.1 Chloride flux and transference number

Under the influence of 60Vdc electrical field in CIPT, ionic migration through a diffusion process becomes an important phenomenon. This process can be expressed with a plug flow model (11) and the migration flux of chloride ions can be obtained in Equation 4.1,

$$J_{cl} = V_{cl} \times C_{cl} \tag{4.1}$$

where V_{cl} is the velocity of chloride front in m/sec and the chloride ion concentration, C_{cl} in mole/l can be related to the current density for chloride ions only, i_{cl} by Equation 4.2,

$$i_{cl} = Z_{cl} \times F \times J_{cl} \tag{4.2}$$

where Z_{cl} is the valency of chloride ion, J_{cl} is the flux of chloride ion, i_{cl} is the current density due to chloride ions only and F is the Faraday's constant. Again, this current density due to chloride ions, i_{cl} can be related to chloride transference number, t_{cl} and current density for all ions (i) by Equation 4.3. The transference number of an ion in an electrolyte solution is the ratio of current carried by that particular ion to the total current carried in the solution (12).

$$i_{cl} = t_{cl} \times i \tag{4.3}$$

The transference number can also be defined in Equation 4.4 (11).

$$t_{cl} = \frac{Z_{cl}^2 \times D_{cl} \times C_{cl}}{\sum Z_j^2 \times D_j \times C_j} \quad (4.4)$$

In Equation 4.4, the following list defines the variables: D_j- the diffusion coefficient of the j^{th} ionic species, C_j-the concentration of chloride ions for j^{th} ionic species and Z_j-the valency of j^{th} ionic species. The computation of transference number can be performed from current intensity circulating through the specimen and from the flux of chlorides resulting from this circulation (12) and it is shown in Equation 4.5,

$$t_{cl} = \frac{z \times F \times J}{i} \quad (4.5)$$

4.5.2 Joule effect and adjusted flux

The electrical current is correlated to the flux of ions by a fundamental electrochemical equation. An electrical current is defined as the amount of electricity passing through a cross-sectional area, S, in a unit time (13) as expressed in Equation 4.6,

$$I = z \times F \times J \times S \quad (4.6)$$

where z is the valency of the chloride ion (z= 1), J is the flux of the chloride ion species, S is the cross sectional area of 50 mm (2 inch) diameter concrete specimen and F is the Faraday constant.

The application of the 60 Vdc in chloride ion penetration test (CIPT) induces an increase in temperature of the electrode solution throughout the 6 hour test period. This accelerates the current flow through permeable concrete mixtures during the test period resulting in a high value of charge passed. Betancourt et al. (6) developed a temperature adjustment to reduce or eliminate this “joule effect” and improve the prediction of charge

passed during the 6- hour time period. The adjusted charge during the 6 hour test can be expressed in Equation 4.7.

$$Q_0 = e^{[\ln(Q_{c\,6hr}) + \beta(1/\delta T - 1/273)]} \tag{4.7}$$

In Equation 4.7, Q_0 is the adjusted charge passed through 6 hour CIPT and β is an experimental constant equal to 1245, Q_{c6hr} is the original charge passed through 6 hour CIPT test, and δT is the difference in temperature increment in Kelvin during the 6 hour test (6). The adjusted average current is obtained by dividing the joule effect adjusted charge passed (Q_0) by time in seconds and it is expressed in Equation 4.8.

$$I_{adj} = \frac{Q_0}{t} \tag{4.8}$$

The adjusted average electrical current during 360 minutes can be substituted into Equation 4.6 to obtain adjusted flux. Chloride transference number (t_{cl}) for all the cementitious mixtures can be obtained by using this adjusted flux and the current density from the CIPT in Equation 4.5.

4.5.3 Concrete resistivity and geometric shape factor

The denominator in Equation 4 is related to the electrical resistivity of concrete (ρ), by Equation 4.9 (11),

$$\frac{1}{\rho} = \frac{F^2}{RT} \times \sum Z_j^2 \times D_j \times C_j \tag{4.9}$$

This resistivity in Equation 4.9 was determined on concrete cylinder for 21 different cementitious mixtures. Resistivity readings from a semi-infinite flat slab represent the standard for resistivity of the material, whereas the resistivity from the curved cylinder has interference from the edge of the cylinder. In order to account for this interference, the data needed to be converted into an equivalent semi-infinite slab resistivity where there are no curvature effects.

Morris et al. (14) developed this correction factor to convert the experimental lab resistivity data performed on concrete cylinder to eliminate the geometrical shape difference between a wide thick slab and concrete cylinder. The experimental resistivity values obtained by using the Wenner Probe device need to be divided by the proper correction factor, which was equal to K = 2.7 for 50 mm (2 inch) probe spacing and 100 mm x 200 mm (4 inch x 8 inch) cylinder. Diffusion coefficients obtained from experimental resistivity data need to be involved with this correction factor for understanding actual real life bridge deck slab data.

4.5.4 Velocity of chloride front and diffusion coefficients

By combining Equations 4.1, 4.2 and 4.3, the velocity of chloride front can be written as:

$$V_{cl} = \frac{J_{cl}}{C_{cl}} = \frac{it_{cl}}{C_{cl} F Z_{cl}} \tag{4.10}$$

Using Equation 4.10, the velocity of chloride front was determined for all the cementitious mixtures and it is shown in Table 4.2. Again, by combining Equations 4.1,

4.2, 4.3, 4.4 and 4.9, this velocity of chloride front can be correlated to the diffusion coefficients for chloride ions only by Equation 4.11.

$$V_{cl} = \frac{iZ_{cl}D_{cl}F\rho}{RT} \tag{4.11}$$

By interchanging the terms, finally the diffusion coefficients for chloride ions only can be obtained in Equation 4.12 using adjusted experimental resistivity data.

$$D_{cl} = \frac{RTV_{cl}}{iZ_{cl}F\rho} \tag{4.12}$$

4.6 Nernst-Einstein Relationship

For all porous materials, the Nernst-Einstein equation expresses the relationship between the electrical resistivity and ion diffusivity, as shown in the Equation 4.13 (15).

$$D = \frac{RT}{Z^2F^2} x \frac{t_i}{\gamma_i C_i \rho} \tag{4.13}$$

In Equation 4.13, D- diffusivity of the chloride ion; R- is the universal gas constant; T- is absolute temperature; Z- is ionic valence; F- is Faraday constant; t_i- is the transfer number of chloride ion; γ_i- activity coefficient for chloride ion; C_i- is concentration of ion i in the pore water; and ρ- is the electrical resistivity. This electrical resistivity is adjusted due to the geometric shape difference as explained previously in plug flow model. It has also been shown that the diffusivity of chloride ions in concrete can be determined by the Nernst-Einstein equation only if the transference number (t_i) is equal to one (16).

In Equation 4.13, for determination of diffusion coefficients all the parameters are known except the activity coefficient. There is need to compute the interaction parameter (I) and then substitute it in the activity coefficient equation to obtain the activity coefficient. The interaction parameter (I) can be defined in Equation 4.14 as follows (17):

$$I = \frac{1}{2}\sum mZ^2 \tag{4.14}$$

where m is the molality and Z is the charge of ions. The value of the interaction parameter (I) can be expressed in Equation 4.15 and the activity coefficient (γ) can be shown in Equation 4.16, (18). The 3% NaCl solution used in the CIPT according to ASTM C1202 is equivalent to 0.5 M and the charge of Na^+ and Cl^- ion is +1 and -1, respectively.

$$I = \frac{1}{2}x(0.5x1^2 + 0.5x(-1)^2) = 0.5 \tag{4.15}$$

$$-\log\gamma = AZ^2[\frac{\sqrt{I}}{1+\sqrt{I}} - 0.2xI] \tag{4.16}$$

In Equation 4.16, A is an empirical constant and equal to 0.5094 at room temperature and valency of chloride ion (Z) is equal to 1. Finally, the value of activity coefficient was determined from Equation 16 and then substituted in Equation 10 to compute the diffusion coefficients for different cementitious materials using adjusted resistivity data due to the geometric shape difference.

4.7 Nernst-Einstein Law

The ability of concrete resistivity to estimate diffusivity is based in one of the Einstein laws which relate the movement of electrical charges to the conductivity of the medium by Equation 4.17 (19),

$$D_e = \frac{k_{cl}}{\rho_{es}} \tag{4.17}$$

where D_e= effective diffusion coefficient, k_{cl} is a factor, which depends on the external ionic concentration, ρ_{es} is the resistivity of concrete saturated water.

The diffusion coefficient of chloride ion in concrete computed by the above equation does not involve chloride binding. However, in real life chloride binding should be considered by introducing a binding factor r_{cl}. Equation 4.17 can be modified and be written as Equation 4.18(12).

$$D_e = \frac{k_{cl}}{\rho_{es} r_{cl}} \tag{4.18}$$

There are some procedures to calculate r_{cl}, but it is not so important, as the paramount importance remains on the use of resistivity to determine parameter of durability multiplied by a binding retardation factor. For the sake of simplicity Andrade et al. (12) assumed the environmental parameter for chloride attack k_{cl}= 20000 ohm-cm^3/year (0.71 ohm-ft^3/year) and the reaction factor was assumed as r_{cl}=2. Table 4.3 shows the value of diffusion coefficients from the Nernst-Einstein law.

4.8 Empirical Method

The determination of diffusion coefficients by measurement of CIPT data is time consuming process. Therefore, it is beneficial to estimate the diffusion coefficients directly from electrical resistivity data. Berke et al. (9) developed an empirical equation to obtain diffusion coefficients from CIPT data as this test is frequently used in quality control and concrete specifications for construction projects. In the study presented herein, geometric correction factor was implemented on electrical resistivity data for computation of diffusion coefficients. Equation 4.19 is the prediction of the effective diffusion coefficients.

$$D_{eff} = 54.6 \times 10^{-8} \times (\text{Re}\,sistivity)^{-1.01} \tag{4.19}$$

Table 4.3 shows the numerical values of diffusion coefficients of the 21 mixture designs from Berke's empirical method. Diffusion coefficients from Nernst-Einstein equation are compared with other theoretical approaches and with Berke's empirical equation for the 21 mixture designs in Fig. 4.1 and the details are discussed in the results section.

4.9 Arrhenius Correction Factor

The diffusion coefficients obtained from the theoretical and empirical approaches using both resistivity and CIPT data presented in the previous sections are based on the temperature of the solution for the 6 hour CIPT experiment for each particular mixture. It has been observed that even a 10°C (18°F) increase of solution temperature results in approximately doubling the value of diffusion coefficients (10). Thus, diffusion coefficients determined on different temperature ranges must be converted to room

temperature (21°C) (70°F) to get a uniform distribution of diffusion coefficients for all the cementitious mixtures. An Arrhenius type factor can be implemented to obtain diffusion coefficients at room temperature for all the mixtures designs as expressed in Equation 4.20.

$$D_2 = D_1(\frac{294}{T})\exp[\frac{U}{R}(\frac{1}{273+T} - \frac{1}{294}) \quad (4.20)$$

In Equation 4.20, T is temperature of the solution after 6 hour CIPT in Kelvin (Fahrenheit), U/R is the activation energy divided by the universal gas constant and it has been estimated to vary between 3850°K (6470°F) and 6000°K (10340 °F) for concrete with water to cementitious materials ratio of 0.6 to 0.4 respectively. Fig. 4.4 shows the effect of the Arrhenius correction factor on diffusion coefficients predicted from the Nernst-Einstein equation.

4.10 Results and Discussion

Table 4.1 shows the unadjusted and adjusted (due to the joule effect) charge passed in the CIPT and the geometrically adjusted resistivity for all 21 cementitious mixtures. It is evident from Table 4.1 that in the case of ternary cementitious mixtures adjustment of charge passed for the joule effect in 6- hour CIPT are significantly smaller compared to control mixtures except for the 85TIP/15F mixture. This small rise is due to the small gradual rise of temperature through ternary cementitious mixtures in 6 hours of CIPT compared to the control mixtures. Table 4.1 also shows high values of electrical resistivity (adjusted for geometric shape factor) for all the ternary cementitious mixtures (more than 12 kOhm-cm) as compared to control mixtures except the mixture 85TIP/15F.

It is apparent from Table 4.2, most of the ternary based cementitious mixtures have lower values of velocity of chloride front (less than $4.0x10^{-8}$ m/sec) except three mixtures namely 85TIP/15F, 65TISM/35G120S and 77TI/20F/3SF. This is due to their high chloride transference number. Table 4.3 shows complete distribution of diffusion coefficients for all 21 cementitious mixtures from all the theoretical and empirical approaches. It is evident from Table 4.3 that the plug flow model for diffusion coefficients of chloride ions only computes significant lower values of diffusion coefficients, whereas, Berke's empirical method remarkable high values of diffusion coefficients are obtained compared to other two methods. Nernst-Einstein equation and Nernst-Einstein law computes diffusion coefficients within similar range. These theoretical and empirical methods are proportional with the Nernst-Einstein method in Fig. 4.1, but they do not provide the same values. In general, all methods compute very low diffusion coefficients for the ternary cementitious mixtures compared to OPC and other control mixtures.

Fig. 4.2 provides an indication of relationship between the adjusted charge passed during 6-hour CIPT and the diffusion coefficients for all the theoretical and empirical methods. It has been observed that as the charge increases, diffusion coefficients increase which are applicable to the OPC and control mixtures. The beneficial effect related to the decrease in charge and the decrease in diffusion coefficients is applicable to all the ternary cementitious mixtures.

Fig. 4.3 shows the comparison of diffusion coefficients versus experimental resistivity for all the cementitious mixtures. It is observed from Fig. 4.3 that diffusion coefficients decrease exponentially as the resistivity increases and vice versa for all the

theoretical and empirical approaches. Plug flow model provides lowest values as it represents an ideal system involving the chloride ions only and excluding the effect of other ions which are also present in the system.

The Arrhenius correction factor shows the temperature effect on the diffusion coefficients of cementitious mixtures, as shown in Fig. 4.4. Permeable cementitious mixtures have the greatest reduction in diffusion coefficients due to conversion of temperature from 6 hour CIPT to 21°C (70°F).

4.11 Summary and Conclusion

The work presented in this paper demonstrates the necessity of the temperature adjustment due to the joule effect and adjustment due to geometric shape difference in computation of diffusion coefficients using the electrical resistivity and the CIPT data. As a result, these adjustments achieved a more accurate and reliable prediction of diffusion coefficients in hardened concrete from different theoretical approaches based on fundamentals of electrochemistry. Significant reduced values of diffusion coefficients for chloride ions only obtained from plug flow model clarified that there is some predominant effect of other ions such as Na^+, K^+, and OH^- in the CIPT and other extended migration test. Ternary cementitious mixtures have large effect for reduction of diffusion coefficients and increase of resistivity to reduce the chloride ingress. The key reason is the high pozzolanic reactivity of supplementary cementitious materials by densifying or refining the concrete pore structure.

The Arrhenius correction factor is also necessary to obtain the diffusion coefficients from different temperature ranges to a standardize test temperature of 21°C (70°F). Overall, the findings of these diffusion coefficients with less effort and expense

for different cementitious mixtures can provide effective decision support in the design of new durable structures in harsh chloride environments.

4.12 Acknowledgements

The authors wish to express their gratitude and sincere appreciation to the Federal Highway Administration Pooled Fund Study TPF-5(117) for support of this research work.

4.13 Notation

C_0 = Chloride ion concentration

I = Electrical current

I = Interaction parameter

Z =Valency of chloride ion

J = Flux of ionic species

J_{cl} = Flux for chloride ion

F = Faraday constant

A = Cross-sectional area

D = Diffusion coefficient

D_{cl} = Diffusion coefficient for chloride ions only

D_{eff} = Effective diffusion coefficient

R = Universal gas constant

T = Absolute temperature in Kelvin

V = Volume of the solution used in CIPT

V_{cl} = Velocity of chloride front

L = Thickness of the concrete specimen

i = Current density

t_i = Transport or Transference number of chloride ion

i_{cl} = Current density carried by chloride ions

n_{cl} = Mole number of chlorides

U = Activation energy

x = Depth

γ = Activity coefficient

ρ_{es} = Resistivity of concrete saturated water

k_{cl} = Factor depending on external ionic concentrations

r_{cl} = Binding factor

m = Molality

A = Empirical constant equal to 0.5094 at room temperature

4.14 References

1. Ahmad, S., Al-Kutti, W.A., Al-Amoudi, B.S.O., and Maslehuddin, M., "Correlations Between Depth of Water Penetration, Chloride Permeability, and Coefficient of Chloride Diffusion in Plain, silica fume, and fly ash Cement Concretes", *Journal of Testing and Evaluation,* V.36, No.2, 2009, pp.1-4.

2. Tikalsky, P.J., Pustka, D., and Marek, P., "Statistical Variations in Chloride Diffusion in Concrete Bridges", *ACI Structural Journal,* V.102, No.3, May 2005, pp.481-486.

3. Azad, A.K., Sharif, A.M., Navaz, M., and Loughlin, K.F., "Chloride Diffusion Coefficient of Concrete in the Arabian Gulf Environment", *Arabian Journal of Science and Engineering,* Dhahran, Saudi Arabia, V.22, No.2B, 1997, pp.169-182.

4. Sengul, O., and Gjorv, O.E., "Electrical Resistivity Measurements for Quality Control During Concrete Construction" *ACI Materials. Journal,* V.105, No.6, 2008, pp.541-547.

5. Whiting, D., "Rapid Measurements of Chloride Permeability of Concrete", *Public Roads,* V.45, No.3, 1981, pp.101-112.

6. Betancourt, J.G.A., and Hooton, R.D., "Study of the Joule Effect on Rapid Chloride Permeability Values and Evaluation of Related Electrical Properties of Concrete", *Cement and Concrete Research*, V.34, No.6, June 2004, pp. 1007-1015.

7. Andrade, C., Rio, O., Castellote, M., and Andrea, R.D., "A NDT Performance Method Based on Electrical Resistivity for The Specification of Concrete Durability", *ECOOMAS Thematic Conference on Computational methods in Tunneling,* Vienna, Austria, August 27-29, 2007, pp.1-9.

8. Riding, A.K., Poole, L.J., Schindler, K.A., Juenger, G.C.M., and Folliard, J.A., "Simplified Concrete Resistivity and Rapid Chloride Permeability Test Method", *ACI Materials Journal,* V.105, No.4, July-August 2008, pp.390-394.

9. Berke, N.S., and Hicks, M.C., "The Life Cycle of Reinforced Concrete Decks and Marine Piles Using Laboratory Diffusion and Corrosion Data", *In corrosion forms and control of infrastructure*, V.Chaker. ASTM STP 1137, *American Society for Testing and Materials,* Philadelphia, 1992, pp.207-31.

10. Berke, N., and Hicks, M., "Predicting Chloride Profiles in Concrete, Proceedings, Corrosion 93, *National Association of Corrosion Engineers Annual Conference,* Houston, 1993, pp.341/1-341/15.

11. Orlova, V.N., Westall, C.J., Rehani, M., and Koretsky, D.M., "The Study of Chloride Ion Migration in Concrete under Cathodic Protection" Final Report-SPR357 Prepared for Oregon Department of Transportation, September, 1999, pp.1-83.

12. Andrade, C., "Calculation of Chloride Diffusion Coefficients in Concrete from Ionic Migration Measurements", *Cement and Concrete Research*, V.23, No.3, 1993, pp.724-742.

13. Bockris, J.O'M., and Reddy, A.K.N., "Modern Electrochemistry", Plenum Press, V.1, 1998.

14. Morris, W., Moreno, E.I. and Sagües, A.A., "Practical Evaluation of Resistivity of Concrete in Test Cylinders Using a Wenner Array Probe", *Cement and Concrete Research*, V.26, No. 12, 1996, pp.1779-1787.

15. Atkins, P.W., "Physical Chemistry", Oxford University Press, Oxford, UK, 1990.

16. Lu, X., "Application of the Nernst-Einstein Equation to Concrete", *Cement and Concrete Research*, V.27, No.2, February1997, pp.293-302.

17. Zemaitis J.F, Clark, D.M., Rafal M., Scrivner, N.C., "Handbook of Aqueous Electrolyte Thermodynamics", *Design institute for physical property data*, New York, 1986.

18. Butler J.N., "Ionic Equilibrium: Solubility and pH Calculations", *John Wiley & Sons*, *New York,* 1998, pp.45.

19. Bard, A.J., and Faulkner, L.R., "Electrochemical Methods. Fundamentals and Applications"- *John Wiley & Sons, Inc. New York,* 1980.

Table 4.1- Charge passed and electrical resistivity for all mixtures

Mix ID	6- hour Charge passed in CIPT (Coulomb)	Adjusted charge passed in CIPT (Coulomb)	Adjusted Electrical resistivity (kOhm-cm)
100TI	4563	3069	6.6
60TI/20F/20F2	4963	3247	5.6
75TISM/25C	4024	2725	6.9
100TIP	3584	2433	7.6
75TI/20F/5SF	1163	1033	13.5
75TI/20F/5M	1621	1373	13.3
60TI/20F2/20G120S	2316	1808	15.7
75TI/20F2/5M	2364	1744	15.8
65TI/30F2/5SF	1168	1010	23.7
67TI/30F2/3SF	1988	1615	13.4
65TIP/35G120S	1845	1546	27.3
75TISM/25F2	3032	2173	12.3
97TISM/3SF	935	848	18.2
77TI/20F/3SF	2549	2010	21.1
62TI/35G120S/3SF	1025	888	23.3
60TI/35G120S/5M	927	814	24.1
75TI/20F2/5SF	1720	1409	24.3
77TI/20F2/3SF	2137	1711	15.7
85TIP/15F	3877	2633	9.6
65TISM/35G120S	2736	2048	14.5
50TI/35G120S/15F	1125	980	17.5

Table 4.2- Velocity of chloride front for all cementitious mixtures

Mix ID	Velocity of chloride front (V_{cl}) (m/sec) x10^{-8}
100TI	5.6
60TI/20F/20F2	5.8
75TISM/25C	4.9
100TIP	4.1
75TI/20F/5SF	2.4
75TI/20F/5M	3.0
60TI/20F2/20G120S	3.7
75TI/20F2/5M	3.4
65TI/30F2/5SF	2.5
67TI/30F2/3SF	3.5
65TIP/35G120S	4.0
75TISM/25F2	3.9
97TISM/3SF	2.0
77TI/20F/3SF	4.3
62TI/35G120S/3SF	2.1
60TI/35G120S/5M	2.0
75TI/20F2/5SF	3.1
77TI/20F2/3SF	3.9
85TIP/15F	4.9
65TISM/35G120S	4.1
50TI/35G120S/15F	2.1

Table 4.3- Diffusion coefficients from different theoretical and empirical approaches

Mix ID	Diffusion coefficients m^2/sec (ft^2x sec) x 10^{-12}			
	Plug Flow model	Nernst-Einstein Equation	Nernst-Einstein law	Berke's empirical method
100TI	1.2	3.10	4.80	8.09
60TI/20F/20F2	1.4	3.71	5.66	9.83
75TISM/25C	1.10	2.92	4.60	7.75
100TIP	0.94	2.65	4.17	7.05
75TI/20F/5SF	0.7	1.43	2.35	3.94
75TI/20F/5M	0.67	1.83	2.38	5.03
60TI/20F2/20G120S	0.54	1.26	2.02	3.38
75TI/20F2/5M	0.52	1.25	2.01	3.36
65TI/30F2/5SF	0.42	0.81	1.34	2.23
67TI/30F2/3SF	0.66	1.47	2.37	3.96
65TIP/35G120S	0.39	0.70	1.16	1.93
75TISM/25F2	0.66	1.76	2.81	4.72
97TISM/3SF	0.52	1.05	1.74	2.91
77TI/20F/3SF	0.43	0.95	1.50	2.51
62TI/35G120S/3SF	0.41	0.81	1.36	2.27
60TI/35G120S/5M	0.40	0.79	1.32	2.19
75TI/20F2/5SF	0.36	0.79	1.30	2.18
77TI/20F2/3SF	0.39	1.25	2.02	3.38
85TIP/15F	0.81	2.10	3.30	5.56
65TISM/35G120S	0.58	1.36	2.19	3.67
50TI/35G120S/15F	0.56	1.09	1.81	3.03

(Legend used to describe percentage of cementitious materials in mix proportions)
Note: 75TI/20F/5M = 75% Type I cement, 20 % Class F Fly ash, 5% metakaolin
(1 m^2 = 10.76 ft^2)

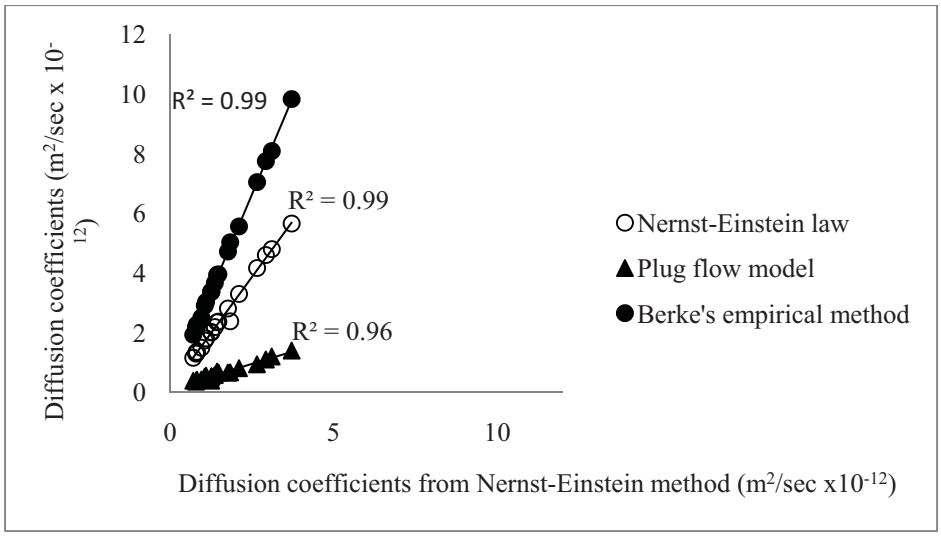

Fig. 4.1- Comparison of diffusion coefficients from different approaches
(1 m^2 = 10.76 ft^2)

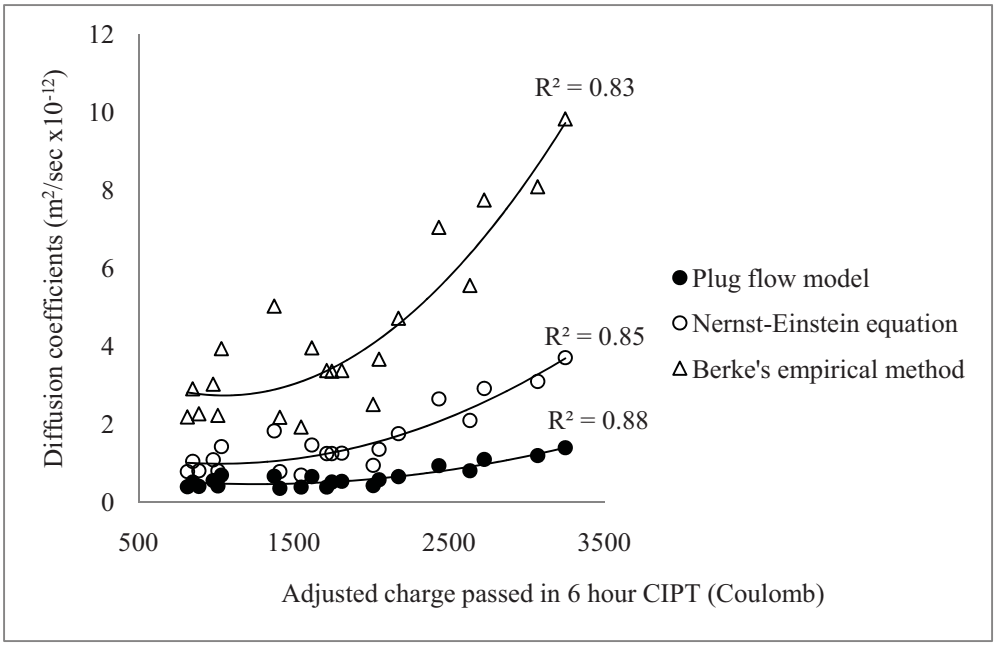

Fig. 4.2 -Diffusion coefficients vs. charge passed for different cementitious materials
(1 m^2 = 10.76 ft^2)

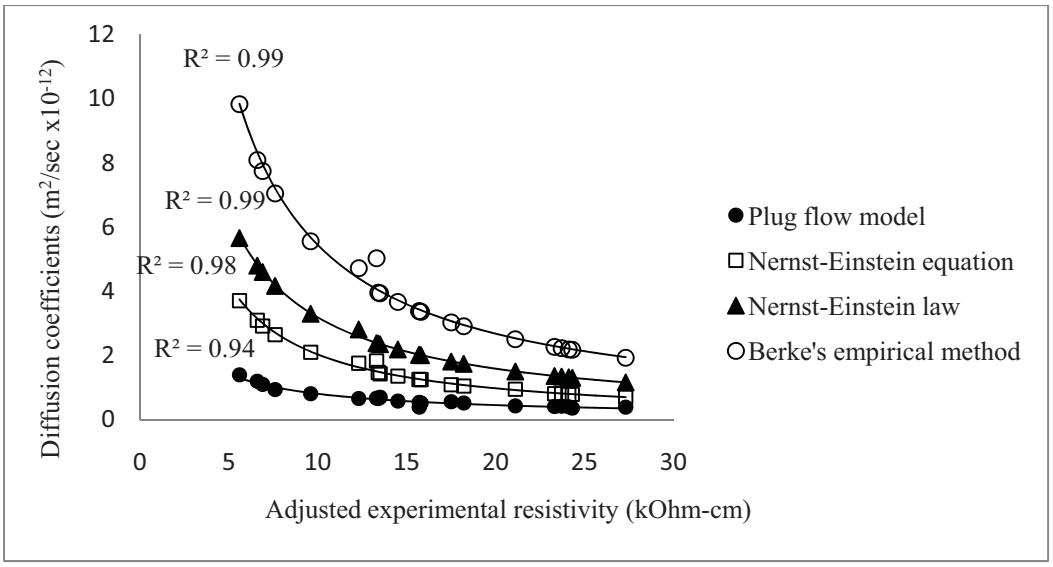

Fig. 4.3- Diffusion coefficients vs. experimental resistivity
(1 m^2 = 10.76 ft^2) (1cm = 0.39 inch)

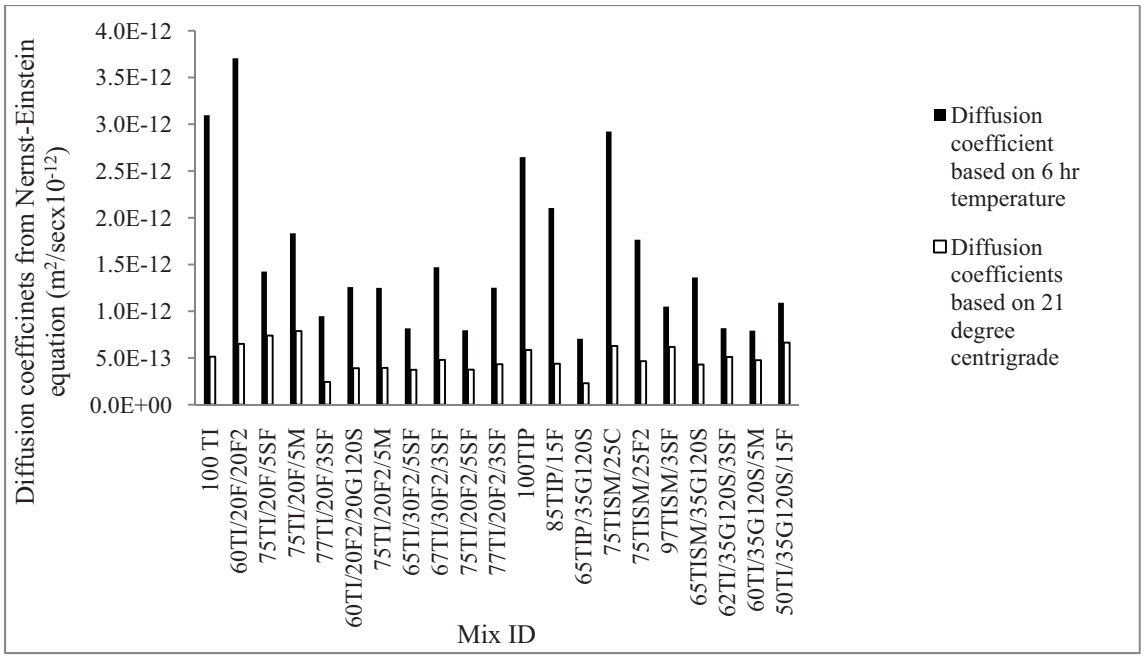

Fig. 4.4 -Effect of temperature on diffusion coefficients (Nernst-Einstein equation)
(1 m^2 = 10.76 ft^2)

CHAPTER 5

CORRELATION OF RESISTIVITY AND CIPT DATA

Pratanu Ghosh, Alex Hammond and Paul J. Tikalsky

Biography: ACI student member **Pratanu Ghosh** is a Research Assistant at the Materials and Structures Research Laboratory at the University of Utah. He received his B.S. from Bengal Engineering College (D.U), India and MASc from the University of Windsor, Canada.

ACI student member **Alex Hammond** is a Research Assistant at the Materials and Structures Research Laboratory at the University of Utah. He received his B.S. from Boise State University and his M.S. from the University of Utah.

ACI Fellow **Paul Tikalsky** is the Chair of the Department of Civil and Environmental Engineering at the University of Utah. He is a member and former Chair of ACI Committee 232 (Fly Ash and Natural Pozzolans), member of ACI Committee 201 (Durability), and Chair of TRB Committee AFN10 (Basic Research and Emerging Concrete Technologies).

(To be submitted in Concrete Research Letter)

5.1 Abstract

Concrete resistance to the penetration of chloride ions from deicing salts is an important performance indicator for mixture design specifications. Chloride Ion

Penetration Test (CIPT) according to ASTM C1202 can be used for approval of concrete mixture designs as an indicator of potential long-term behavior. However, it is time consuming and not conducive to quality control/ quality assurance (QC/QA) testing of field cured concrete. The Wenner probe device characterizes the electrical resistance of concrete, which has a role both in the initiation and propagation of chloride induced corrosion. This paper demonstrates the connected physics relationship between these two tests and the correlation of the test results with incorporation of essential adjustments due to the joule effect and geometric shape difference. Using different HPC and control mixtures, the electrical resistivity data are well correlated with the CIPT and provides reliable prediction of concrete resistance to chloride ingress with less effort and expense.

Keywords: chloride ingress, joule effect, corrosion, resistivity, CIPT

5.2 Introduction

Chloride based deicing salts are commonly used on bridges and pavements during winter conditions to improve driving and safety. These salts migrate down to the reinforcing steel through small pores in the concrete, driven by the diffusion process. Over time, the chlorides in these salts react with the reinforcing steel, breaking down the passivating layer on the steel and causing the steel reinforcement to oxidize and subsequently corrode. The corroding steel eventually delaminates the concrete, resulting in the need to replace bridge decks, substructures, and pavements. Performance-based or high performance concrete specifications need measures that predict concretes which resist the intrusion of chloride ions. Chloride Ion Penetration Test (CIPT) (1-2) is one of the testing procedures that has been used to predict concrete resistance to chloride ion penetration for the last two decades. This test is designed to verify mixture designs in a

laboratory, but not for in situ quality control measures. Further, this test provides a relative measure of the resistance of concrete to the ingress of chloride ions, but not a measure of a fundamental material property of concrete.

A different approach of evaluating the resistance of concrete to transport chloride ions can make use of basic physics and material properties. A Wenner probe device measures the electrical resistivity of concrete using a fixed electrical current and voltage measurement. It has been used extensively for investigation of chloride ingress. This class of device reduces the time spent on sample preparation and testing as compared to the CIPT. It also provides for a scientific measurement of properties that include the effects of material quality, mixing, transportation, placement and curing found in situ, rather than laboratory preparation conditions.

5.3 Research Significance

It is necessary to obtain correlation between the electrical resistivity and the CIPT data in order to use the Wenner probe device for evaluation of a performance measure of mixture designs and in situ properties of constructed facilities by Highway Agencies. This research presented herein addresses reliable correlation between the two tests to determine durability of concrete structures in completed constructions in a more efficient manner. As a result, the Wenner probe device can be used for in situ measurement of electrical resistivity of bridge deck.

5.4 Background

Chloride ion ingress is one of the major problems that affect the durability of concrete structures such as bridge decks, concrete pavements and other structures

exposed to chloride salts during winter. Typically chloride resistance of concrete is determined by Chloride Ion Penetration Test (CIPT) according to ASTM C1202 specification. The total charge passed in coulomb in 6 hour of CIPT is considered a relative measure of the resistance to chloride ingress of the concrete. Feldman et al. (3) conducted research to investigate usefulness of the CIPT as a method of testing chloride ion penetration. It was determined that the physical characteristics of the concrete specimens in the CIPT were changed by the high impressed voltage and vacuum saturation procedure of the test. Therefore, the results obtained from this test potentially lead to incorrect measurements. One major limitation of the CIPT is the high current flow through permeable concrete mixtures results in a "joule effect." The increase in temperature effectively decreases the electrical resistance and encourages the current to flow more rapidly and produce more heat which further accelerates the current flow (4).

The other existing method of determination of concrete resistance to the chloride ion penetration is the electrical resistivity by Wenner probe device. It was originally designed to determine soil resistivity in soil strata, but has been adapted for concrete (5). Research has been conducted to investigate the effects of probe spacing and other factors on resistivity readings (6-9). The Florida Department of Transportation has developed a method to standardize procedures for collection of resistivity readings (10).

Experimentation using the Wenner device on 529 sample sets was conducted by Kessler et al. at the Florida Department of Transportation (11) to investigate whether resistivity can be used as a quality control measure in place of the CIPT. Their findings indicate that there is a good correlation between the CIPT and resistivity with the application of geometric correction factor. Torri et al. (12) found a good correlation

between the charge passed in the CIPT, initial direct current and the electrical resistivity. It was observed that charge passed was one of the most effective indicators for the evaluation of chloride permeability for different set of cementitious mixtures. Marriaga et al. (13) studied the reliability of the CIPT and resistivity test on the basis of chloride resistance of Ground Granulated Blast Furnace Slag (GGBFS) mixtures with different levels of replacements. They established that electrical resistivity and the total charge passed is an indirect measure of the chloride penetration suitable for both OPC and GGBS mixtures. Riding et al. (14) developed a simplified method which is similar to CIPT procedure except for the specimen and gasket size to determine concrete resistivity as an index of concrete permeability. To eliminate the gradual temperature rise problem only one current reading was taken (after 5 minutes) that could be applied to measure the concrete resistivity. An empirical correlation between the new method and the standard CIPT method established the validity and promise of the new simplified method. The disadvantage of this method is its application and suitability on core field samples as it has not yet been determined (14).

Most of the existing studies for finding the correlation between the CIPT and electrical resistivity data are not based on fundamentals of physics relationship and lack HPC mixtures data. The purpose of this research was to find scientific correlation between the CIPT results and the results obtained from a Wenner probe resistivity device by Ohms law for several ternary, binary and control cementitious mixtures. It has been observed that there is a good correlation in the testing results based on the essential adjustments due to the joule effect and geometric shape difference.

5.5 Experimental Investigation

Different types of ternary, binary cementitious mixtures along with control mixtures with a water/cementitious materials ratio of 0.44, typical of exposed bridge deck concrete, were designed to give a wide range of values for this experimental program. All mixtures contained 256 kg (564 lb) of the cementitious material with a Coarse Aggregate Factor (CAF) of 0.67. Limestone coarse aggregate of size 19 mm (3/4 inch) meeting ASTM C33 No.67 gradation and ASTM C33 silica sand were used. Tests were performed on mixtures using:

- ASTM Type I cement (TI)
- Portland-pozzolan blended cement(TIP (20))
- Slag blended portland cement (TISM[TIS (25)])
- Limestone blended cement (E)

Mineral additives used:

- Ground granulated blast furnace slag (G120S)
- Fly ash (Types C, F and F2)
- Silica fume(SF)
- Metakaolin(M)

Table 5.1 shows the concrete mixture compositions. Medium range water reducing admixture and air entraining agent were also used to meet required slump flow and other durability performance specifications. Chloride ion penetration test (CIPT) was performed with different ternary, binary cementitious mixtures including the control mixtures. For each mixture, two 100 mm x 200 mm (4 inch x 8 inch) cylinders were cast and wet cured for 14 days and then they were air cured in lab conditions until the 98th day

for testing. Ninety-eight days (i.e., 14 weeks) was selected as sufficient time for pozzolanic reaction to develop. Experimentation with a Wenner Probe device was conducted for 26 different concrete mixtures to determine concrete cylinder resistivity on 98 days and this data were utilized to obtain correlation with the CIPT data. Concrete cylinders of 100 mm x 200 mm (4 inch x 8 inch) were cast and placed in a wet curing room in accordance with ASTM C192. They were wet cured for 98 days for electrical resistivity measurements to comply with continuous Saturated Surface Dry (SSD) condition. A minimum of two specimens were tested for each of the concrete mixtures for the CIPT and electrical resistivity data measurement. The average value of the specimen readings was reported to minimize the variation.

5.6 Analytical Development

It is necessary to determine the resistivity from the CIPT data in order to compare with the results obtained using the Wenner probe device. Both of these testing methods are related by Ohms law, shown in Equation 1, which relates voltage (V), current (I), and resistance (R) in an electrical circuit.

$$I = \frac{V}{R} \tag{5.1}$$

The CIPT can be modeled as an electrical circuit consisting of a power source, steady voltage drop, and a resistor. The basic equation for electrical resistivity (ρ) of this resistor is expressed in Equation 5.2,

$$\rho = R * \frac{A}{l} \tag{5.2}$$

where R is the resistance of the resistor, A is the cross sectional area and l is the thickness of the specimen.

The CIPT has a constant voltage drop (60 Vdc) across the resistor with a measured current value in a 6- hour time interval. As the dimensions of the specimen are also known, resistivity can be directly computed. The resistivity (ρ) of the specimen used in the CIPT can be determined by substituting the value of resistance (R) from Equation 5.1 into Equation 5.2 and it is expressed in Equation 5.3.

$$\rho = \frac{V \times A}{I \times l} \tag{5.3}$$

5.6.1 Joule effect and theoretical resistivity

The application of the 60 Vdc in CIPT induces an increase in temperature of the electrode solution throughout the 6- hour test period. This accelerates the current flow (I) through permeable concrete mixtures during the test period resulting in a high value of charge passed. Betancourt et al. (4) developed a temperature adjustment to reduce or eliminate this "joule effect" and improve the prediction of charge passed during a 6- hour time period. The adjusted charge during the 6- hour test can be expressed in Equation 5.4.

$$Q_0 = e^{[\ln(Q_{c\,6\,hr}) + \beta(1/\delta T - 1/273)]} \tag{5.4}$$

In Equation 5.4, Q_0 is the adjusted charge passed through 6 hours CIPT and β is an experimental constant equal to 1245, Q_{c6hr} is the original charge passed through the 6-hour CIPT test, and δT is the difference in temperature increment in Kelvin during the 6 hour test *(4)*. Table 5.1 depicts the 6- hour unadjusted charge and adjusted charge for 26

different cementitious mixtures. The adjusted average current is obtained by dividing the joule effect adjusted charge passed (Q_0) by time in seconds and it is expressed in Equation 5.5.

$$I_{adj} = (\frac{Q_0}{t}) \tag{5.5}$$

This adjusted average electrical current is then substituted in Equation 5.3 to obtain theoretical resistivity as shown in Equation 5.6 for all the cementitious mixtures.

$$\rho_{the} = \frac{VA}{I_{adj}l} \tag{5.6}$$

5.6.2 Geometric correction factor and experimental resistivity

The Wenner probe device measures the electrical resistivity of concrete and this technique uses a series of four probes connected to a power source. The spacing of the probes is constant (a=5.1 cm [2 inches]). This spacing dimension is always used in the lab to maintain uniformity of electrical resistivity measurement. A known current is passed between the two outer probes and the resulting voltage drop across the two inner probes is measured. A diagram of this arrangement is shown in Fig. 5.2. The theoretical concept for determining the resistivity using the Wenner probe device is shown in Equation 5.7,

$$\rho_{measured} = 2 * \pi * a * \frac{V}{I} \tag{5.7}$$

where "*a"* is the distance between probes.

Current is not one- dimensional; it is a three- dimensional field. When resistivity is measured on a rounded cylinder using the Wenner probe device, the current is restrained within the concrete. Further, interference is caused by the concrete and air interface. Resistivity readings from a semi-infinite flat slab represent the standard for resistivity of the material, whereas the resistivity from the curved cylinder has interference from the edge of the cylinder. In order to account for this interference, the data needed to be converted into an equivalent semi-infinite slab resistivity where there are no curvature effects. Morris et al. (15) developed this adjustment factor (K) to convert the experimental lab resistivity data performed on a concrete cylinder to eliminate the geometrical shape difference between a wide thick slab and concrete cylinder. The experimental resistivity values obtained by using the Wenner Probe device need to be divided by the proper correction factor, which was equal to K = 2.7 for 50 mm (2 inch) probe spacing and 100 mm x 200 mm (4 inch x 8 inch) cylinder. Experimental resistivity data need to be involved with this correction factor for understanding real life bridge deck slab data. The Florida Department of Transportation (10) also used this adjustment as expressed in Equation 8 to develop the limits for the FDOT resistivity testing method (15).

$$\rho_{real} = \frac{\rho_{measured}}{K} \tag{5.8}$$

Using Equation 5.8, the theoretical electrical resistivity data from the CIPT method can be compared to real experimental data obtained using the Wenner probe device for all 26 different cementitious mixtures. This geometric adjustment factor was verified in the lab to make sure it worked with the lab specimens.

5.6.3 Comparison of charge

As the Wenner probe testing technique also follows Ohm's law, current through the resistor can be computed by rearranging Equation 5.3 and it is expressed in Equation 5.9.

$$I = \frac{VA}{\rho l} \tag{5.9}$$

The converted coulomb value was determined by multiplying the current value (I) by the CIPT duration (6 hours = 21,600 seconds) and is shown in Equation 5.10. The resulting value is the theoretical coulomb calculated from the Wenner probe resistivity device readings.

$$Q_{the} = I * t \tag{5.10}$$

This theoretical coulomb value is compared with the coulomb value obtained from the CIPT for all cementitious mixtures. The results for both testing procedures can be analytically combined as an evaluation tool for concrete with the application of both geometric correction factor and the adjustment due to the joule effect.

5.6.4 Comparison with empirical method

As the CIPT and electrical resistivity are two important parameters in durability modeling of concrete, there is always research interest to correlate the data between them. Berke et al. (16) developed an empirical equation to obtain correlation between CIPT and experimental resistivity data as this test is frequently used in quality control and concrete specifications for construction projects. Equation 5.11 was used to derive correlations

between the two tests. In the study presented herein, adjustments due to the joule effect and geometric correction factor are included in the derived correlation equation for all 26 different cementitious mixtures.

$$\rho_{emp} = 4887x(Q_0)^{-0.832} \tag{5.11}$$

Correlation of both testing methods is presented in Fig. 5.1 through Fig. 5.9 for both adjusted and unadjusted resistivity. Data for both testing methods along with empirical methods are presented in Table 5.1 and Table 5.2.

5.7 Results

In order to verify a relationship using Ohms law, three different ways of analyzing the data needed to be investigated. The first type of analysis done was to calculate equivalent coulomb values from resistivity data and compare it to the CIPT coulomb data. The second method was to compute equivalent resistivity from the CIPT data to compare with the Wenner probe resistivity data. The third type of analysis done was to compare the CIPT coulomb data and Wenner probe resistivity data.

To develop a relationship between the CIPT and resistivity, data were collected and shown in Fig. 5.1 through Fig. 5.7. Each data point represents average values of resistivity with an average of 2 specimens (8 readings per cylinder specimen) for each mixture, and at least 2 specimens for the CIPT. There is a strong need for using the joule effect adjustment and geometric correction factor to relate these two testing methods through Ohms law. This necessity for these adjustments has been clearly observed by comparing coulomb values from the CIPT with calculated coulomb from resistivity as shown in Fig. 5.1 through Fig. 5.3 and in Table 5.1. The closer the line is to a 1:1

relationship, the better the relationship is between these two methods using Ohms law. Fig. 5.1 shows the adjusted (including joule effect and geometric correction factor) and raw (no adjustment) coulomb relationship. The correlation is close to the 1:1 relationship with the adjustments. To understand how each of these adjustments affects the data, they are plotted separately in Fig. 5.2 and Fig. 5.3, keeping the joule effect adjustment or geometric correction unchanged for each plot. The trend in Fig. 5.2 is due to the excessive heating of the specimens caused by the large current flow through the permeable and control mixtures. Both adjustments are incorporated to account for most of the differences in the coulomb relationship through Ohms law for these two testing methods.

A similar trend is observed in the coulomb value comparisons for calculated resistivity in Fig. 5.4 through Fig. 5.6 and Table 5.2. Similar to the coulomb comparisons, either the joule effect adjusted values or the geometric corrected values are kept the same for each plot to investigate the effect of the adjustment. With the adjustments, it is evident that the relationship is much closer to a 1:1 relationship than without these adjustments. Two sets of data are presented in Fig. 5.5, one showing the CIPT raw data converted to resistivity and the other showing the joule effect adjusted data in the computation for the CIPT data keeping unchanged geometrically adjusted resistivity. The relationship between the calculated resistivity from the CIPT data and the experimentally determined resistivity is closer to a 1:1 relationship with the implementation of joule effect adjustment. Fig. 5.6 shows the effects of varying the geometric correction factor while keeping the adjusted CIPT data unchanged. It has been observed that there is a change in slope between the joule effects adjusted values and the

raw data values. The prime reason for this change in slope is due to the excessive heating of the test specimens through highly permeable mixtures requiring more adjustment.

In Fig. 5.7, a theoretical line is presented to represent coulomb values based on the CIPT in correlation with electrical resistivity computed from the CIPT along with the raw data for comparisons. There is a relationship between the CIPT and resistivity readings based on the fit of the trend line to the data and the proximity of the trend line to the theoretical line.

It has been observed that the adjusted predictive line in Fig. 5.7 is much closer to the theoretical values obtained from the CIPT with the incorporation of adjustments due to the joule effect and geometric correction factor. There still exists a variance between the theoretical and adjusted values; however, this can be explained by looking at the values of surface resistivity vs. concrete resistivity. Surface resistivity is determined by the Wenner probe device and only determines the resistivity a small distance into the concrete (up to a depth equal to the probe spacing). Concrete conductivity is determined through the CIPT over the entire depth of the specimen. The difference between the theoretical and empirical readings is due to the presence of more paste at the surface of the concrete. The surface of concrete has a different resistivity than the center of the concrete where less paste exists.

These Wenner probe resistivity and CIPT coulomb data were also compared with Berke's empirical method to investigate the correlation of the tests and this comparison has expressed in Fig. 5.8 and 9. It has been observed that resistivity values from Berke's empirical method correlated well with Wenner probe resistivity and the theoretical resistivity from the CIPT data. There are some scattered points in case of Wenner probe

resistivity values, which measure surface resistivity as compared to resistivity over entire depth of specimen in case of CIPT and Berke's empirical method.

5.8 Summary and Conclusions

In order to use chloride ion penetration as part of a durability acceptance criterion, an effective and simpler means of testing concrete test needs to be used. This research demonstrates the good correlation between the CIPT and Wenner probe data to justify the use of Wenner probe device as an expedited method for investigation of chloride ion ingress. The CIPT testing results and results obtained using a Wenner probe can be related through Ohms law for blended and unblended cement concrete mixtures. This correlation of data becomes reliable with the incorporation essential adjustments due to the joule effect and geometric shape factor. This is particularly true for mixtures with higher permeability. Comparison with Berke's empirical method was also necessary to obtain strong relationship between the data of two testing methods. This finding from this analysis also supports the use of the Wenner probe device as a possible quality assurance/quality control (QA/QC) tool in concrete field testing.

5.9 References

1. AASHTO Standard T277, "Standard Method of Test for Electrical Indication of Concrete's Ability to Resist Chloride", American Association of State Highway and Transportation Officials, Washington, D.C., U.S.A, 2005.

2. ASTM Standards vol. 04.01, 04.02, American Society for Testing and Materials, Philadelphia, PA, 2007.

3. Feldman, R.F., Chan, G.W, Brousseau, R.J., and Tumidajski, P.J. "Investigation of the Rapid Chloride Permeability Test" *ACI Materials Journal*, V. 91, No. 2, 1994, pp.246-255.

4. Julio-Betancourt, G.A, and Hooton, R.D., "Study of the Joule Effect on Rapid Chloride Permeability Values and Evaluation of Related Electrical Properties of Concretes", *Cement and Concrete Research*, V. 34, 2004, pp.1007 - 1015.

5. Ewins, A.J., "Resistivity Measurements in Concrete", *British Journal of NDT*, Northampton, UK, V. 32, 1990, pp. 120-126.

6. Gowers, K.R., and Millard, S.G., "Measurement of Concrete Resistivity for Assessment of Corrosion Severity of Steel using Wenner Technique", *ACI Materials Journal*, V. 96, No. 5, 1999, pp.536-541.

7. Sengul, O., and Gjorv, O.E., "Electrical Resistivity Measurements for Quality Control during Concrete Construction", *ACI Materials Journal*, V. 105, No. 6, 2008, pp.541-547.

8. Stanish, K.D., Hooton, R.D., Thomas, M.D.A., "Testing the Chloride Penetration Resistance of Concrete: A Literature Review", FHWA Contract DTFH61-97-R-00022 University of Toronto, Toronto, Ontario, Canada. June 31, 2000.

9. Smith, K., "Evaluating Concrete Bridge Design Factors using Concrete Resistivity" Penn State University Master's Thesis, 2002, pp. 92-113, pp. 151-152.

10. FDOT Standard FM5-578, "Florida Method of Test for Concrete Resistivity as an Electrical Indicator of its Permeability," Florida Department of Transportation, 2004 (FM 5-578).

11. Kessler, R.J., Powers, R.F., and Paredes, M.A., "Resistivity Measurements of Water Saturated Concrete as an Indicator of Permeability", *NACE International Corrosion Conference 2005*, Houston, Texas, Paper 5261, pp. 1 – 10.

12. Torri, K, Sasatani, T., and Kawamura, M., "Application of Rapid Chloride Permeability Test to Evaluate the Chloride Ion Penetration into Concrete", Durability of Concrete, ACI, SP 170-21, 1997, pp.421-435.

13. Marriaga, J.L., Claisse, P., and Ganjian, E., "Application of Traditional Techniques on Chloride Resistance Assessment of GGBS Concrete", *Second International Conference on Sustainable Construction Materials and Technologies*, Università Politecnica delle Marche, Ancona, Italy, June 28 - June 30, 2010, pp.1911-1921.

14. Riding, K.A., Poole, J.L., Schindler, A.K., Juenger, M.C.G., and Folliard, K.J., "Simplified Concrete Resistivity and Rapid Chloride Permeability Test Method", *ACI Materials Journal*, Vol. 105, No.4, 2008, pp. 390-394.

15. Morris, W., Moreno, E.I. and Sagües, A.A., "Practical Evaluation of Resistivity of Concrete in Test Cylinders using a Wenner Array Probe", *Cement and Concrete Research*, Vol. 26, No. 12, 1996, pp. 1779-1787.

16. Berke, N.S., and Hicks, M.C., “The Life Cycle of Reinforced Concrete Decks and Marine Piles Using Laboratory Diffusion and Corrosion Data”, In corrosion forms and control of infrastructure, V.Chaker, ASTM STP 1137, *American Society for Testing and Materials*, Philadelphia, 1992, pp.207-31.

Table 5.1 – Wenner probe resistivity conversions to coulomb

	Wenner probe Method				
Mixture	Measured Resistivity ($\rho_{measured}$)	Geometric K Factor	Geometric Adjusted Resistivity(ρ_{real}) (GAR)	Calculated Coulombs from GAR (Q_{the})	Coulomb from Berke's empirical method (Q_{emp})
	kΩ*cm (kΩ*in)		kΩ*cm (kΩ*in)	Coulombs	Coulomb
75TI/20F/5M	28.7 (11.3)	2.7	10.6 (4.2)	1711	1591
60TI/30F/10F2	8.4 (3.3)	2.7	3.1 (1.2)	5857	6972
60TI/20F2/20G120S	42.4 (16.7)	2.7	15.7 (6.2)	1158	992
75TI/20F2/5M	42.6 (16.8)	2.7	15.8 (6.2)	1152	985
67TI/30F2/3SF	36.3 (14.3)	2.7	13.4 (5.3)	1352	1200
60TI/20F/20F2	14.8 (5.8)	2.7	5.5 (2.2)	3328	3500
100TIP	20.5 (8.1)	2.7	7.6 (3.0)	2394	2373
60TI/30F2/10C	17.0 (6.7)	2.7	6.3 (2.5)	2887	2973
75TISM/25C	18.7 (7.3)	2.7	6.9 (2.7)	2630	2665
75TISM/25F2	30.6 (12.1)	2.7	11.3 (4.5)	1603	1473
97TISM/3SF	49.3 (19.4)	2.7	18.2 (7.2)	997	831
75TI/20F/5SF	36.4 (14.3)	2.7	13.5 (5.3)	1349	1190
100TI	17.9 (7.0)	2.7	6.6 (2.6)	2746	2811
65TI/30F2/5SF	64.0 (25.2)	2.7	23.7 (9.3)	767	605
65TIP/35G120S	73.8 (29.0)	2.7	27.3 (10.8)	666	510
60TI/20F/20G120S	36.3 (14.3)	2.7	13.4 (5.3)	1354	1200
100E	16.7 (6.6)	2.7	6.2 (2.4)	2938	3031
80E/20G120S	29.8 (11.7)	2.7	11.0 (4.3)	1650	1521
95E5SF	46.0 (18.1)	2.7	17.0 (6.7)	1068	902
62TI/35G120S/3SF	62.8 (24.7)	2.7	23.3 (9.2)	782	617
60TI/35G120S/5M	65.1 (25.6)	2.7	24.1 (9.5)	754	593
75TI/20F2/5SF	65.6 (25.8)	2.7	24.3 (9.6)	748	587
77TI/20F2/3SF	42.4 (16.7)	2.7	15.7 (6.2)	1158	992
65TISM/35G120S	39.2 (15.4)	2.7	14.5 (5.7)	1253	1092
50TI/35G120S/15SF	47.2 (18.6)	2.7	17.5 (6.9)	1040	871
85TIP/15F	25.8 (10.2)	2.7	9.6 (3.8)	1902	1792

Note: 75TI/20F/5M = 75% Type I cement, 20% Class F fly ash, 5% metakaolin

Table 5.2 – CIPT conversions to resistivity

Mixture	CIPT data			
	Unadjusted Average CIPT charge (Q)	Joule Effect Adjusted CIPT charge (Q_0)	Calculated Resistivity(ρ_{the}) from the CIPT	Resistivity (ρ_{emp}) from Berke's empirical method
	Coulomb	Coulomb	kΩ*cm (kΩ*in)	kΩ*cm (kΩ*in)
75TI/20F/5M	1621	1369	13.3 (5.2)	12.0 (4.7)
60TI/30F/10F2	6786	3871	4.7 (1.8)	5.1(2.0)
60TI/20F2/20G120S	2316	1804	10.1 (4.0)	9.5 (3.8)
75TI/20F2/5M	2363	1877	9.7 (3.8)	9.2 (3.6)
67TI/30F2/3SF	1987	1611	11.3 (4.4)	10.5(4.1)
60TI/20F/20F2	5490	3431	5.3 (2.1)	5.6 (2.2)
100TIP	4023	2715	6.7 (2.6)	6.8 (2.7)
60TI/30F2/10C	6137	3558	5.1 (2.0)	5.4 (2.1)
75TISM/25C	4023	2725	6.7 (2.6)	6.8 (2.7)
75TISM/25F2	3032	2173	8.4 (3.3)	8.2 (3.2)
97TISM/3SF	935	845	21.5 (8.5)	17.9 (7.1)
75TI/20F/5SF	1163	1032	17.6 (6.9)	15.2 (6.0)
100TI	4562	3068	5.9 (2.3)	6.1 (2.4)
65TI/30F2/5SF	1512	1308	13.9 (5.5)	12.5 (4.9)
65TIP/35G120S	1176	1040	17.5 (6.9)	15.1 (5.9)
60TI/20F/20G120S	2000	1709	10.6 (4.2)	10.0 (3.9)
100E	5890	3649	5.0 (2.0)	5.3 (2.1)
80E/20G120S	1970	1703	10.7 (4.2)	10.0 (3.9)
95E5SF	1656	1415	12.9 (5.1)	11.7 (4.6)
62TI/35G120S/3SF	984	872	20.9 (8.2)	17.5 (6.9)
60TI/35G120S/5M	698	627	29.0 (11.4)	23.0 (9.1)
75TI/20F2/5SF	1230	1071	17.0 (6.7)	14.7 (5.8)
77TI/20F2/3SF	1900	1555	11.7 (4.6)	10.8 (4.3)
65TISM/35G120S	1568	1318	13.8 (5.4)	12.4 (4.9)
50TI/35G120S/15SF	1437	1216	15.0 (5.9)	13.3 (5.2)
85TIP/15F	3634	2555	7.1 (2.8)	7.1(2.8)

Note: 75TI/20F/5M = 75% Type I cement, 20% Class F fly ash, 5% metakaolin

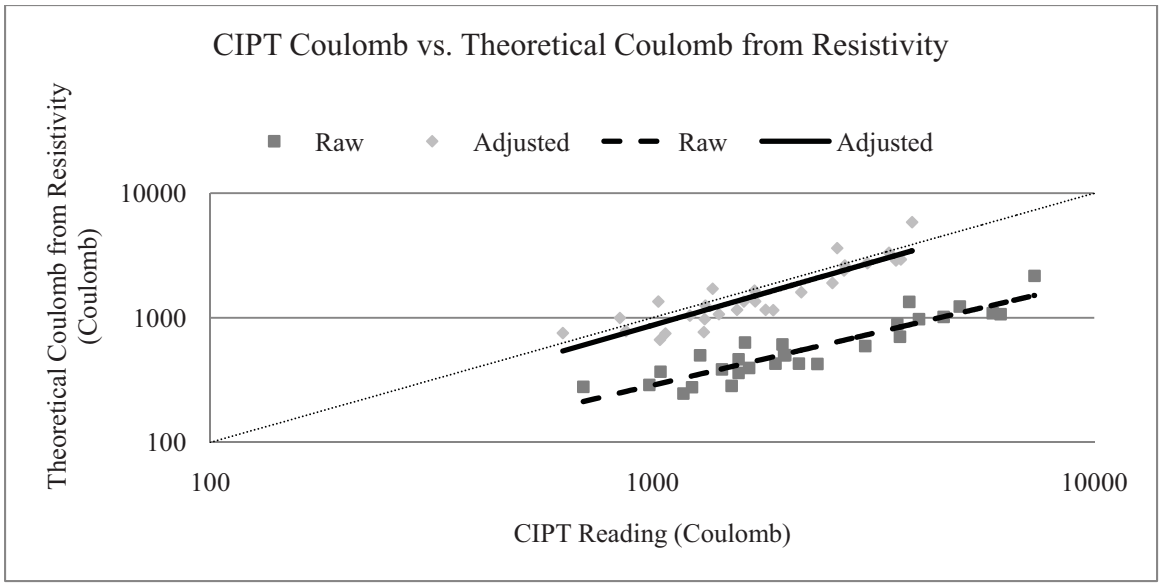

Fig. 5.1 – Raw CIPT coulomb vs. adjusted coulomb from Wenner probe resistivity data (joule effect and geometric shape adjustment)

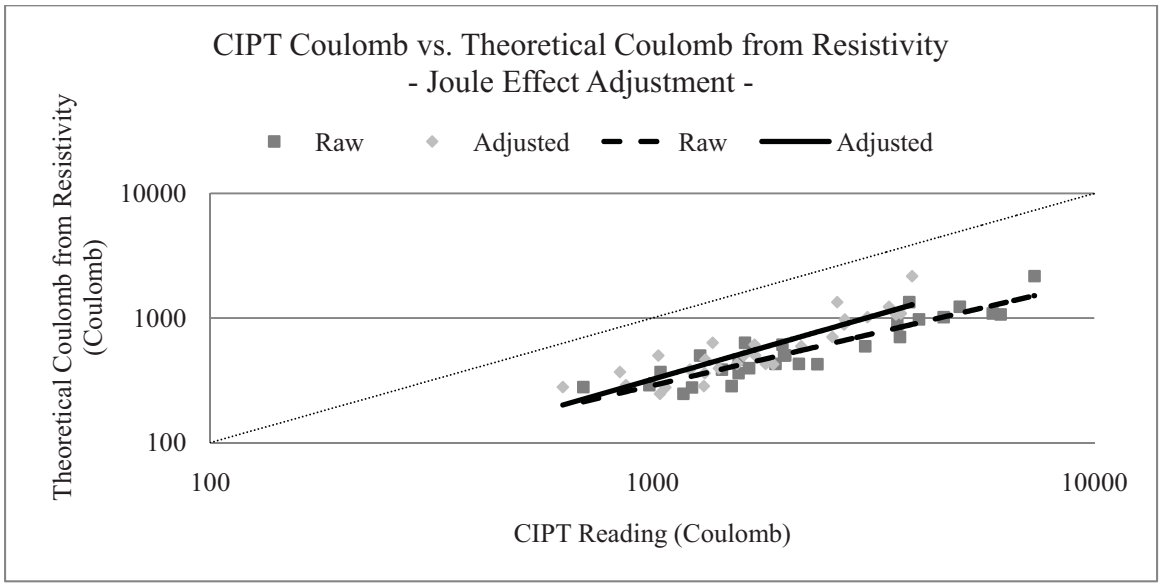

Fig. 5.2 – Raw CIPT coulomb vs. adjusted coulomb from Wenner probe resistivity (only joule effect adjustement)

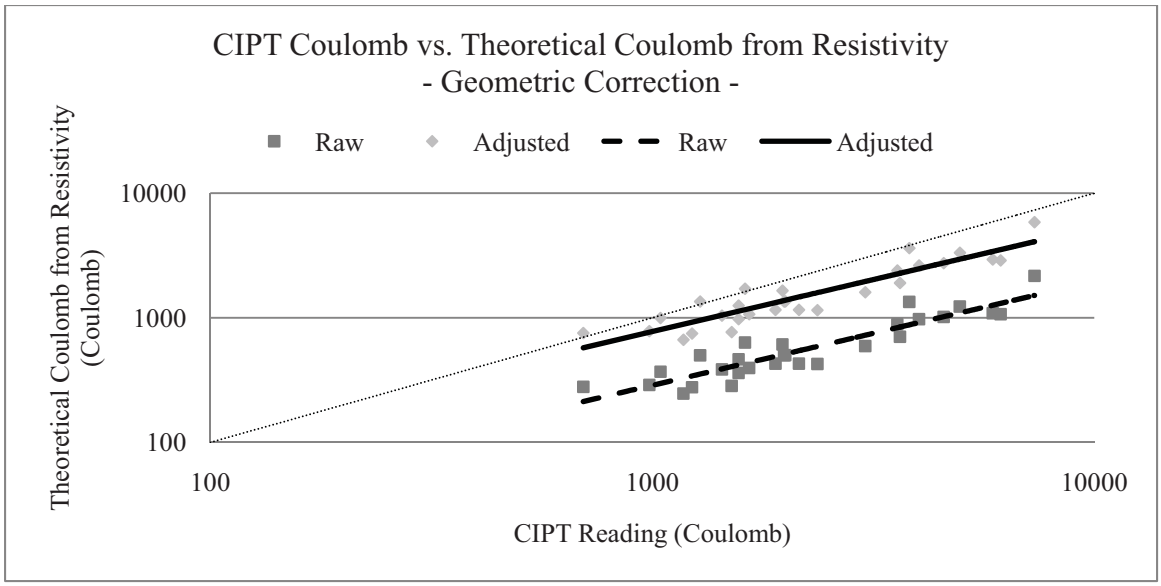

Fig. 5.3 – Raw CIPT coulomb vs. adjusted coulomb from Wenner probe resistivity (only geometric shape adjustment)

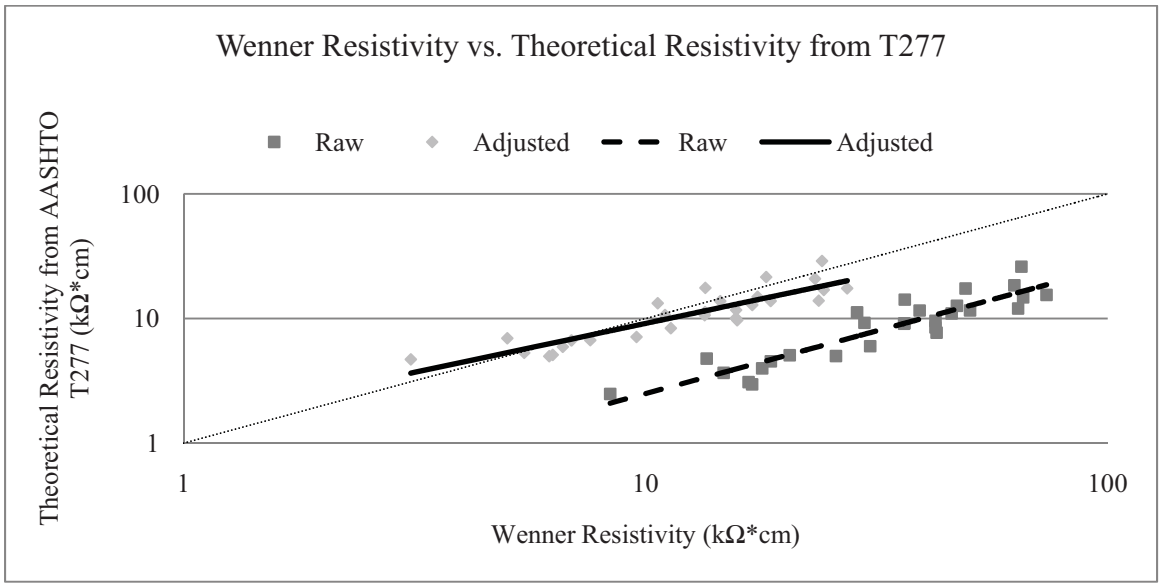

Fig. 5.4 – Raw Wenner probe resistivity vs. adjusted resistivity from CIPT (joule effect and geometric correction)
(1inch = 2.54cm)

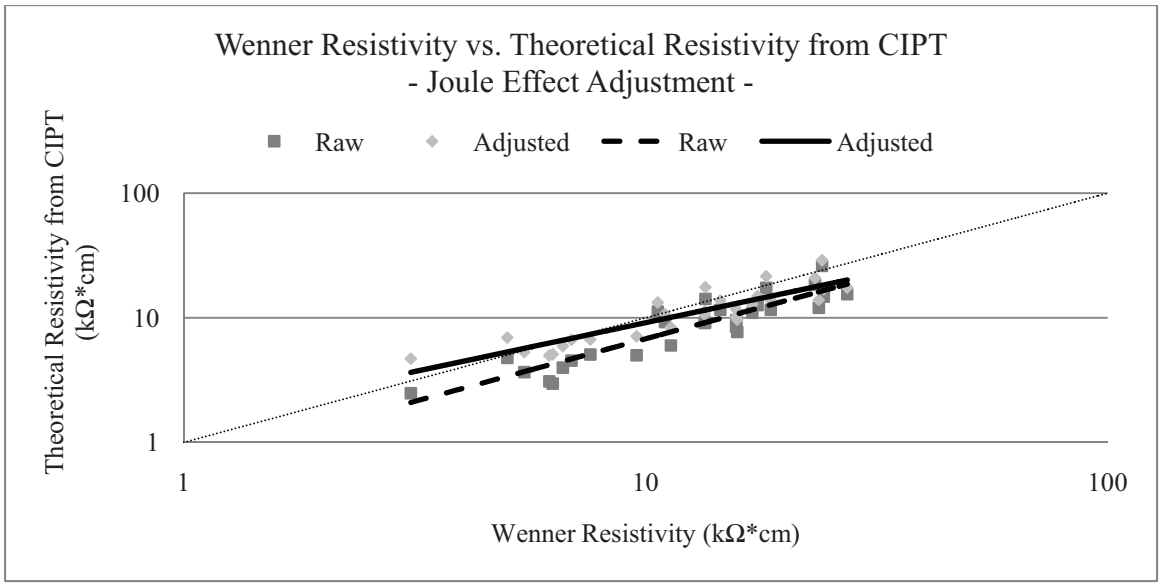

Fig. 5.5 – Wenner probe resistivity vs. Theoretical resistivity from CIPT (Only joule effect adjustment) (1inch = 2.54cm)

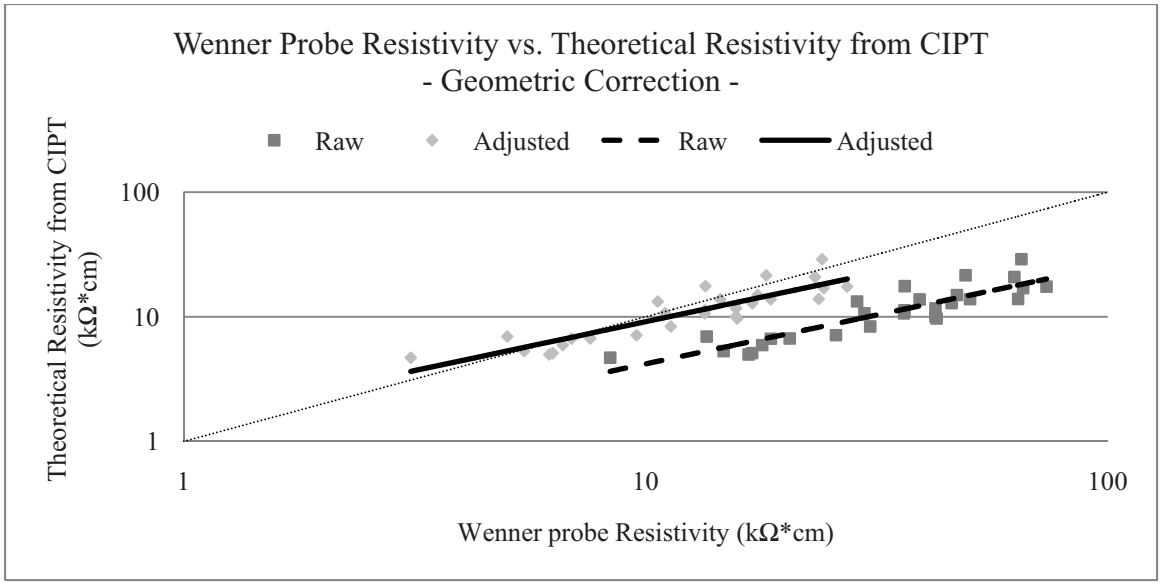

Fig. 5.6 – Raw Wenner probe resistivity and adjusted resistivity from CIPT (Only geometric shape adjustment)
(1inch =2.54 cm)

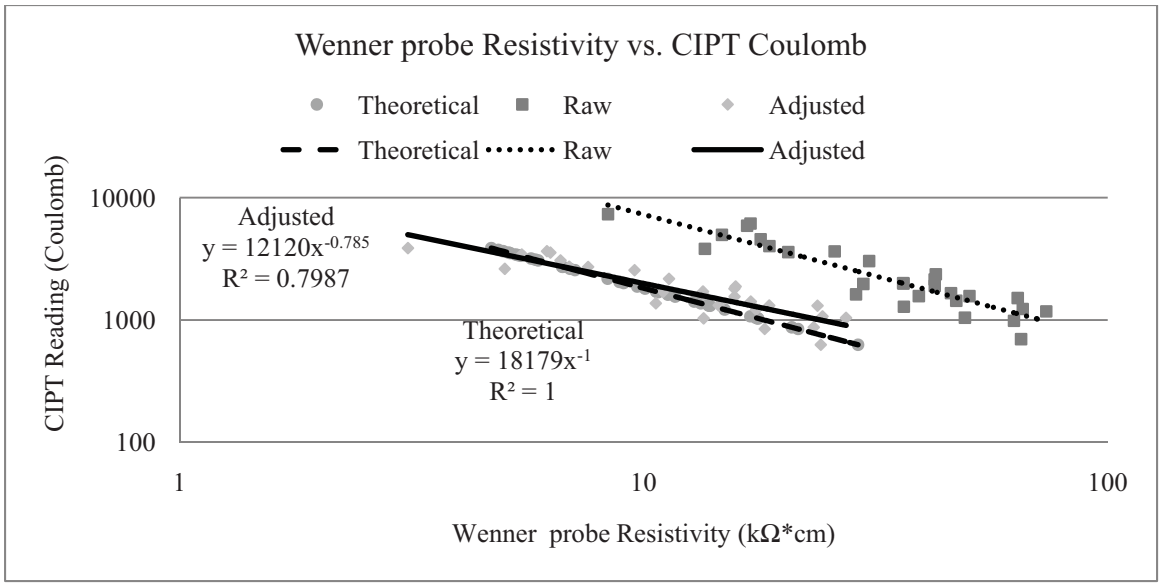

Fig. 5.7 – Wenner probe resistivity vs. CIPT coulomb (1inch = 2.54cm)

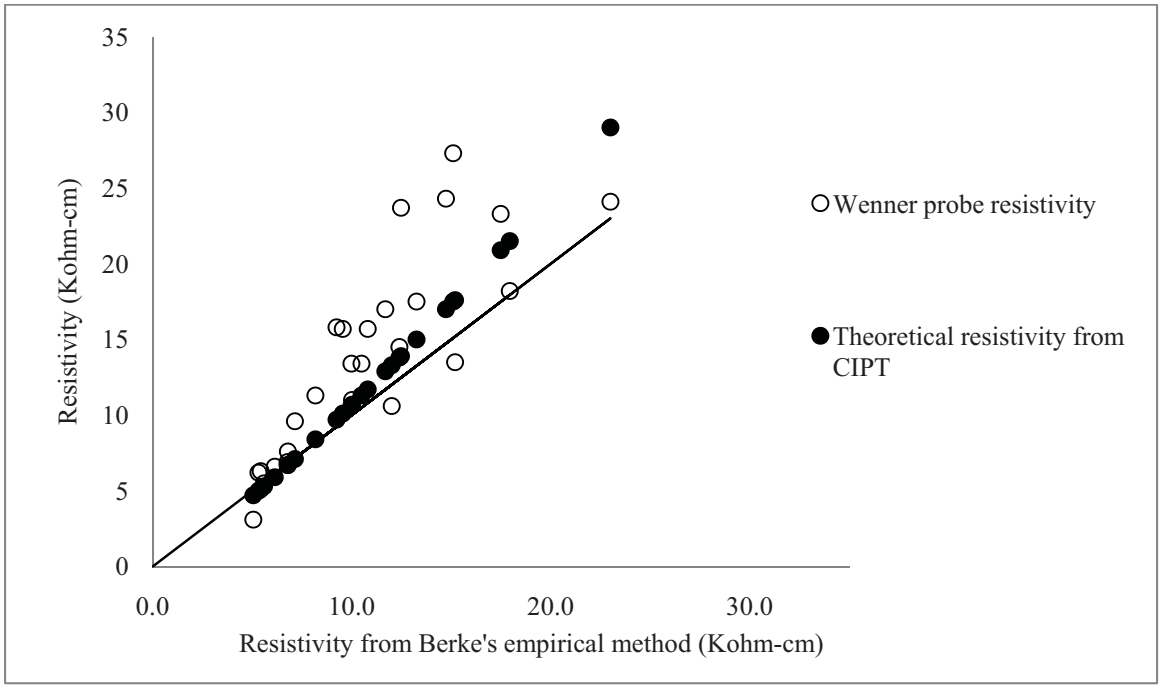

Fig. 5.8- Comparison of resistivity from empirical, experimental and theoretical methods
(1 inch=2.54 cm)

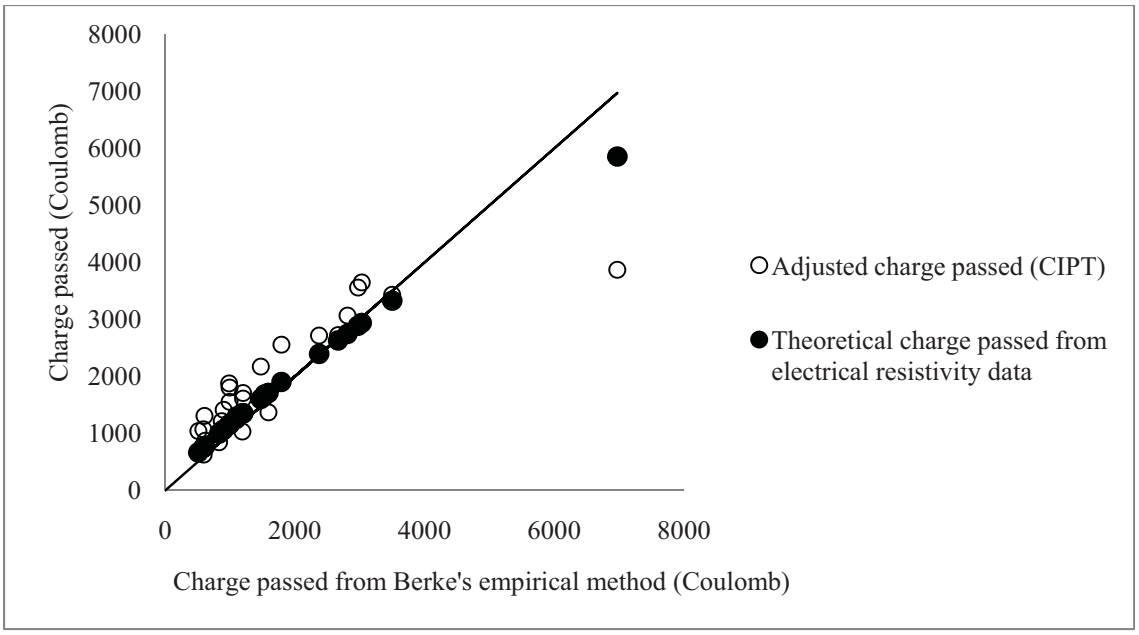

Fig. 5.9- Comparison of charge passed from empirical, CIPT and theoretical methods

(1 inch=2.54 cm)

CHAPTER 6

EFFECT OF HPC SYSTEM ON CONDUCTIVITY AND DIFFUSION

Pratanu Ghosh and Paul J. Tikalsky

Biography: ACI student member **Pratanu Ghosh** is a Research Assistant at the Materials and Structures Research Laboratory at the University of Utah. He received his B.S. from Bengal Engineering College (D.U), India and MASc. from the University of Windsor, Canada.

ACI Fellow **Paul Tikalsky** is the Chair of the Department of Civil and Environmental Engineering at the University of Utah. He is a Fellow of the Engineering Academy of the Czech Republic. He is a member and former Chair of ACI Committee 232 (Fly Ash and Natural Pozzolans), member of ACI Committee 201 (Durability), and Chair of TRB Committee AFN10 (Basic Research and Emerging Concrete Technologies).

(To be submitted in ACI Materials Journal)

6.1 Abstract

Chloride ingress is one of the major contributing factors to the corrosion of reinforced concrete structures exposed to deicing salts. Electrical conductivity and diffusion coefficients are material properties that indicate the resistance to chloride ion transport to concrete. This paper presents an approach to determine the conductivity using measurements from chloride ion penetration test (CIPT) data. Steady state

conditions were verified by comparing the numerical values of conductivity during 5 minute, 10 minute, 30 minute and 360 minute testing period. The Nernst-Einstein relationship was used to determine the diffusion coefficients from the conductivity values for different binary and ternary cementitious systems including the control mixtures. This method of computing the diffusion coefficients includes the necessary adjustments due to the joule effect. Computed diffusion coefficients and conductivity measurements data showed that ternary cementitious materials can be designed to have low diffusion coefficients and high resistance to chloride ion transport compared to ordinary portland cement (OPC) and other permeable control mixtures. The computation of the corrosion initiation time presented herein has shown that these improved diffusion coefficients for ternary cementitious mixtures delay the corrosion initiation of concrete structures exposed to chloride laden environments.

Keywords: Chloride diffusion, ternary, conductivity, corrosion, joule effect, steady-state

6.2 Introduction

One of the major premature deterioration processes in concrete structures is the reinforcement corrosion by chloride ingress. Diffusion is one of the properties that control the rate of chlorides and ions entering into concrete structures. The chloride salt ingression into concrete can take place in several ways, such as flow under a pressure differential, termed as “permeability,” capillary movement into the pores termed as “adsorption” and transport due to the difference in concentration, termed as “diffusion” (1). Among these transport phenomena, diffusion is the most detrimental process related to the chloride ingress in concrete. As a consequence, the chloride diffusion coefficient is a necessary component in predicting the time of corrosion initiation and the rate of

reinforcement corrosion (2). Typically the diffusion coefficients are determined by sampling concrete at different depths and fitting the profiles of acid soluble chloride concentrations versus sample depths using Crank's solution following Fick's second law (3). This was one of the possible methods a decade ago despite being highly variable. The problem of such a method is that a powdered concrete sample at any depth sample may represent a mortar or an aggregate material at a particular location, not the composite behavior of concrete material. The existing method is the chloride ion penetration test (CIPT) following ASTM C1202 specification (4). In this testing procedure, the transport of chloride ions is accelerated by applying an external electrical field. The current passed through an electrical cell containing the concrete specimen is measured at 5 minute intervals for a 6- hour time period. The resistance to chloride ion penetration is assessed by the total charge passed during the 6- hours (5). One major limitation of the CIPT results is that they do not account for the current exclusively carried by chloride ions as distinguished from the total ions in the migration process (6). Another limitation of the CIPT is the high current flow in permeable concrete mixtures results in a "joule effect". The increase in temperature effectively decreases the electrical resistance and encourages the current to flow more rapidly and produce more heat which further accelerates the current flow (7). Riding et al. developed a simplified method which is similar to CIPT procedure except for the specimen and gasket size to determine concrete resistivity as an index of concrete permeability. To eliminate the gradual temperature rise problem only one current reading was taken (after 5 minutes) that could be applied to measure the concrete resistivity. An empirical correlation between the new method and the standard CIPT method established the validity and promise of the new simplified method. The

disadvantage of this method is its application and suitability on core field samples as it has not yet been determined (8). Snyder et al. have established that Ohmic heating during the 6- hour CIPT makes the raw data an unreliable measurement of any specimen transport property from the results (9). Despite the limitations of the CIPT, it is still regarded as repeatable experimental procedure for investigation of chloride ion ingress.

Electrical conductivity is a secondary parameter in durability modeling of concrete structures. Lane established that the electrical properties of concrete correlated well with the durability of the concrete as an indirect measure of the capillary pore system and are a direct measure of the concrete's electrical conductivity which affects steel corrosion in concrete (10). Shi established that CIPT is actually an indication of electrical conductivity of the concrete which depends upon the pore solution chemistry of the concrete. Results of this study showed that supplementary cementing materials such as silica fume, fly ash and ground blast furnace slag may have a significant effect on the chemistry or electrical conductivity of pore solution, depending on the alkali content of the supplementary cementing material, replacement level and age (11). Smith et al. have shown the significant advantage of using supplementary cementitious materials (SCM) in development of high performance concrete. Their study revealed that use of SCM results in high values of concrete resistivity (inverse of electrical conductivity), cause a smaller likelihood of corrosion initiation (12). Thomas et al. showed that ternary based cementitious materials had high resistance to the penetration of chloride ions using the diffusion experimentation method. They emphasized that ternary cementitious mixtures have low diffusivity at an early age and relatively large decay in diffusivity over time (13).

Most of the existing models for estimation of corrosion initiation time and service life are not involved with a significant number of ternary cementitious material's diffusion coefficients. The emphasis of this paper is on a reliable estimation of the diffusion coefficients directly from electrical conductivity measurements from CIPT data with incorporation of essential components of past research and adjustments due to the joule effect and subsequently computing corrosion initiation time. This study also attempts to investigate influence of diffusion coefficients and corrosion initiation time on several ternary cementitious mixtures of quality assurance specimens.

6.3 Research Significance

It is necessary to include variations of the diffusion coefficients of concrete with different cementitious materials to enhance the service life prediction of concrete structures, and establish some concrete mixtures with diffusion coefficients that minimize the ingress of chlorides. This research presented herein addresses the computation of diffusion coefficients from electrical conductivity measurements with the incorporation of essential adjustments due to the joule effect. These adjustments of data provide an improved and reliable prediction of chloride diffusion coefficients and corrosion initiation time with strong theoretical basis for several ternary based cementitious materials in concrete structures.

6.4 Experimental Investigation

Different types of binary and ternary cementitious mixtures along with control mixtures with a water/cementitious materials ratio of 0.44, typical of exposed bridge deck concrete, were designed to give a wide range of values for this experimental program. All

mixtures contained 340 kg/m^3 of the cementitious material with a Coarse Aggregate Factor (CAF) of 0.67. Limestone coarse aggregate of size 19 mm meeting ASTM C33 No.67 gradation and ASTM C33 silica sand was used. Tests were performed on mixtures using:

- ASTM Type I cement (TI)
- Portland-pozzolan blended cement(TIP (20))
- Limestone blended cement (E)
- Slag blended portland cement [TIS (25)]

Mineral additives used:

- Ground granulated blast furnace slag (G120S)
- Fly ash (Types C, F and F2)
- Silica fume (SF)
- Metakaolin (M)
- Volcanic tuft (S)

Table 6.1 shows the concrete mixture compositions. Medium range water reducing admixture and air entraining agent were also used to meet required slump flow and other durability performance specifications. Chloride ion penetration test (CIPT) was performed with different ternary cementitious mixtures including the control mixtures to use its data for computation of equivalent steady state diffusion coefficients. For each mixture, two 100 mm x 200 mm (4 inch x 8inch) cylinders were cast and wet cured for 14 days and then they were air cured in lab conditions until the 98th day for testing. Ninety Eightdays (i.e., 14 weeks) was selected as sufficient time for pozzolanic reaction to develop. The concrete cylinders were cut to 50 mm (2 inches) slices and vacuum

saturated with de aerated water. In the testing process, each cell was filled with 3% NaCl solution on one side (cathode) and 0.3M NaOH solution on the other side (anode). A potential difference of 60Vdc was applied across each cell during which the current and temperature were recorded every 5 minutes for 6 hours. A minimum of two specimens were tested for each of the concrete mixtures. The average value of the specimen readings was reported to minimize the variation.

6.5 Conductivity and Joule Effect

The electrical conductivity of concrete can be determined from resistance of concrete and the geometry of the cylinder used in the CIPT and is expressed in Equation 6.1,

$$\sigma = \frac{l}{RA} \tag{6.1}$$

where σ is the conductivity in Siemens/m (Siemens/ft), l is the length of the specimen in m (ft), R is the resistance in ohms and A is the cross-sectional area of the specimen in m^2 (ft^2).

The RCPT is an electrical test operating under Ohm's law (Equation 6.2) in which the test result is a direct function of the resistance of the test specimen (7).

$$V = IR \tag{6.2}$$

where V is the applied voltage in CIPT in volt and I is the current passing through the circuit. Substituting the value of resistance (R) from Equation 6.2 to Equation 6.1, the electrical conductivity can be expressed in Equation 6.3.

$$\sigma = \frac{lI}{VA} \tag{6.3}$$

6.5.1 Joule effect

The application of the 60 Vdc in chloride ion penetration test (CIPT) induces a large current flow from the beginning of the 6- hour test period. The resistor in this circuit consequently increases temperature and accelerates the current flow through permeable concrete mixtures during the test period resulting in a high value of charge passed. Betancourt et al. (7) developed a temperature adjustment to reduce or eliminate this "joule effect" and improve the prediction of charge passed during the 6- hour time period. The adjusted charge during the 6- hour test can be expressed in Equation 6.4.

$$Q_0 = e^{[\ln(Q_{c\,6hr}) + \beta(1/\delta T - 1/273)]} \tag{6.4}$$

In Equation 6.4, Q_0 is the joule effect adjusted charge passed through the 6- hour CIPT and β is an experimental constant equal to 1245, Q_{c6hr} is the original charge passed through the 6- hour CIPT test, and δT is the difference in temperature increment in Kelvin (Fahrenheit) during the 6- hour test (7). The adjusted average current is obtained by dividing the joule effect adjusted charge passed (Q_0) by time in seconds and it is expressed in Equation 6.5.

$$I_{adj} = \frac{Q_0}{t} \tag{6.5}$$

The adjusted average electrical current during 360 minutes can be substituted into Equation 6.2 to get adjusted resistance and then in Equation 6.1 to obtain the adjusted

electrical conductivity during 360 minutes. Table 6.1 shows the electrical conductivity rate during 5- minute, 10- minute, 30- minute and 360- minute intervals.

Electrical conductivity of concrete calculated from 5 minutes to 30 minutes data are nearly identical, because they contain minimal joule effect. The 360 minutes raw data produced a much higher electrical conductivity. When adjusted for the joule effect the electrical conductivity is within 10% of the 5 and 30 minutes results indicating that the joule effect is not only needed for coulomb readings but also for conductivity. Fig. 6.1 shows the need for the incorporation of the joule effect adjustments. This indicates that the high current passed through concrete mixtures during the 6-hour test due to application of the 60 Vdc is not realistic and the "joule effect" was examined by performing long term migration test (36 hours with 10 Vdc) along with CIPT procedure for the 6-hour test for four different mixtures. Fig. 6.2 and 6.3 show the joule effect on two concrete mixtures for the CIPT as well as long term migration test in terms of excessive current passed and temperature rise.

6.6 Diffusion Coefficients from Electrical Conductivity

Electrical conductivity values adjusted for the joule effect during 360 minute emulates that steady state condition for the 6 hour of CIPT. Using Nernst-Einstein-relation, the diffusion coefficient D_{eff} can be derived from conductivity σ_{eff} and the salt concentration in the sample c_i and it is expressed in Equation 6.6, (14)

$$D_{eff} = \sigma_{eff} \frac{kT}{Z^2 Fec_i} \tag{6.6}$$

where, k- Boltzmann constant, T- Temperature in Kelvin, Z- Charge number, F- Faraday constant, and e- Electron charge. The diffusion coefficients for all the cementitious mixtures are computed on 360 minutes by using Equation 6.6.

6.7 Corrosion Initiation Time

Since chloride ingress occurs under transient conditions, Fick's second law of diffusion in terms of Crank's solution (15) can be used to predict the time variation of chloride concentration for one-dimensional flow, and it can be expressed in Equation 6.7.

$$C(x,t) = C_0(1 - erf(\frac{x}{2\sqrt{Dt}})) \quad (6.7)$$

In Equation 6.7, $C_{(x,t)}$ is the chloride concentration at depth x after time t; C_o is the chloride concentration at the surface; D is the diffusion coefficient; t is the time of exposure; and erf is the error function. The onset of corrosion of the reinforcing steel is assumed to start when the concentration of chlorides at the level of the reinforcement has reached or exceeded critical chloride threshold level C_{cth}. The average value of chloride threshold of the black bar is taken as 0.98 kg/m^3 (16) and the average value of surface chloride concentration is computed to 2.18 kg/m^3 (17). Considering d_c is the depth of concrete cover (50 mm), the time to corrosion initiation can be expressed in Equation 6.8 by using the diffusion coefficients obtained from Nernst-Einstein equation. It is to be noted that this corrosion initiation time is for solid properly compacted concrete.

$$T_i = \frac{{d_c}^2}{4D[erf^{-1}(1 - \frac{C_{cth}}{C_0})^2} \quad (6.8)$$

6.8 Results

The values of electrical conductivity obtained from the CIPT data are in a similar range from 5 minutes to 30 minutes and they are shown in Table 6.1. However, high values are obtained where 360 minutes data are obtained. In situ concrete is not exposed to sustained elevated temperatures. This phenomenon is evidenced by Fig. 6.1 and 6.2 for two different mixtures one with 60Vdc for 6 hours and the other with 10Vdc for 36 hours of time. Fig. 6.1 and 6.2 shows that temperature and current become nearly constant with the application of 10V dc over a 36-hour time period in comparison with high temperature and current passed due to application 60Vdc over a 6-hour time period. Considerations for the joule effect are necessary to adjust the current and therefore electrical conductivity. Fig. 6.3 depicts this adjustment of electrical conductivity during 360 minutes and shows that it is nearly constant as compared to the 5-minute electrical conductivity. This small difference in values of electrical conductivity (σ) implies further chloride ingress has been stopped and equivalent steady state condition has nearly been reached within the 6 hours of CIPT where adjustments for the joule effect are incorporated.

Table 6.2 shows the distribution of diffusion coefficients and corrosion initiation time for all the cementitious mixtures. It is evident from Table 6.2 that most of the ternary cementitious mixtures performed well in computation of corrosion initiation time (more than 50 years) except the control mixtures and some other permeable mixtures. Ternary mixtures' beneficial effect related to the reduced charge passed during the 6 hours of CIPT and lower influence of the Joule effect. Combination of two fly ashes and blended cement (TIP and TISM) in combination with other fly ash did not provide

beneficial effect to extend the corrosion initiation by computing corrosion initiation time less than 50 years. It has also been observed that limestone blended cement in combination with different pozzolans showed remarkable reduced corrosion initiation time.

Fig. 6.4 shows that charge passed and the increase of temperature during 6 hours of CIPT are correlated well with each other (R^2=0.95). It also signifies that control mixtures and some other permeable mixtures, namely 100 TI, 100TIP, 80TI/20C, 60TI/20C/20F2, 60TI/30C/10F, produce high values of charge passed due to large increment of temperature from the starting of the test to the end of the 6-hour CIPT. However, most of the ternary based cementitious mixtures produce insignificant increment of temperature due to minimal joule effect.

Fig. 6.5 established a relationship between 360 minutes electrical conductivity with 5 minutes electrical conductivity in terms of temperature rise in 6 hour of CIPT. This relationship becomes significantly established whenever the joule effect is predominant on some permeable and control mixtures.

Fig. 6.6 shows group wise statistical distribution of diffusion coefficients of different cementitious mixtures. The box (2-3-7-6) represents the range of diffusion coefficients those lay between the first quartile (Q1) and the third quartile numbers (Q3). Thus, the bottom most line (line 2-3) of the box represents the first quartile number (Q1) and the topmost line (line 6-7) represents the third quartile number (Q3). The horizontal line inside the box (line 4-5) represents the median value of diffusion coefficient. The vertical line below and above the box represent the remaining values of diffusion coefficients excluding the outlier. It is evident from Fig. 6.6 that all the Class C mixtures

combined with other fly ashes have high value of diffusion coefficients (2.34E-12 - 2.59E-12 m^2/sec) (25.18E-12-27.86E-12 ft^2/sec). On the other hand, most of the Class F, F2, slag, TIP and TISM group of mixtures performed remarkably well in reduction of diffusion coefficients except for some of the ternary mixtures namely Class F2 and one TISM mixture combined with other pozzolans in the ternary blends. These mixtures are shown as outliers in their respective group.

Electrical conductivity is an important component in the computation of diffusion coefficients. For some permeable mixtures, namely 100 TI, 75TISM/25C, the adjusted chloride electrical conductivity reduces the diffusion coefficients by a large extent (25 to 30%). It has been observed from Fig. 6.7 that the adjusted electrical conductivity correlated well with the diffusion coefficients predicted by the Nernst-Einstein equation. It can be concluded from Fig. 6.7 that the joule effect is the prominent factor in computing diffusion constants for permeable concrete mixtures and the joule effect does not have a predominant effect on impermeable concrete mixtures. This observation has clear implication of significant achievement of ternary mixtures on reduction of diffusion coefficients and electrical conductivity.

6.9 Summary and Conclusion

The work presented in this paper demonstrates the necessity of the temperature adjustment due to the joule effect in understanding the equivalent steady state condition of the diffusion process. As a result, this adjustment indicated a more accurate and reliable prediction of the electrical conductivity in hardened concrete within 6 hours of the CIPT. Thus, the Nernst-Einstein relationship is applicable to compute equivalent

steady state diffusion coefficients for several ternary cementitious mixtures including the control mixtures from the CIPT data using electrical conductivity measurements.

Ternary cementitious mixtures have a large effect for reduction of diffusion coefficients and electrical conductivity to increase long term resistance for chloride ion penetration. The key reason is the densification of the matrix brought about by the pozzolanic reactions of pozzolans tries to close the pores and results in reducing permeability.

Some of the pozzolans in combinations of two fly ashes in the ternary blend did not produce desirable results in the computation of diffusion coefficients and corrosion initiation time. Diffusion coefficients show negative influence on replacement of limestone blended cement, some of the portland-pozzolan cement and slag modified portland cement combined with other pozzolans as they compute significant lower values of corrosion initiation time.

Overall, the findings of these diffusion coefficients for ternary cementitious mixtures can provide effective decision support in the design of new durable structures in harsh chloride environments.

6.10 Acknowledgements

The authors wish to express their gratitude and sincere appreciation to the Federal Highway Administration Pooled Fund Study TPF-5(117) for support of this research work.

6.11 References

1. Ahmad, S., Al-Kutti, W.A., Al-Amoudi, B.S.O., and Maslehuddin, M., " Correlations Between Depth of Water Penetration, Chloride Permeability, and Coefficient of Chloride Diffusion in Plain, silica fume, and fly ash Cement Concretes", *Journal of Testing and Evaluation,* V.36, No.2, 2009, pp.1-4.

2. Azad, A.K., Sharif, A.M., Navaz, M., and Loughlin, K.F., "Chloride Diffusion Coefficient of Concrete in the Arabian Gulf Environment", *Arabian Journal of Science and Engineering,* Dhahran, Saudi Arabia, V.22, No.2B, 1997, pp.169-182.

3. Nokken, M., Boddy, A., Hooton, R.D., and Thomas, M.D.A, "Time Dependent Diffusion in Concrete-Three Laboratory Studies", *Cement and Concrete Research*, V.36, No.1, January 2006, pp.200-207.

4. ASTM C1202-05, "Electrical Indication of Concrete's Ability to Resist Chloride Ion Penetration", *ASTM V04.02,* ASTM*,* Philadelphia, PA, 2005.

5. Whiting, D., "Rapid Measurements of Chloride Permeability of Concrete", *Public Roads,* V.45, No. 3, 1981, pp.101-112.

6. Suryavanshi, A.K., Swami, R.N., and Cardew, G.E., "Estimation of Diffusion Coefficients for Chloride Ion Penetration Into Structural Concrete", *ACI Materials Journal,* V.99, No.5, September 2002, pp.441-449.

7. Betancourt, J.G.A., and Hooton, R.D., "Study of the Joule Effect on Rapid Chloride Permeability Values and Evaluation of Related Electrical Properties of Concrete", *Cement and Concrete Research,* V.34, No.6, June 2004, pp. 1007-1015.

8. Riding, A.K., J.L. Poole, K.A., C.G.M. Juenger, and J.K. Folliard, "Simplified Concrete Resistivity and Rapid Chloride Permeability Test Method", *ACI Materials Journal*, Vol.105, No. 4, 2008, pp. 390-394.

9. Snyder, K.A., C. Ferraris, N.S. Martys, and E.J. Garboczi. Using Impedance Spectroscopy to Assess the Viability of the Rapid Chloride Test for Determining Concrete Conductivity. *Journal of Research of the National Institute of Standards and Technology*, Vol.105, No.4, 2000, pp.497-509.

10. Lane, S., "Supplanting the rapid chloride permeability test with a quick measurement of concrete conductivity", Final Report to Virginia Transportation Research Council, Charlottesville, Virginia, March 2005, pp.1-13.

11. Shi, C., "Effect of Mixing Proportions of Concrete on its Electrical Conductivity and the Rapid Chloride Permeability Test (ASTM C1202 Or ASSHTO T277) Results", *Cement and Concrete Research*, V.34, 2004, pp.537-545.

12. Smith, M.K., Andrea, J.S., and Tikalsky, P.J., "Performance of Supplementary Cementitious Materials in Concrete Resistivity and Corrosion Monitoring Evaluation", *ACI Materials Journal*, Vol.101, No.5, 2004, pp.385-390.

13. Thomas, M.D.A, Shehata, M.H., Sashiprakash, S.G., Hopkins, D.S., and Cali, K., "Use of Ternary Cementitious Systems Containing Silica Fume and Fly Ash in Concrete", *Cement and Concrete Research*, Vol. 29, No.8, 1999, pp.1207-1214.

14. T. Kudo, K. Fueki, Solid State Ionics, VCH, Tokyo, 1990, p.62.

15. Crank, J. The Mathematics of Diffusion, 2nd Edition, Oxford University Press, London, 1975.

16. Darwin, D., Browning, J., O'Reilly, M., Xing, L., and Ji, J., "Critical Chloride Corrosion Threshold of Galvanized Reinforcing Bars", *ACI Materials Journal*, Vol.106, No.2, 2009, pp. 176-183.

17. Pyc, W. Field Performance of Epoxy-Coated Reinforcing Steel in Virginia Bridge Decks, Doctoral Dissertation, Virginia Polytechnic Institute and State University, Blacksburg, Virginia, U.S.A, 1998.

Table 6.1- Electrical conductivity for different cementitious mixtures

Mix ID		Electrical conductivity (Siemens/m)			
	5 min	10 min	30 min	Raw 360 min	Adjusted 360 min
100 TI	0.0188	0.0181	0.0196	0.0269	0.0148
80TI/20C	0.0215	0.0219	0.0237	0.0282	0.0164
60TI/20C/20F2	0.0220	0.0221	0.0251	0.0324	0.0171
60TI/30C/10F2	0.0210	0.0210	0.0233	0.0313	0.0162
60TI/30C/10F	0.0239	0.0245	0.0272	0.0320	0.0179
80TI/20F	0.0228	0.0227	0.0249	0.0358	0.0180
60TI/20F/20F2	0.0185	0.0196	0.0218	0.0288	0.0157
60TI/30F/10F2	0.0192	0.0195	0.0211	0.0262	0.0154
77TI/20F/3SF	0.0117	0.0114	0.0116	0.0149	0.0097
75TI/20F/5SF	0.0059	0.0058	0.0054	0.0071	0.0050
60TI/20F/20G120S	0.0077	0.0069	0.0069	0.0090	0.0055
75TI/20F/5M	0.0073	0.0073	0.0073	0.0100	0.0066
65TI/30F/5SF	0.0036	0.0036	0.0035	0.0044	0.0032
67TI/30F/3SF	0.0056	0.0056	0.0054	0.0071	0.0050
50TI/30F/20G120S	0.0049	0.0048	0.0049	0.0062	0.0045
65TI/30F/5M	0.0055	0.0054	0.0053	0.0072	0.0049
80TI/20F2	0.0096	0.0093	0.0094	0.0137	0.0085
60TI/30F2/10C	0.0213	0.0214	0.0243	0.0385	0.0172
75TI/20F2/5SF	0.0074	0.0075	0.0078	0.0103	0.0068
77TI/20F2/3SF	0.0101	0.0099	0.0100	0.0120	0.0083
60TI/20F2/20G120S	0.0101	0.0100	0.0100	0.0140	0.0087
75TI/20F2/5M	0.0109	0.0106	0.0106	0.0141	0.0084
65TI/30F2/5SF	0.0061	0.0060	0.0056	0.0066	0.0049
67TI/30F2/3SF	0.0090	0.0090	0.0088	0.0120	0.0078
65TI/30F2/5M	0.0127	0.0126	0.0130	0.0191	0.0111
65TI/35G120S	0.0067	0.0067	0.0063	0.0079	0.0056
50TI/35G120S/15F	0.0057	0.0056	0.0054	0.0064	0.0047
50TI/35G120S/15F2	0.0063	0.0062	0.0061	0.0073	0.0053
62TI/35G120S/3SF	0.0052	0.0052	0.0051	0.0059	0.0043
60TI/35G120S/5M	0.0045	0.0045	0.0045	0.0054	0.0039
100TIP	0.0134	0.0141	0.0156	0.0231	0.0118
85TIP/15C	0.0204	0.0207	0.0219	0.0309	0.0150
85TIP/15F	0.0155	0.0154	0.0158	0.0232	0.0129
85TIP/15F2	0.0085	0.0084	0.0080	0.0122	0.0073
65TIP/35G120S	0.0070	0.0070	0.0068	0.0093	0.0075
97TIP/3SF	0.0048	0.0048	0.0047	0.0057	0.0042
95TIP/5M	0.0037	0.0037	0.0037	0.0045	0.0033
75TIP/25C	0.0237	0.0242	0.0284	0.0401	0.0210
75TIP/25F	0.0177	0.0175	0.0192	0.0265	0.0149
75TIP/25F2	0.0210	0.0209	0.0233	0.0335	0.0169
50TIP/50G120S	0.0047	0.0047	0.0046	0.0056	0.0042
100TISM	0.0142	0.0153	0.0164	0.0255	0.0130
75TISM/25C	0.0151	0.0151	0.0164	0.0241	0.0132
75TISM/25F2	0.0122	0.0117	0.0124	0.0193	0.0105
65TISM/35G120S	0.0120	0.0118	0.0119	0.0162	0.0099
97TISM/3SF	0.0045	0.0045	0.0043	0.0057	0.0041
100E	0.0185	0.0187	0.0195	0.0312	0.0149
80E/20S	0.0163	0.0158	0.0167	0.0290	0.0144
80E/20F	0.0156	0.0155	0.0153	0.0250	0.0130
80E/20F2	0.0162	0.0164	0.0179	0.0251	0.0140
80E/20G120S	0.0122	0.0118	0.0116	0.0171	0.0099
80E/20C	0.0139	0.0137	0.0142	0.0208	0.0118
95E/5SF	0.0036	0.0036	0.0035	0.0049	0.0034
95E/5M	0.0060	0.0060	0.0060	0.0084	0.0055

Table 6.2- Diffusion coefficients and corrosion initiation time for different mixtures

Mix ID	Diffusion coefficients (m^2/sec)	Corrosion Initiation time (Years)
100 TI	2.10.E-12	30
80TI/20C	2.35.E-12	27
60TI/20C/20F2	2.49.E-12	26
60TI/30C/10F2	2.34.E-12	27
60TI/30C/10F	2.59.E-12	25
80TI/20F	2.58.E-12	25
60TI/20F/20F2	2.22.E-12	29
60TI/30F/10F2	2.19.E-12	29
77TI/20F/3SF	1.34.E-12	67
75TI/20F/5SF	6.65.E-13	96
60TI/20F/20G120S	7.34.E-13	57
75TI/20F/5M	8.93.E-13	71
65TI/30F/5SF	4.27.E-13	149
67TI/30F/3SF	6.63.E-13	96
50TI/30F/20G120S	5.92.E-13	108
65TI/30F/5M	6.50.E-13	98
80TI/20F2	1.15.E-12	56
60TI/30F2/10C	2.49.E-12	26
75TI/20F2/5SF	9.12.E-13	70
77TI/20F2/3SF	1.13.E-12	57
60TI/20F2/20G120S	1.20.E-12	53
75TI/20F2/5M	1.15.E-12	55
65TI/30F2/5SF	6.55.E-13	74
67TI/30F2/3SF	1.07.E-12	60
65TI/30F2/5M	1.53.E-12	42
65TI/35G120S	7.49.E-13	85
50TI/35G120S/15F	6.26.E-13	102
50TI/35G120S/15F2	7.02.E-13	91
62TI/35G120S/3SF	5.67.E-13	113
60TI/35G120S/5M	5.21.E-13	123
100TIP	1.64.E-12	39
85TIP/15C	2.14.E-12	30
85TIP/15F	1.80.E-12	35
85TIP/15F2	9.82.E-13	65
65TIP/35G120S	9.98.E-13	94
97TIP/3SF	5.59.E-13	114
95TIP/5M	4.35.E-13	147
75TIP/25C	3.04.E-12	21
75TIP/25F	2.09.E-12	31
75TIP/25F2	2.43.E-12	26
50TIP/50G120S	5.56.E-13	115
100TISM	1.82.E-12	35
75TISM/25C	1.84.E-12	35
75TISM/25F2	1.45.E-12	44
65TISM/35G120S	1.35.E-12	47
97TISM/3SF	5.43.E-13	118
100E	2.10.E-12	25
80E/20S	2.03.E-12	31
80E/20F	1.81.E-12	30
80E/20F2	1.94.E-12	33
80E/20G120S	1.35.E-12	58
80E/20C	1.63.E-12	39
95E/5SF	4.42.E-13	69
95E/5M	7.33.E-13	87

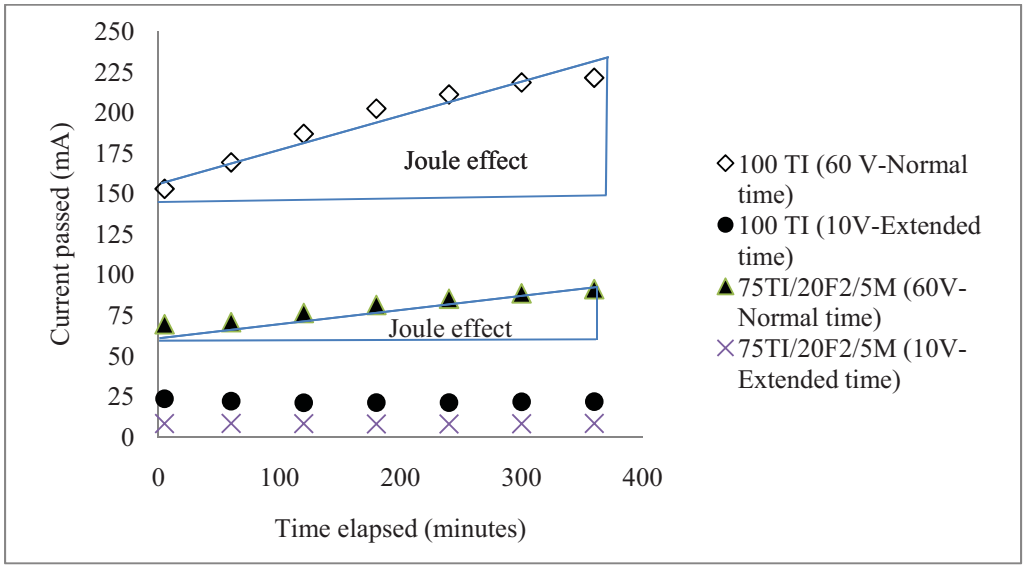

Fig. 6.1- Joule effect on two concrete mixtures in terms of current passed

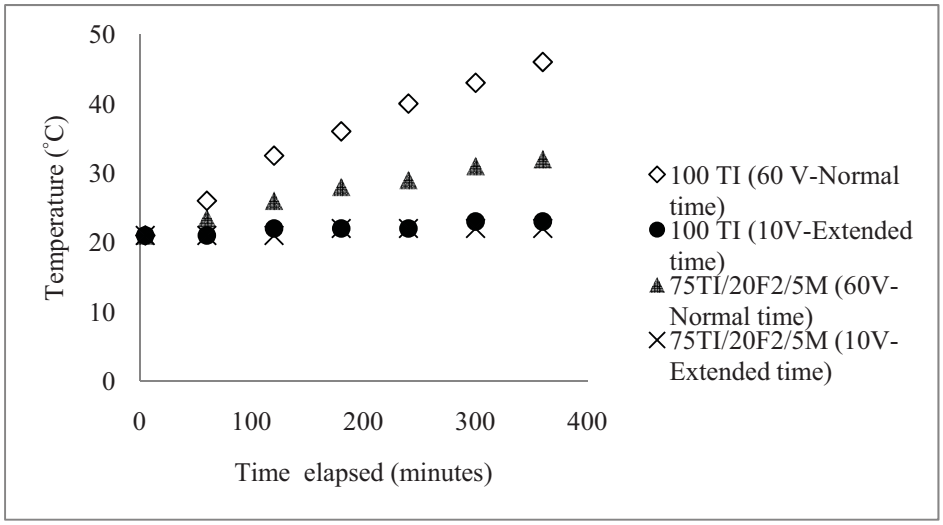

Fig. 6.2- Joule effect on two concrete mixtures in terms of temperature rise (1°F = °C x 1.8+32)

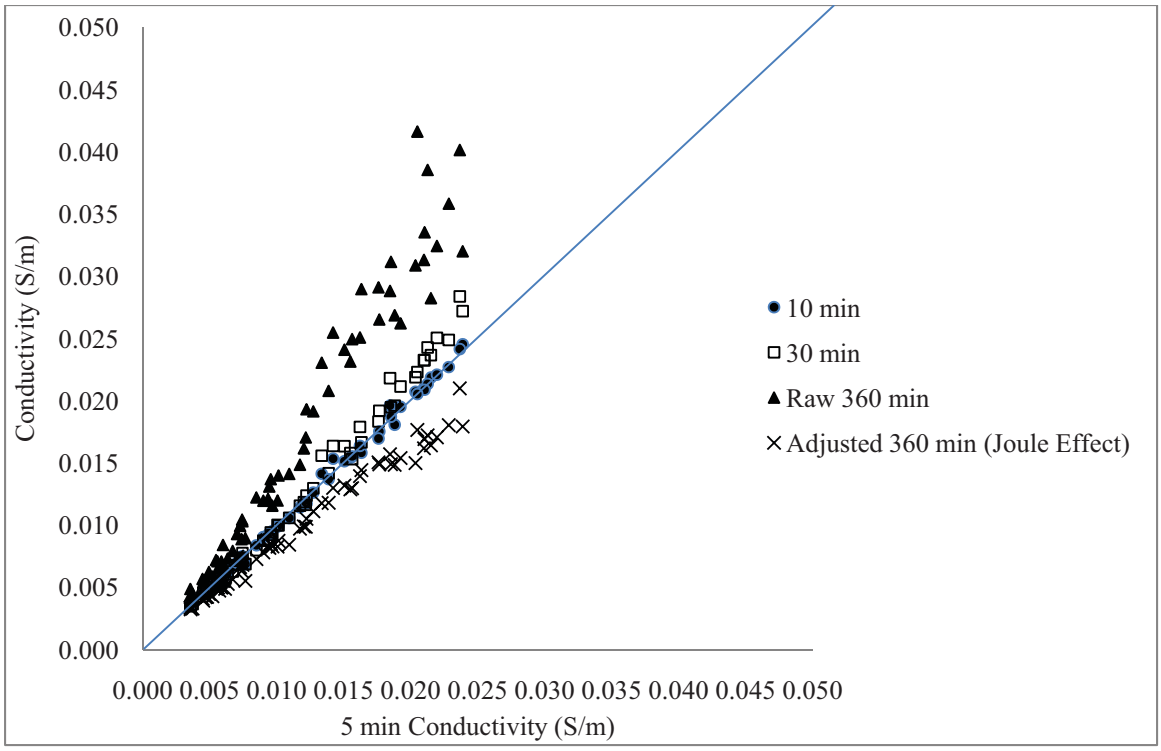

Fig. 6.3- Comparison of chloride migration rate from 5 minutes to 360 minutes

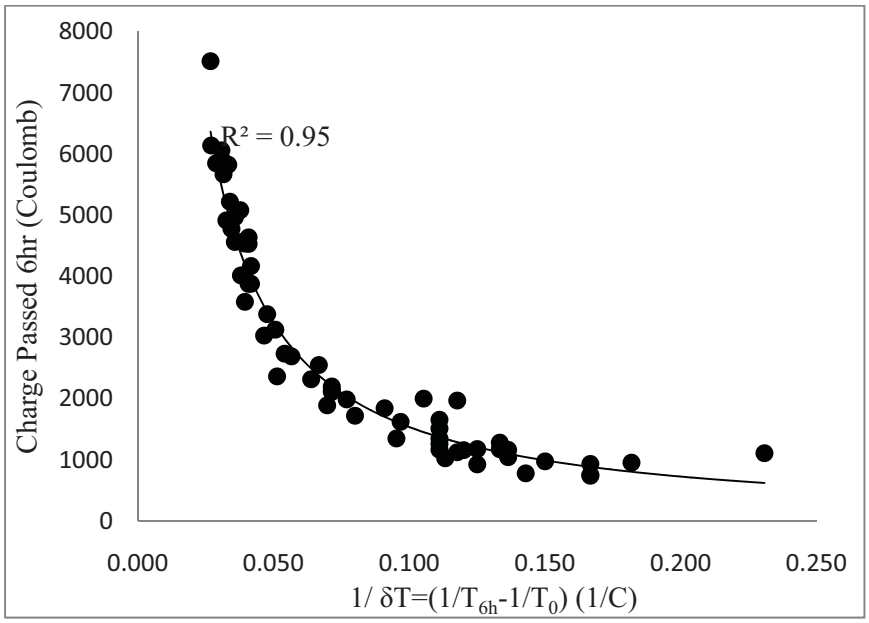

Fig. 6.4- Effect of temperature increment on charge passed on different mixtures

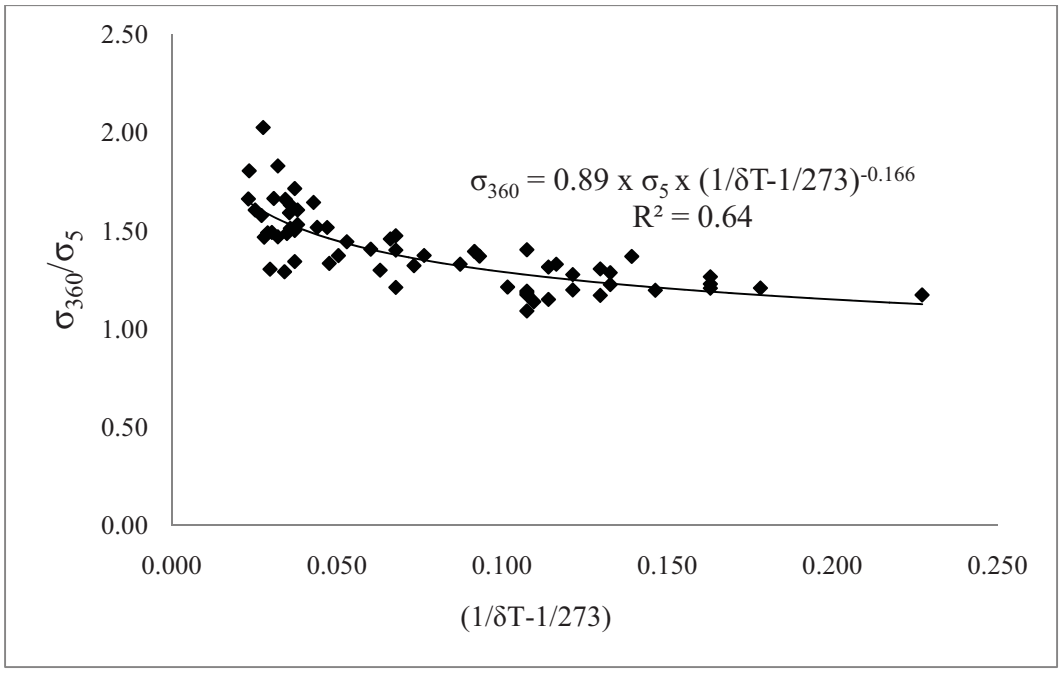

Fig. 6.5 - Relationship between 5 minute and 360 minute electrical conductivity

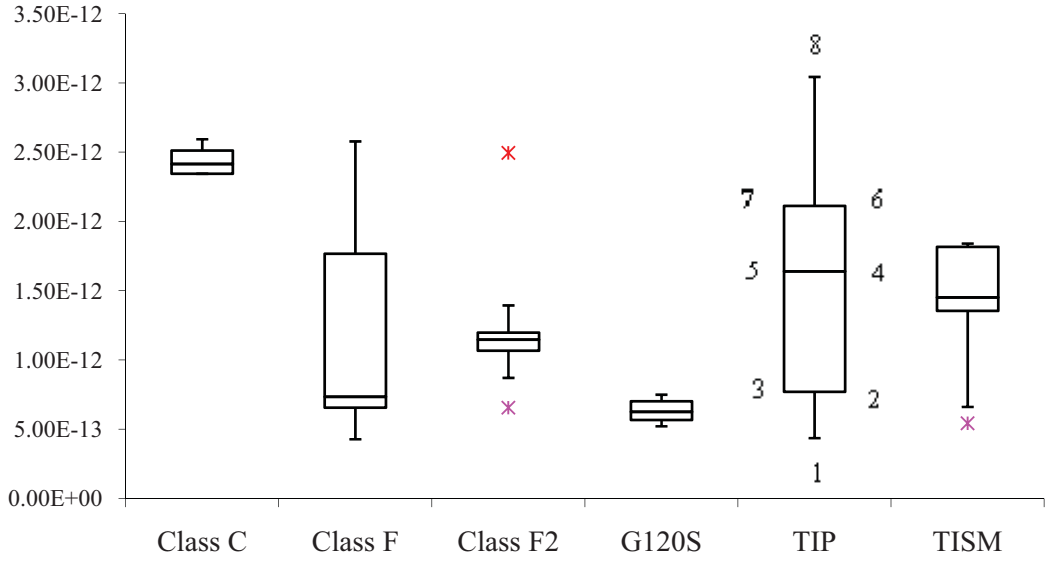

Fig. 6.6 – Group wise distribution of diffusion coefficients on different Cementitious mixtures

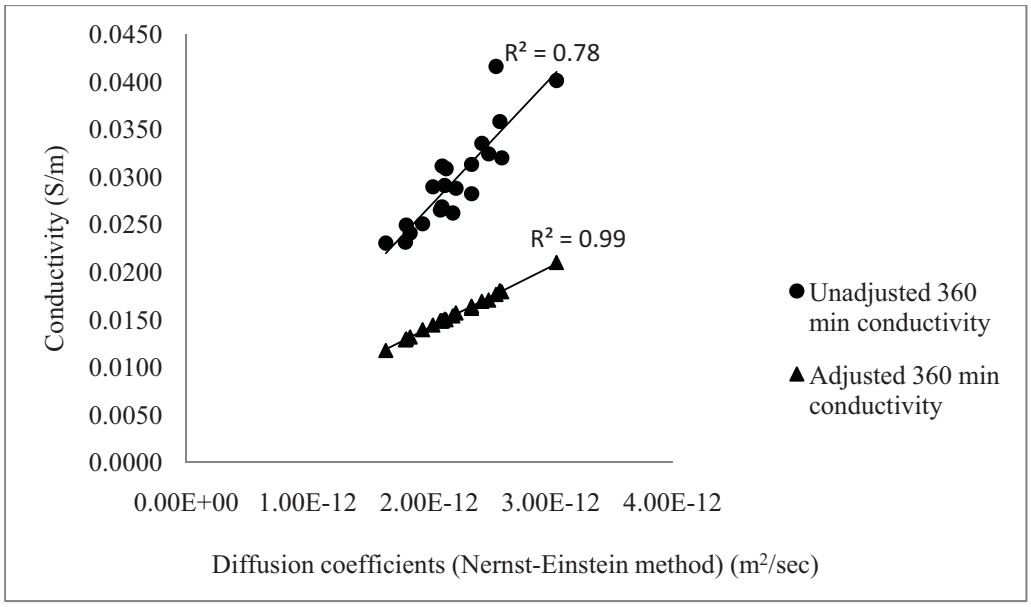

Fig. 6.7 Correlation between conductivity and diffusion coefficients

CHAPTER 7

PROBABILISTIC CORROSION INITIATION MODEL

Pratanu Ghosh, Petr Konečný and Paul J. Tikalsky

Biography: ACI student member **Pratanu Ghosh** is a Research Assistant at the Materials and Structures Research Laboratory at the University of Utah. He received his B.S. from Bengal Engineering College (D.U), India and MASc. from the University of Windsor, Canada.

Petr Konečný is currently a lecturer in the Department of Civil Engineering in VSB-Technical University of Ostrava.

ACI Fellow **Paul Tikalsky** is the Chair of the Department of Civil and Environmental Engineering at the University of Utah. He is a member and former Chair of ACI Committee 232 (Fly Ash and Natural Pozzolans), member of ACI Committee 201 (Durability), and Chair of TRB Committee AFN10 (Basic Research and Emerging Concrete Technologies).

(To be submitted in ACI Materials Journal)

7.1 Abstract

A finite element based probabilistic reinforced concrete bridge deck corrosion initiation model is established that includes the uncertainties in the physical models of chloride penetration into concrete. The model is focused on uncertainties in the governing

parameters that include concrete diffusivity, concrete cover depth, surface chloride concentration, holidays in reinforcements, coatings and critical chloride threshold level for onset of corrosion in steel reinforcement with excessive cracks. The objective of this research is based on the formulation of probabilistic corrosion initiation model with the inclusion of distribution of High Performance Concrete (HPC) diffusion coefficients along with control mixtures computed from four different approaches and to investigate the performance of several corrosion resistant steel reinforcements. The distribution of the other governing parameters is generated from either detailed field survey or laboratory experimental investigation. This study shows the variability and sensitivity of estimation of the time to onset of corrosion using the Monte Carlo technique. Results from this probabilistic analysis estimates the corrosion free service life for the design of concrete structures in harsh chloride environments with respect to methods for diffusion coefficients computation.

Keywords: SBRA, diffusion coefficient, Monte Carlo simulation, Probabilistic modeling

7.2 Introduction

Chloride induced corrosion of reinforcing steel in concrete bridge decks and other concrete structure is one of the major problems in the USA for premature deterioration. As a result, safety, serviceability and durability of concrete structures are reduced with increase of life cycle cost. The possible solution to minimize the impact of corrosion is the reduction of chloride ingress and implementation of different corrosion resistant steel reinforcement to optimize life cycle cost. Though models for chloride ingress and corrosion development have been studied [see, e.g., (1-11)], there are still many issues that must be addressed to become useful engineering tools, especially with regard to

randomness of pertinent input variables. Tikalsky et al. (12) and Konečný et al. (13) used the Monte Carlo technique in a corrosion model to show the variability on estimation of the time to onset of corrosion and the required depth of concrete cover to extend the service life up to 100 years. Shim (14) demonstrated that the resulting probability distribution is most sensitive to the chloride diffusion coefficients. Lounis et al. (15) presented a research approach for the probabilistic modeling of the chloride induced corrosion of carbon steel reinforcement in concrete structures considering the uncertainties of the governing parameters such as concrete diffusivity, surface chloride concentration, concrete cover depth, and threshold chloride level. The parameters were modeled as random variables and the distribution of the corrosion time and probability of corrosion rate are determined by using Monte Carlo simulation. Kirpatrick et al. (16) established a probabilistic model to estimate the time required for first repair and subsequent rehabilitation of concrete bridge decks exposed to chloride salts. Their model expands on the existing deterministic model using two different types of resampling technique namely simple and parametric boot strap with emphasis on diffusion portion of diffusion cracking model. Provided results from two methods subsequently agreed the condition of 10 bridge decks in Virginia in terms of rehabilitation assessment.

All of the previously mentioned probabilistic corrosion models lack the distribution of performance based diffusion coefficients data of various high performance cementitious materials along with the performance of several corrosion resistant steel reinforcements. It is desirable thus to perform research to incorporate reliable diffusion coefficients of HPC materials and investigates the performance of several steel reinforcements to delay chloride induced corrosion initiation.

7.3 Research Significance

This research indicates the road map to formulation of the probabilistic corrosion initiation model of a typical reinforced concrete bridge deck with different steel reinforcements with respect to chloride ingress using Simulation-Based Reliability Assessment (SBRA) method. This numerical model also accounts for the scatter of input random variables with regard to diffusion, surface cracks and reinforcing steel protection type (i.e., black bar, epoxy coating bar, galvanized bar and ASTM A1035 steel). The model combines a finite element model (13) and the Simulation Based Reliability Assessment (SBRA) method that is introduced in (17) and proposed for application with chloride ingress by Tikalsky et al. (12) and (18). The objective of this research is based on the formulation of probabilistic corrosion initiation model with the inclusion of distribution of HPC diffusion coefficients computed from Chloride Ion Penetration Test (CIPT) and electrical resistivity data, the variation of surface chloride concentration from the field data of Virginia bridge decks (19) and the variation of critical chloride threshold for reinforcing steel (20). This study shows the variability and sensitivity on estimation of the time to onset of corrosion using the Monte Carlo technique.

7.4 Chloride Induced Corrosion

Chloride induced corrosion is a complex electrochemical process which consists of the cathode, anode and the electrolyte. Saturated concrete acts as an electrolyte which facilitates the flow of electrons from anode to cathode. In the anode iron losses its electrons to form Fe^{2+} and this is an oxidation reaction. In the cathode, oxygen dissolves to form hydroxyl ions (OH^-) and this is a reduction reaction. The anodic product Fe^{2+} reacts with the cathodic product OH^- to produce hydrated ferrous oxide (Fe_2O_3. H_2O).

This hydrated ferrous oxide can be further converted to red brown rust and black magnetite to form a stable passive layer around the steel reinforcement. Chloride enters through the cover of concrete to the reinforcing steel and starts to attack this stable passive film. When the concentration of chlorides reaches a critical level that is generally referred as critical chloride threshold, the passive layer breaks down and the corrosion is initiated.

Tutti's model is one of the first attempts to develop service life model of concrete structures in corrosion process and it can be expressed by Equation 7.1 (21),

$$t_{service} = t_{initiation} + t_{propagation} \tag{7.1}$$

where initiation is the period before the onset of corrosion and tpropagation is the time for corrosion to reach an unacceptable damage level once it has started. The initiation time period is primarily influenced by the concrete diffusion coefficients, concrete cover, surface chloride concentration, temperature, level of saturation and the required concentration at the level of reinforcing steel to initiate corrosion. The model adopted in this paper focuses only on this initiation period.

7.5 Chloride Transportation Model

The chloride salt ingression into concrete bridge deck can take place in several ways, namely permeability, adsorption or diffusion (22). Among these transport phenomena, diffusion is the most detrimental process related to the initiation of corrosion in steel reinforcement. It is widely accepted that Fick's 2nd law of diffusion can represent the rate of chloride penetration into concrete as a function of depth and time, see (23).

The solution (referred to as the Crank's Solution) of the governing differential equation is given as Equation 7.2 (24),

$$C_{x,t} = C_0\left[1 - erf\left(\frac{x}{\sqrt{4D_c t}}\right)\right] \tag{7.2}$$

where $C_{x,t}$ is the concentration of chlorides at time t (years) and depth x (meters), C_0 is the concentration of chlorides at the surface directly inside the concrete and D_c is the apparent diffusion coefficient (m^2/year).

Polynomial derivation of Equation 7.2 is a feasible approach for probabilistic model with respect to 1-D problem. However, it does not account for cracks and must be modified to account for time dependent changes in material property or boundary conditions.

7.5.1 Performance assessment

Severity of the chloride ingress can be assessed by comparing the chloride threshold value C_{th} with the chloride concentration at the exposed areas of reinforcing steel. This value will depend on the type and preparation of the reinforcing steel and the constituents of the concrete as well as other factors. The performance function, RF_t, of a bridge deck is expressed as the time-dependent exceedance of the corrosion initiation threshold by the location dependent chloride concentration, $C_{xy,t}$. Reliability function RF=R(Resistance) - S(Load effects) is analyzed using the Monte Carlo technique and random variables can be described by bounded histogram as well as continuous distributions. The performance function characterizing the above described limit state is expressed as:

$$RF_t = (R - S) = (C_{th} - C_{xy,t}) \quad (7.3)$$

The highest concentration $C_{xy,t}$ surrounding one of the epoxy-coating damaged areas was selected as the critical case where corrosion would occur first whereas the highest concentration on the reinforcement level was selected for the computation for other types of reinforcement protection. Measure of reliability or performance (reliability level) is expressed by probability of failure P_f. It needs to be noted that "failure" in studied case does not mean structural failure. P_f means here corrosion initiation likelihood. The performance of the system was estimated by the probability of chloride threshold exceedance (corrosion initiation) at a specific age $P_{f,t}$.

$$P_{ft} = P(C_{th} - C_{xy,t} < 0) \quad (7.4)$$

7.5.2 2-D finite diffusion model with crack effect

This proposed model focuses on the chloride transportation in reinforced concrete bridge decks with cracks and on the estimation of chloride ion concentration in particular locations on the embedded reinforcing steel bars or damaged areas of epoxy-coated bars. Although transverse reinforcing steel bars are susceptible to corrosion, the presented model is focused on longitudinal steel because longitudinal bars will cross the crack while only one transverse bar (closest to the crack) is affected by rapid chloride ingress through crack.

The 2-D finite element model (13) based on Ficks 2nd law of diffusion focuses on the movement and accumulation of chloride ions to the level of reinforcing steel during the initiation period of corrosion. The analysis is 2-D in order to cover the interaction

between the effect of crack on the chloride ion ingress and the holidays in the epoxy coating.

The commercial software ANSYS was used (25). The assumptions for the applied model are explained in (13). The 4-noded thermal solid element PLANE55 was used for the chloride diffusion analysis because of the analogy between the mechanisms of thermal flow and ion diffusion. The 0.25 m thick deck was vertically divided into 25 elements that are 10 mm by 10 mm in size.

7.6 SBRA Application

The SBRA Module for ANSYS is a tool for managing the probabilistic Monte Carlo simulation process with random variables distributions characterized by frequency histograms according to (18). The SBRA Module (13) runs the FEM Macro containing the diffusion process description. Random variable parameters in the FEM macro were automatically replaced by randomly generated variables throughout the Monte Carlo simulations. Random parameters are described next.

The level of acceptable probability of corrosion initiation is not well defined yet. Tikalsky (18) discusses the target probabilities and states the probability that the structure will perform for 50 years at 3 out of 4 (respective P_d would be 25 %) and the probability that the structure will perform for 100 years is 1 out of 2. Teplý (26) discusses the Pd for the corrosion imitation according to EN1990 and recommended value of the target probability for serviceability (irreversible state) as P_d = 7%. The key issue in durability assessment is a comparison of computed likelihood of corrosion initiation $P_{f,t}$ with target probability P_d as indicated in next equation.

$$P_{f,t} \leq P_d \tag{7.5}$$

Designed reliability and performance levels should be maintained throughout the intended service life. Acceptable corrosion initiation likelihood $P_f <= 0.25$ is selected here because the corrosion initiation does not immediately threaten safety ($P_d<7\times10^{-5}$) nor serviceability ($P_d < 0.07$).

7.7 Governing Input Parameters

7.7.1 Diffusion coefficient

Incorporation of the variation of reliable diffusion coefficients for HPC materials in probabilistic model is a significant part as diffusion coefficient plays a major role in corrosion initiation. Histograms for diffusion coefficients for different HPC materials along with control mixtures are computed from four different approaches, namely Nernst-Plank, Zhang-Gjorv, Nernst-Einstein and the plug flow model method (27)(28)(29). First two approaches compute equivalent steady state diffusion coefficients from chloride ion penetration test (CIPT) data with the essential adjustment for the joule effect. The other two approaches compute the diffusion coefficients from experimental concrete resistivity as well as CIPT data with the adjustment of geometric shape factor. Among the four methods, plug flow model calculates diffusion coefficients exclusively for chloride ions. Generally, CIPT and other extended migration tests include the effect of several ions such as Na^+, K^+, OH^- along with the effect of Cl^- ions. Therefore, sometimes it is difficult to understand the influence of other ions in the computation of diffusion coefficients. Since the plug flow model calculates diffusion coefficients for chloride ions only, it provides the lowest values of diffusion coefficients compared to other three methods. Four different types of simulation were run for comparison of probability of corrosion

initiation. Fig. 7.1 (a), (b) and Fig. 7.2 (a), (b) show the diffusion coefficients histogram for the previously mentioned four approaches.

7.7.2 Cover depth

Cover depth is an important parameter, which affects corrosion initiation. Therefore, it is essential to incorporate variation of cover depth in corrosion initiation model. Histogram of cover depth, presented in (30), is based on the measurement of chloride penetration and concrete cover from more than 200 samples taken from 40 bridge decks constructed under a single specification.

7.7.3 Chloride threshold for corrosion resistant steel

Alternative corrosion resistant reinforcement has already been in use for the last 30 years in the USA as a measure of corrosion protection strategy. The most widely used corrosion resistant steel is epoxy coated rebar for corrosion protection. The implementation of new corrosion-resistant steel reinforcement has been limited due to the lack of quantitative data on the corrosion threshold of the specific reinforcement. The values of critical chloride threshold of different corrosion resistant steel can be utilized in the numerical model to predict life expectancy of concrete bridge decks reinforced with different corrosion resistant steel. In this SBRA model, performance of epoxy coating, galvanized rebar, ASTM A1035 steel is compared on the basis of probability of failure on corrosion initiation time with black bar as control reinforcement. The chloride threshold distribution for black bar, galvanized steel, ASTM A1035 steel (low carbon chromium) is based on the experimental data published in (20). The chloride threshold distribution for epoxy-coated reinforcement is considered to be based on the black bar performance (Fig.

7.4 (a)) while the performance of the epoxy coating is assessed by the evaluation of the chloride ion concentration at the nearest holiday to the crack. Fig. 7.5 shows the histogram of chloride threshold of ASTM A1035 steel.

7.7.4 Other random variable parameters

It is beneficial to use the variation of distribution of surface chloride concentration to get reliable prediction of corrosion initiation time. To meet this requirement, the frequency of surface chloride concentration is prepared on the basis of field data obtained from Virginia bridge decks (19).

Holidays in epoxy coated reinforcement also play an important role in corrosion initiation in epoxy coating rebar. For this reason, frequency distribution of holidays is prepared from the existing data of Virginia bridge decks to investigate the performance of epoxy coated rebar (19).

Distribution for crack depth is based on the engineering estimation by exponential distribution. Minimal value is zero depth and maximal value is all the way through the deck thickness.

Crack spacing distribution is assumed to be correlated with deck thickness and width of model slab is equal to the random variable crack spacing. For this paper the worst case scenario is used with frequent cracks throughout all bridges. Spacing of the cracks is also estimated as a normal distribution with the mean value 0.7 m that is circa three times the thickness of the slab. Standard deviation is 0.15. The distribution is truncated within boundaries <0.25, 1.15> m.

Table 7.1 summarizes deterministic and random input variables for specified analyses.

7.7.5 Precision of Monte Carlo simulation

The SBRA module governs the probabilistic analysis with 10,000 Monte Carlo simulation steps. The error of resulting probabilities obtained by the Monte Carlo simulation can be estimated using Equation 7.6 because the precision depends on the number of simulations.

$$[-\varepsilon;\varepsilon]=[-t\sigma;t\sigma]=\left[-t\sqrt{\frac{P_f(1-P_f)}{N}};t\sqrt{\frac{P_f(1-P_f)}{N}}\right] \tag{7.6}$$

where ε is confidence region, N is the number of simulations, P_f is desired precision and t represents the confidence level. If the probability of corrosion initiation is P_f = 1/100, total simulation steps will be N=10,000. For 90% confidence level (t=1.6449) the resulting probabilities will be P_f = 0.01±0.0016. This precision is reasonable with respect to the performed study even though the confidence interval boundaries change depending on the value of estimated probability.

7.8 Results

The sample output for epoxy coated reinforcement is indicated next on the example with diffusion constant derived using the Nernst-Plank method. The chloride ion concentration at the rebar level at the exposed reinforcing steel areas and performance function distributions are shown after 100 years in service. The ACI threshold C_{th}=0.2% is shown in Fig. 7.7 (a) for illustration purposes only. The performance function, which is also shown in Fig. 7.7 (b), consists of random variable chloride concentration as well as random variable threshold based on the particular distribution.

Probability of corrosion initiation on the epoxy-coated reinforcement for service life 100 years is $P_{f,100}$=26.6% as can be seen on Fig. 7.7 (b). The probabilities can be obtained throughout the whole service life and the corrosion initiation risk can be drawn as a function of time (see Fig.7.8). For the epoxy-coated reinforcement and diffusion coefficient computed using the Nernst-Plank method, the corrosion initiation risk P_f reaches 25% in 88.8 years of service.

7.8.1 Reinforcement protection type comparison

The performance of four types of reinforcement embedded in the concrete bridge deck exposed to deicing agents is studied, namely black bar, galvanized bar, epoxy-coated bar and ASTM A1035 type rebar.

The resulting probabilities of corrosion initiation throughout the simulated service life (from 5 to 100 years) are shown in the Fig. 7.9 (including epoxy-coated reinforcement presented in Fig. 7.8). Acceptable lifespan can be evaluated similarly as for the epoxy-coated reinforcement.

From the simulation results, it can be observed that epoxy-coated reinforcement performs the best in the first 15 years. The ASTM A1035 steel provides better results after that initial 15 years. Its corrosion risk is almost uniform throughout the lifespan changing from 3 to 5 %. The corrosion initiation risk for ASTM A1035 steel does not exceed the 25% limit over the studied period. The galvanized steel starts with corrosion risk of 11.4 % and ends up with 28.8 %. The acceptable performance lasts for 70.6 years. Performance of epoxy-coating and galvanized steel becomes similar after 50 simulated years of service. The black bar corrosion risk is two times larger (20.7 - 56.1 %) than of galvanized steel while the acceptable lifespan (12.6 years) is 5.6 times lower. The

resulting performance prediction and probability is strongly dependent on the critical chloride threshold level of selected reinforcement types. The threshold distribution is completely based on the lab data being used in (20).

7.8.2 Diffusion coefficient type comparison

The study is accompanied by the diffusion coefficient computation method effect on the acceptable service life evaluation. Performance of four different types of diffusion coefficient computation is studied (Nernst-Plank, Zhang-Gjorv, Nernst-Einstein and Plug flow). The epoxy-coated reinforcement behavior is selected for that comparison. The effect on the other types of reinforcement is similar to that of epoxy coated reinforcement.

The shortest time to unacceptable reinforcement performance is being provided by the application of diffusion constant histogram derived using the Zhang-Gjorv method (51.9 years). Nernst-Plank and Nernst-Einstein provided similar results (88.8 years and 83.5 years, respectively). If the Plug-flow model (diffusion coefficients model for chloride ions only) derived histogram is selected, the acceptable performance would sustain more than 100 years.

7.9 Discussion

The numerical simulation of bridge deck with crack indicates that the ASTM A1035 steel type reinforcement provides the best protection with respect to chloride induced corrosion risk comparing to epoxy-coated steel and galvanized steel. It needs to be noted that this result is based on the numerical simulation and under laid assumptions

being made. The further laboratory and field tests are necessary to verify the effectiveness of ASTM A1035 steel protection.

The epoxy coated reinforcement performs better comparing to galvanized steel especially in the first five decades. The advantage of epoxy-coated reinforcement seems to be caused by the holiday crack interaction effect. Reduced frequency of holidays and increased crack specially leads to better performance of epoxy-coating in the first five decades.

7.10 Conclusions

1. This research demonstrates the necessity of the formulation of probabilistic corrosion initiation model of HPC materials with inclusion of reliable diffusion coefficients and several corrosion resistant steel reinforcements.

2. Application of corrosion resistant reinforcement can extend the acceptable performance of severely cracked bridges significantly according to the performed numerical simulation. Galvanized rebar extends the service life 5.6 times, epoxy-coating 7 times, and ASTM A1035 more than 8 times compared to the black bar.

3. Selection of the methodology for the computation of diffusion coefficient affects the service life significantly as well. Acceptable bridge deck performance with epoxy-coated reinforcement varies from 51.9 years (Zhang-Gjorv method) up to more than 100 years (Plug flow method).

4. The authors considers the Plug Flow model of diffusion coefficients is the preferred method for computation of extended corrosion free service life as it provides the lowest values of diffusion coefficients (Only for chloride ions) compared to the other three methods. However, for equivalent steady state diffusion coefficient computation, the

Nernst-Plank method is the preferred method as it provides lower values of diffusion coefficients compared to the Zhang-Gjorv method (27). But, further research is needed to compute reliable diffusion coefficients from actual field core samples to compare with lab data. It is also to be noted that the diffusion coefficients included in this model are not age dependent.

5. In addition to designing low diffusion concrete, the quality of rebar coatings and shrinkage crack frequency can be designed to prolong life span of bridge decks.

6. This numerical model does not take into account corrosion in epoxy coating or propagation stage of galvanized rebar. Proper maintenance, installation and alternative corrosion protection strategy according to environmental condition should be implemented along with the use of corrosion resistant steel in HPC materials.

7.11References

1. Zemajtis, J., "Modeling the Time to Corrosion Initiation for Concretes with Mineral Admixtures and/or Corrosion Inhibitors in Chloride Laden Environments", Dissertation at Virginia Polytechnic Institute and State University, Virginia, USA, 1998.

2. Weyers, R.E., Pyc, W., and Sprinkel, M.M., "Estimating the Service Life of Epoxy-Coated Reinforcing Steel", *ACI Materials Journal*, V. 95, No.5, 1998, pp. 546-557.

3. Boddy, A., Bentz, E., Thomas, M. D. A., and Hooton, R.D., "An Overview and Sensitivity Study of a Multi- Mechanistic Chloride Transport Model", *Cement and Concrete Research*, V. 29, 1999, pp. 827-837.

4. Alisa, M., Andrade, C., Gehlen, J., Rodriques, and Vogels, R., "Modeling of Degradation", European Union – Brite Eurram, CT95-0132, Project BE95-1347, Document BE95-1347/R0, 1998.

5. Teplý, B., Novák, D., Keršner, Z., and Lawansuit, W., "Deterioration of Reinforced Concrete: Probabilistic and Sensitivity Analyses", Acta Polytechnica, Prague, Czech Republic, 1999.

6. Papadakis, V.G., "Effect of Supplementary Cementing Materials on Concrete Resistance against Carbonation and Chloride Ingress", *Cement and Concrete Research*, V. 30, No.2, 2000, pp. 291-299.

7. Bentz, E., and Thomas, M. D. A., Life-365 Service Life Prediction Model, Computer Program for Predicting the Service Life and Life-Cycle Costs of Reinforced Concrete Exposed to Chlorides, 2001.

8. Wheeler, M., "Parameters Influencing the Corrosion Protection Service Life of Epoxy Coated Reinforcing Steel in Virginia Bridge Decks", Master's thesis, Virginia Polytechnic Institute and State University, Blacksburg, Virginia, U.S.A, 2003.

9. Lounis, Z., and Amleh, L., "Reliability-Based Prediction of Chloride Ingress and Reinforcement Corrosion of Aging Concrete Bridge Decks", Probabilistic Modeling of Deterioration Process in Concrete Structures, 3rd IABMAS Workshop on Life-Cycle Cost Analysis and Design of Civil Infrastructure Systems/JCSS Workshop, March 24-26, Lausanne, Switzerland, 2004.

10. Lounis, Z., "Probabilistic Modeling of Chloride Contamination and Corrosion of Concrete Bridge Structures", Uncertainty Modeling and Analysis, Proceedings of 4th International Symposium, pp. 447-451, September 21-24, Maryland, U.S.A, 2003.

11. Daigle, L., Lounis, Z., and Cusson, D., "Numerical Prediction of Early-Age Cracking and Corrosion in High Performance Concrete Bridges– Case Study", Available online: http//www.tac-atc.ca/english/pdf/conf2004/Daigle.pdf.

12. Tikalsky, P.J., Pustka, D., and Marek, P., "Statistical Variations in Chloride Diffusion in Concrete", *ACI Structural Journal*, V.102, No.3, 2005, pp.481-486.

13. Konečný, P., Tikalsky, P. J., and Tepke, D. G., "Performance Evaluation of Concrete Bridge Deck Affected by Chloride Ingress: Simulation-Based Reliability Assessment and Finite Element Modeling" In Transportation Research Record: *Journal of the Transportation Research Board*, No. 2028, Transportation Research Board of the National Academies, Washington, D.C., pp. 3-8, 2007.

14. Shim, H., "Design & Analysis of Corrosion Free Service Life of Concrete Structures Using Monte Carlo Method", *KSCE Journal of Civil Engineering*, V.9, No.5, 2005, pp.377-384.

15. Lounis Z., Zhang, J., and Daigle., L., "Probabilistic Study of Chloride Induced Corrosion of Carbon Steel in Concrete Structures", Probabilistic Mechanics and Structural Reliability, 9th ASCE Joint specialty conference on, Albuquerque, New Mexico, July 26-28, 2004, pp.1-6.

16. 16. Kirpatrick, J.T., Weyers, E.R., Abderson-Cook, M.C., and Sprinkel, M.M., "Probabilistic Model for the Chloride Induced Corrosion Service Life of Bridge Decks", *Cement and Concrete Research*, V. 32, 2002, pp.1943-1960.

17. Marek, P., Guštar, M., and Anagnos, T., "Simulation-Based Reliability Assessment for Structural Engineers", CRC Press, Inc., Boca Raton, Florida, 1995.

18. Tikalsky, P., "Chapter 20 Durability and Performance-Based Design Using SBRA, Probabilistic Assessment of Structures Using Monte Carlo Simulation, Basics Exercises", 2nd Edition, ISBN:80-86246-19-1, ITAM Academy of Sciences Czech Republic, 2003.

19. Pyc, W., "Field performance of Epoxy-Coated Reinforcing Steel in Virginia Bridge Decks", Doctoral Dissertation, Virginia Polytechnic Institute and State University, Blacksburg, Virginia, U.S.A, 1998.

20. Darwin, D., and Browning, J., "Critical Chloride Corrosion Threshold of Galvanized Reinforcing Bars", *ACI Materials Journal*, V.106, No.2, 2009, pp.176-183.

21. Tutti, K., "Corrosion of Steel in Concrete", CBI Research Report 4:82, Swedish Cement and Concrete Research Institute, Stockholm, Sweden, 1982.

22. Ahmad, S., Al-Kutti, W.A., Al-Amoudi, B.S.O., and Maslehuddin, M., "Correlations Between Depth of Water Penetration, Chloride Permeability, and Coefficient of Chloride Diffusion in Plain, Silica Fume, and Fly Ash Cement Concretes", *Journal of Testing and Evaluation*, V.36, No.2, 2009, pp.1-4.

23. Hooton, R.D., Thomas, M.D.A., and Standish, K., "Prediction of Chloride Penetration in Concrete", Publication FHWA-RD-00-142, Federal Highway Administration, Washington, D.C., pp. 405, 2001.

24. Collepardi, M., Marcialis, A., and Turrizuani, R., "Penetration of Chloride Ions into Cement Pastes and Concretes", *Journal of American Ceramic Research Society*, V.55, No.10, 1972, pp. 534-535.

25. Ansys 11.0 Release Documentation, 2009.

26. Teplý, B., Keršner, Z., Rovnaník, P., and Chromá, M., "Durability vs. Reliability of RC Structures. Durability of Building Materials and Components", Proceedings of 10DBMC International Conference on, Lyon, France, April 17-20, 2005.

27. Pratanu, G., Hammond, A., and Tikalsky, P., "Prediction of Equivalent Steady State Chloride Diffusion Coefficients", *ACI Materials Journal*, V.108, No.1, pp. 88-94, January-February 2011.

28. Orlova, V.N., Westall, C.J., Rehani, M., and Koretsky, D.M., "The Study of Chloride Ion Migration in Concrete under Cathodic Protection", Final Report-SPR357, Oregon Department of Transportation, Oregon, September, pp.1-83, 1999.

29. Gjorv, E.O., and Sengul, O., "Electrical Resistivity Measurements for Quality Control during Concrete Construction", *ACI Materials Journal*, V.105, No.6, 2008, pp.541-547.

30. Sohanghpurwala, A.A., and Scannell, W.T., "Verification of Effectiveness of Epoxy-Coated Rebars", Final Report Project No. 94 005, Pennsylvania Department of Transportation, 1994, pp.97.

Table 1- Random and deterministic input values for ANSYS model

Parameter	Range	Distribution
Diffusion Coefficient D_c [$10^{-12}m^2/s$](Plug-flow)	0.36-2.69	Histogram (Fig.7.1 (a))
Diffusion Coefficient D_c [$10^{-12}m^2/s$](Nernst-Einstein)	0.71-3.71	Histogram (Fig.7.1 (b))
Diffusion Coefficient D_c [$10^{-12}m^2/s$](Nernst-Plank)	0.59-4.50	Histogram (Fig.7.2 (a))
Diffusion Coefficient D_c [$10^{-12}m^2/s$](Zhang-Gjorv)	1.02-7.72	Histogram (Fig.7.2 (b))
Rebar Depth (Cover) R_{ebd} [m]	0.04-0.11	Histogram (Fig.7.3)
Frequency of holidays M_{ashn} [m^{-1}]	0-10	Histogram (Fig.7.6 (a))
Crack Spacing $Crck_s$ [m]	0.25-1.15	Normal Distribution N(0.7,0.15)
Crack Depth $Crck_{dpt}$ [m]	0-Depth	Exponential Distribution
Relative Damage Area Position $Crack_i$	0-1	Uniform distribution
Surface Soluble Chloride Concentration C_0 [%]	0.2-1.6	Histogram (Fig.7.6 (b))
Chloride Threshold (epoxy-coated bar) C_{th} [%]	0.09-0.50	Histogram (Fig.7.4 (a))
Chloride Threshold (black bar) C_{thb} [%]	0.09-0.50	Histogram (Fig.7.4 (a))
Chloride Threshold (galvanized bar) C_{thg} [%]	0.04-1.23	Histogram (Fig.7.4 (b))
Chloride Threshold (ASTM A1035 bar) C_{thg} [%]	0.34-1.74	Histogram (Fig.7.5)
Depth of Slab D_{epth} [m]	0.25	Constant value
Life Span t [years]	100	Constant value

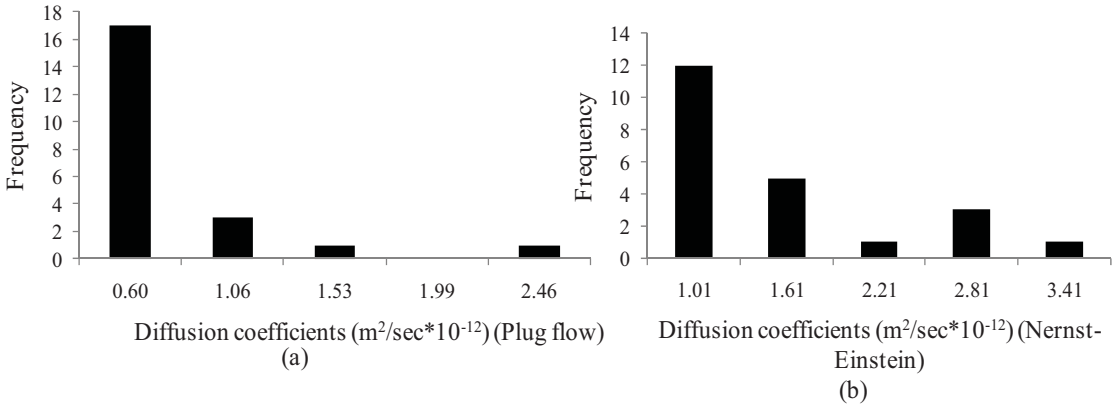

Fig 7.1 Histograms for diffusion coefficients (a) Plug flow model, (b) Nernst-Einstein method

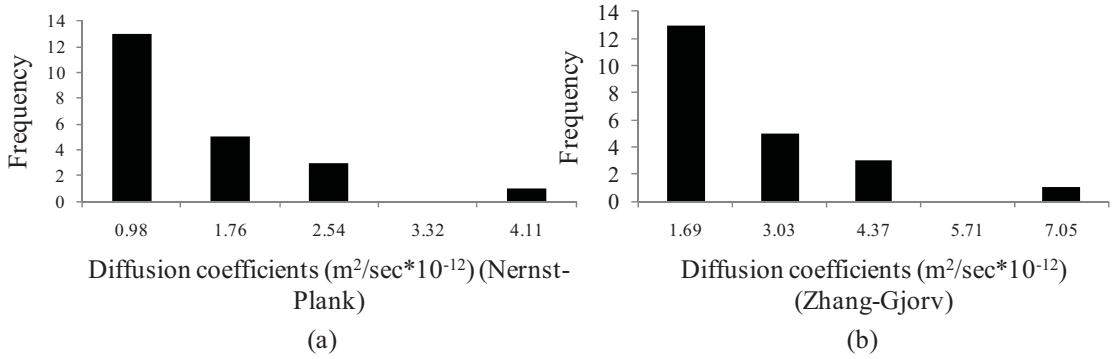

Fig. 7.2 Histograms for diffusion coefficients (a) Nernst-Plank method, (b) Zhang-Gjorv method

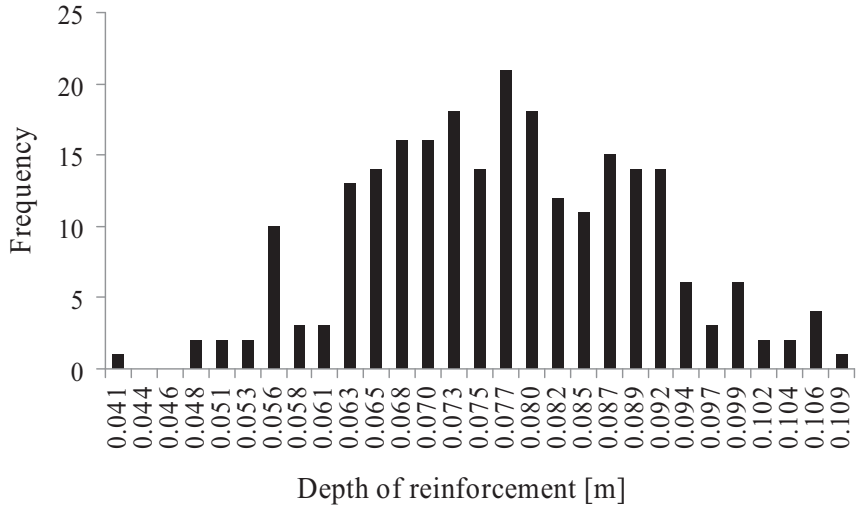

Fig. 7.3 Histogram for cover (Depth of reinforcement) (*30*)

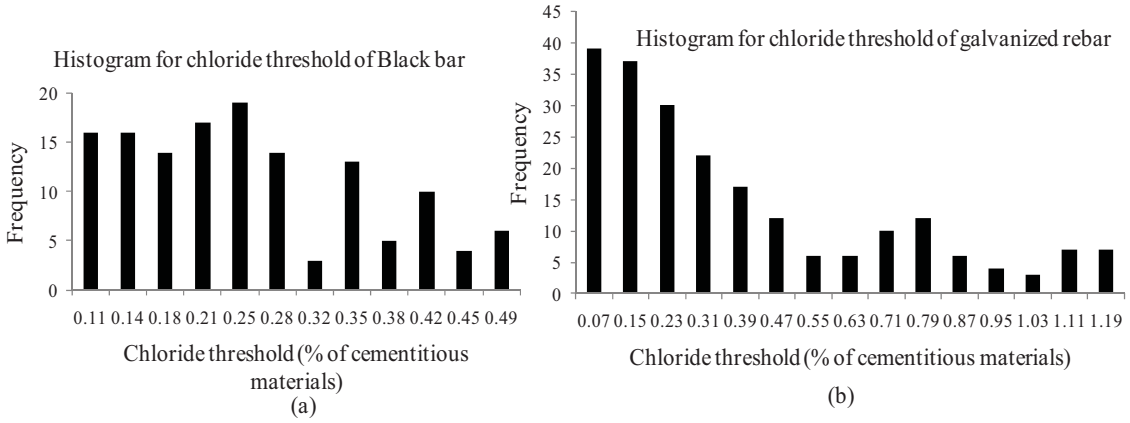

Fig. 7.4 Histograms for chloride threshold (a) black bar and (b) galvanized rebars (20)

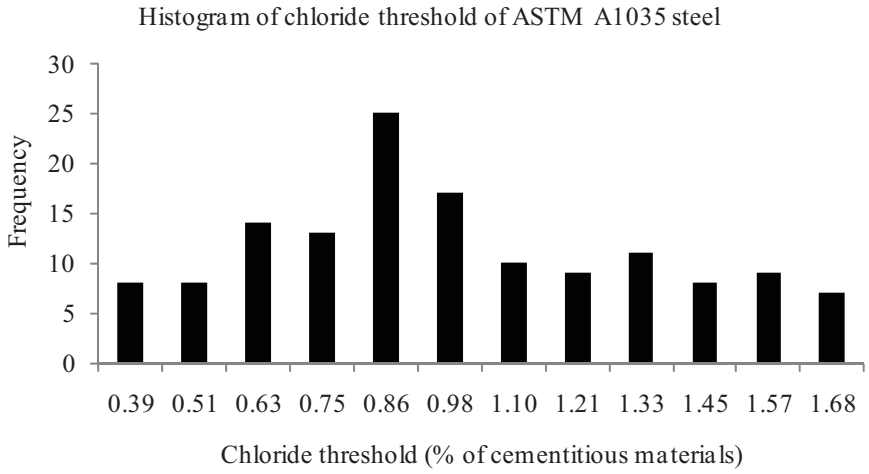

Fig. 7.5 Histogram for chloride threshold of ASTM A1035 steel (20)

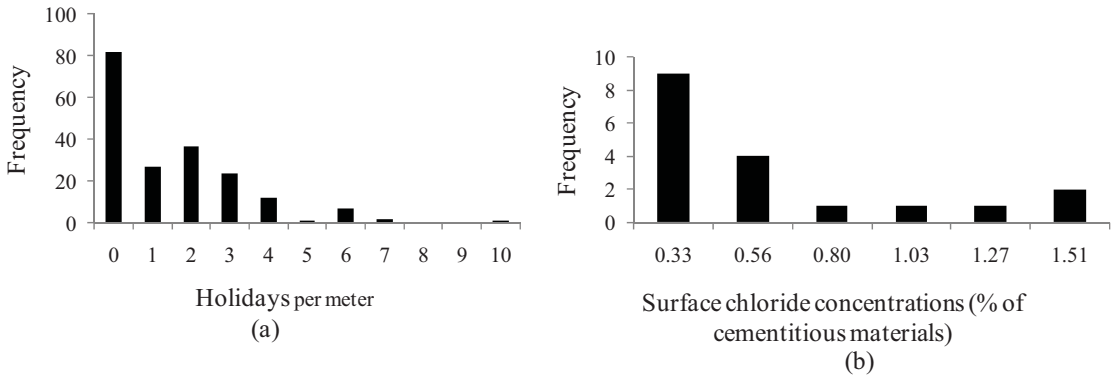

Fig. 7.6 Histograms for frequency (a) holidays and (b) surface chloride concentration (19)

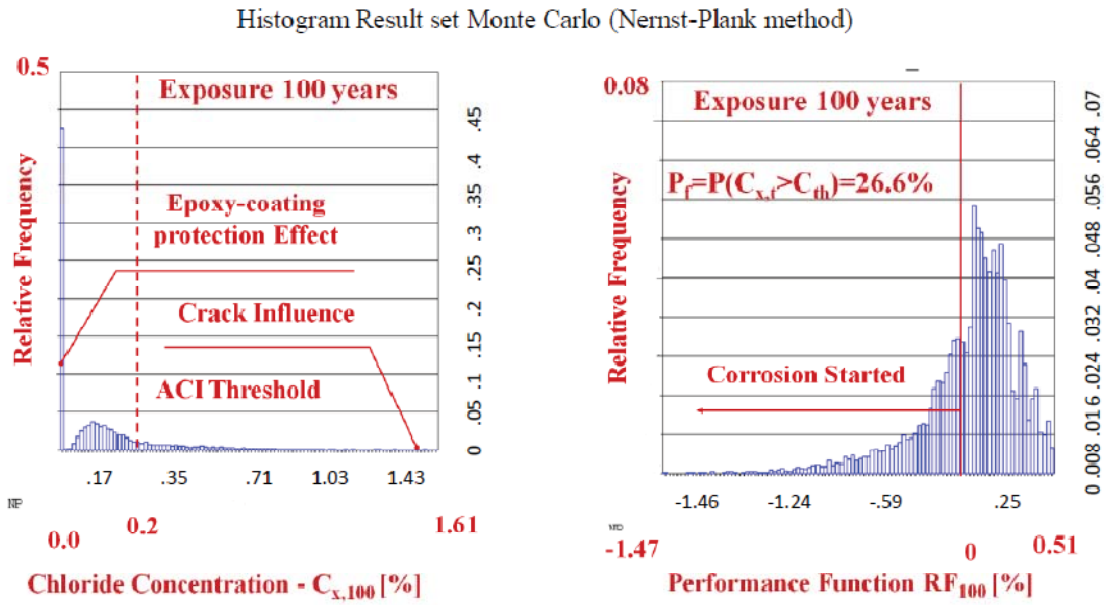

Fig. 7.7 (a) Chloride ion concentration $C_{xy,t}$ and (b) performance function RF_t for epoxy coated reinforcement in 100 years

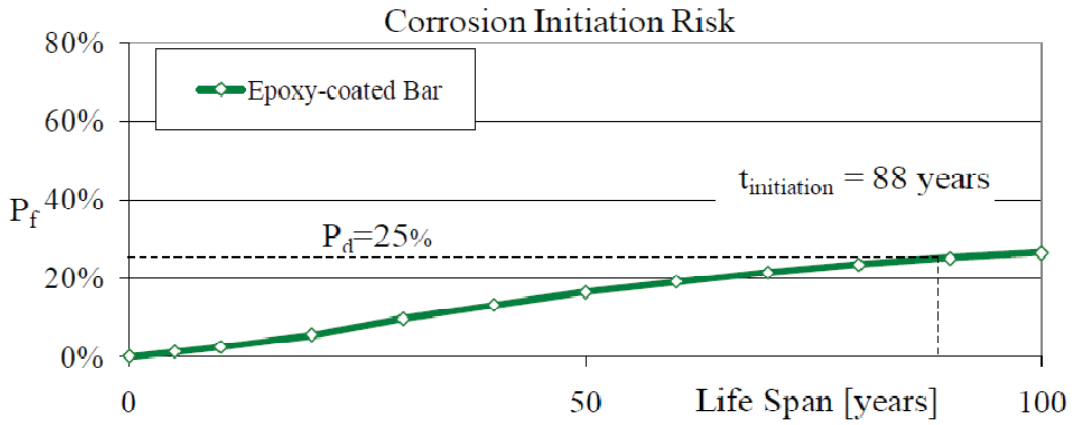

Fig. 7.8 Performance of Epoxy-coated reinforcement (Nernst-Plank method)

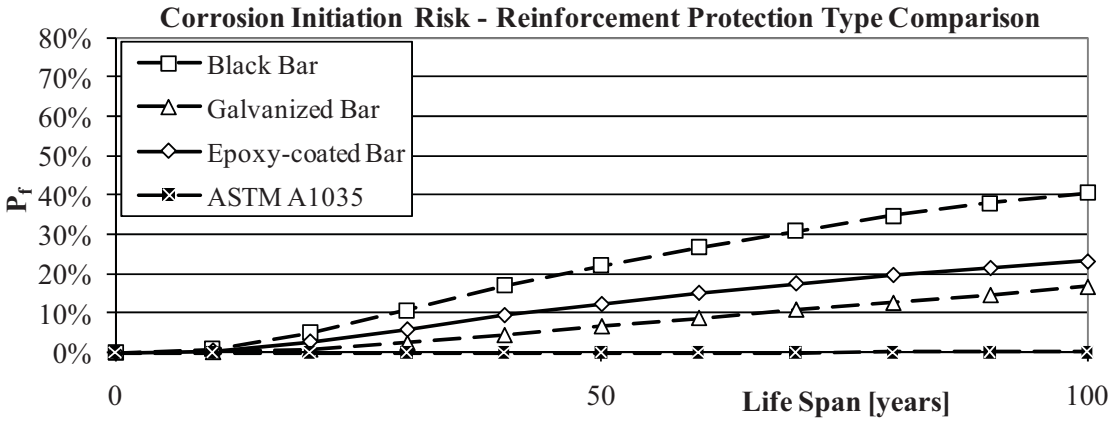

Fig. 7.9 Performance of all the reinforcements (Nernst-Plank method)

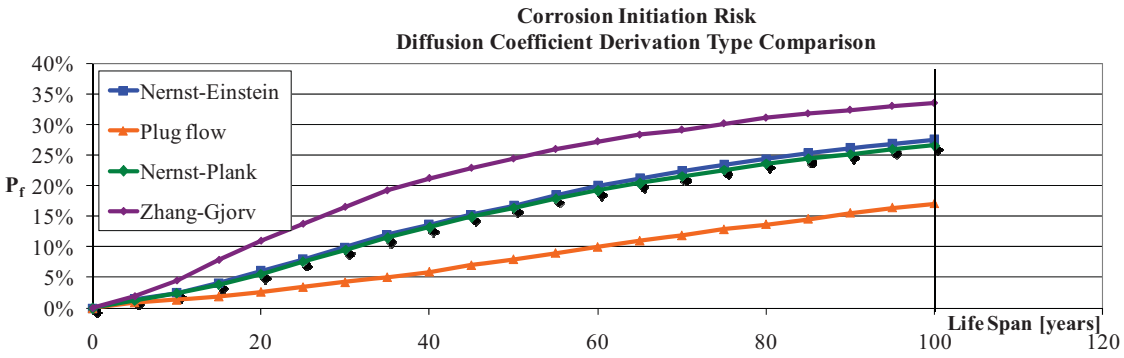

Fig. 7.10 Performance of all the methods for diffusion coefficient evaluation (epoxy-coated reinforcement)

CHAPTER 8

SUMMARY AND CONCLUSIONS

The main body of the research presented herein examined different strategies to delay chloride induced corrosion initiation in bridge decks, pavements and other concrete strictures. This investigation was done through two different goals namely computation of reliable improved HPC diffusion coefficients from two standardized testing procedures and formulation of probabilistic corrosion initiation model with inclusion of these reliable HPC diffusion coefficients and several corrosion resistant steel reinforcements. These two goals helped in improving the pore structure and the hardened concrete with regard to chloride ingress in corrosion initiation process. These two goals are achieved through different analyses, methodologies and corrosion initiation model as discussed in Chapter 3 to 7. The following conclusions can be drawn from the research studies as presented in Chapter 3 to 7:

1) Chapter 3 presented the necessity for application of the CIPT data to compute equivalent steady state diffusion coefficients from different theoretical approaches namely Nernst-Plank, Nernst-Einstein and Zhang-Gjorv methods. Temperature adjustment due to the joule effect helps in understanding the steady state condition of the diffusion process. As a result, this adjustment achieved a more accurate and reliable prediction of the chloride diffusion coefficients in hardened concrete based on fundamental of electrochemistry within 6 hours of the CIPT.

2) Chapter 4 illustrated the method of computation of reliable diffusion coefficients from both the CIPT and experimental resistivity data. The necessity of the temperature adjustment due to the joule effect and adjustment due to geometric shape difference helps in achieving a more accurate and reliable prediction of diffusion coefficients in hardened concrete from different theoretical approaches namely Plug flow, Nernst-Einstein relationship and Nernst-Einstein law. Significant reduced values of diffusion coefficients for chloride ions only obtained from plug flow model clarified that there is some predominant effect of other ions such as Na^+, K^+, and OH^- in the CIPT and other extended migration test.
3) Chapter 5 demonstrated the good correlation of data between the CIPT and Wenner Probe electrical resistivity data. Therefore, these testing procedures can be used to investigate chloride ion penetration as part of a durability acceptance criterion. The CIPT testing results and results obtained using a Wenner probe can be well related through Ohms law for blended and unblended cement concrete mixtures. This correlation of data becomes only reliable with the incorporation essential adjustments due to the joule effect and geometric shape factor. The finding from this analysis also supports the use of Wenner probe device as a possible quality assurance/quality control (QA/QC) tool in concrete field testing.
4) Chapter 6 presented the method of computation of electrical conductivity of different ternary, binary cementitious mixtures along with some control mixtures. Finally, reliable prediction of diffusion coefficients through Nernst-Einstein equation is obtained by using equivalent steady state electrical conductivity

measurement. This method of computation also involved the adjustments due to the joule effect. It has been observed that ternary cementitious mixtures have large effect for reduction of diffusion coefficients and increase of electrical conductivity to increase long term resistance for chloride ion penetration. The key reason is that the densification of the matrix brought about by the pozzolanic reactions of pozzolans tries to close the pores and results in reducing permeability.

5) Chapter 7 addressed the necessity of the formulation of probabilistic corrosion initiation model of HPC materials with inclusion of reliable diffusion coefficients and several corrosion resistant steel reinforcements. This model shows the variability and sensitivity on estimation of the time to onset of corrosion using the Monte Carlo technique with the application of Simulation Based Reliability Assessment (SBRA) method. Application of corrosion resistant reinforcement can extend the acceptable performance of severely cracked bridges significantly according to the performed numerical simulation. Galvanized rebar extend the service life 5.6 times, epoxy-coating 7 times, and ASTM A1035 more than 8 times compared to the black bar. Selection of the methodology for the computation of diffusion coefficient affects the service life significantly as well. Acceptable bridge deck performance with epoxy-coated reinforcement varies from 51.9 years (Zhang-Gjorv method) up to more than 100 years (Plug flow method).

This study focuses on only corrosive environments, where chloride-induced corrosion is of major concern. Corrosion of reinforcement due to the exposure to chemical

environment such as CO_2 induced corrosion has not been considered in this work. Overall, the findings from these research analyses can provide effective decision support in the design of new durable structures in harsh chloride environments.

CHAPTER 9

FUTURE RESEARCH STUDY

The study presented in this dissertation discusses the potential strategies to delay chloride induced corrosion initiation. The performance of several corrosion resistant steel reinforcements presented in the SBRA model is completely dependent on the data of critical chloride threshold of steel reinforcements based on a specific laborartory investigation. The numerical simulation of bridge deck with crack indicates that the ASTM A1035 steel type reinforcement provides the best protection with respect to chloride induced corrosion risk comparing to epoxy-coated steel and galvanized steel. It is to be noted that the findings from this analysis are based on the numerical simulation and under laid assumptions being made. Additional laboratory and field tests are necessary to verify the effectiveness of ASTM A1035 and other steel protection. This numerical model needs to be validated in the future with field data of bridge decks for chloride concentrations on periodic time intervals, electrical resistivity of concrete and critical chloride threshold of corrsion resistant steel reinforcements.

It is also to be noted that the probabilistic model described in this dissertation does not take into account active corrosion propagation of corrosion resistant steel reinforcements. This corrosion propagation process is a complex process and is necessary to understand for computation total service life/residual life of concrete structures in

chloride induced corrosion deterioration. Optimal decision making about repair and maintenance of reinforced concrete structures can only be feasible once corrosion propagation time or time to cracking/spalling of concrete cover is available. Therefore, the corrosion cracking model needs to be developed in future study focusing on active reinforcement corrosion together with suitable probabilistic numerical model and software tools. This would enable the user to compute the propagation period and assess RC structure's safety and durability.